

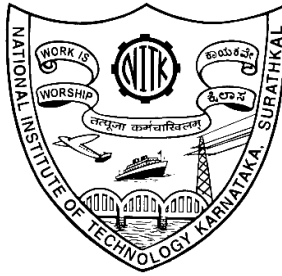
**HYDRAULIC MODELLING OF
UNSTEADY FLOW AND FLOOD
ROUTING IN NETHRAVATHI RIVER
BASIN, INDIA**

Thesis

Submitted in partial fulfilment of the requirements for the degree of
DOCTOR OF PHILOSOPHY

by

**PRAMODKUMAR
165130AM16F08**



**DEPARTMENT OF WATER RESOURCES & OCEAN
ENGINEERING
NATIONAL INSTITUTE OF TECHNOLOGY KARNATAKA
SURATHKAL, MANGALORE – 575 025
APRIL 2022**

**HYDRAULIC MODELLING OF
UNSTEADY FLOW AND FLOOD
ROUTING IN NETHRAVATHI RIVER
BASIN, INDIA**

Thesis

Submitted in partial fulfilment of the requirements for the degree of
DOCTOR OF PHILOSOPHY

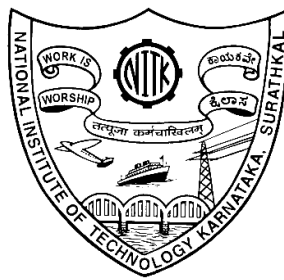
by

**PRAMODKUMAR
165130AM16F08**

Under the guidance of

**Dr. M. K. NAGARAJ
Professor**

**Dr. Paresh Chandra Deka
Professor**



**DEPARTMENT OF WATER RESOURCES & OCEAN
ENGINEERING
NATIONAL INSTITUTE OF TECHNOLOGY KARNATAKA
SURATHKAL, MANGALORE – 575 025
APRIL 2022**

D E C L A R A T I O N

By the Ph.D. Research Scholar

I hereby *declare* that the Research Thesis entitled “**HYDRAULIC MODELLING OF UNSTEADY FLOW AND FLOOD ROUTING IN NETHRAVATHI RIVER BASIN, INDIA**”, which is being submitted to the **National Institute of Technology Karnataka, Surathkal** in partial fulfilment of the requirements for the award of the Degree of **Doctor of Philosophy** in the **Department Of Water Resources & Ocean Engineering** is a *bonafide report of the research work carried out by me*. The material contained in this Research Thesis has not been submitted to any University or Institution for the award of any degree.



165130AM16F08, PRAMODKUMAR

(Register Number, Name & Signature of the Research Scholar)

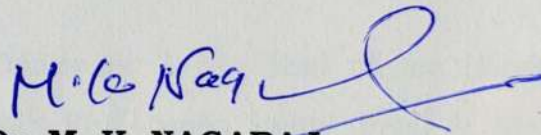
Department of Water Resources and Ocean Engineering
National Institute of Technology Karnataka, Surathkal

Place: NITK-Surathkal

Date: **25-04-2022**

C E R T I F I C A T E

This is to certify that the Research Thesis entitled "**HYDRAULIC MODELLING OF UNSTEADY FLOW AND FLOOD ROUTING IN NETHRAVATHI RIVER BASIN, INDIA**" submitted by **PRAMODKUMAR** (Register Number: 165130 AM16F08) as the record of the research work carried out by him, is *accepted as the Research Thesis submission* in partial fulfilment of the requirements for the award of degree of **Doctor of Philosophy**.



Dr. M. K. NAGARAJ
Professor (Retd)
Research Guide



Prof. Dodamani B M
Chairman (DRPC)
Dept. of Water Resources & Ocean Engineering
Chairman - DRPC

Department of Water Resources and Ocean Engineering
National Institute of Technology Karnataka, Surathkal

ACKNOWLEDGEMENT

With deep sense of gratitude, I express my heartfelt thanks to my research supervisor Dr. M. K. Nagaraj, Retired Professor, and late Dr. Paresh Chandra Deka, Professor Department of Water Resources and Ocean Engineering, NITK for their invaluable guidance, encouragement and motivation throughout my research work. I am indebted to them for their wholehearted interest and keenness in every phase of research work and thesis preparation. Their moral support, guidance, interactions, discussions and precious suggestions have greatly helped me to complete this research work. It has been my greatest opportunity and pleasure to work under them. Their crucial comments have guided me to publish my research work in acclaimed International Journals. I would also like to convey my sincere thanks to my Research Progress Assessment Committee members, Dr. Varija K., Department of Water Resources and Ocean Engineering, and Dr. C. P. Devatha, Department of Civil Engineering for providing valuable suggestions, comments and encouragement at various stages of this research work.

I would like to thank Prof. B M Dodamani, Head of the Department of Water Resources and Ocean Engineering and the former Heads Prof. Amba Shetty, Prof. A. Mahesha and Prof. Dwarakish G S, for all the support throughout my stay at NITK campus. I am also thankful to all faculty and staff of Water Resources and Ocean Engineering Department for their help and support.

My special thanks to Mr. Balakrishna, GIS Lab, who made sure that laboratory facilities were working fine all the time and helped me out whenever in trouble. My sincere thanks to Mr. Seetharam, and Mr. Anil Kumar Water Resources and Ocean Engineering Department for their help in procuring data and department facilities. I am grateful for the help and co-operation rendered by non-teaching staff and office staff of Water Resources and Ocean Engineering Department.

I gratefully acknowledge the emotional support and encouragement provided by my dear colleague Dr. Harish Kumar Shivamogga, helped me to collect data, write paper, and thesis and who pushed me every time to walk extra-mile towards the goal. I am

indebted to the support, technical suggestions and all the help rendered by Dr. Deepak, whose contributions during paper writing is incredible.

My special thanks to Dr. Rajesh Kalli, Dr. Biswajit, Dr. Alok Kumar, Mr. Pandu Shetty and Mr. Sahaj K V best friends of mine who stood by me throughout this journey with their support, suggestions and timely help extended at NITK.

I am forever grateful to my father Sri. Neelkanth, Kappadi, mother Smt. Madhavi Kappadi, my brother Mr. Prashanth Kumar and my sister Bhuvaneshwari who provided me the best education and encouraged in all my endeavors. I am grateful to my wife Mrs. Vidyashree Kappadi, who has been influential in motivating me in this journey with her moral support and cooperation.

I lovingly acknowledge the moral support and help extended by my research colleagues during this journey. Their informal support and encouragement has been very crucial. I am grateful to everybody who helped and encouraged me during this research work.

Pramodkumar

Dedication

I dedicate this thesis to my beloved parents, my caring wife and beautiful daughter Hritika for their eternal love

&

Along with those close to my heart

Family members and Friends

ABSTRACT

River systems need improved hydraulic models in order to better simulate river conditions at different points in time. Flooding is one of the changes in the flow characteristics of a river. Also, Channel roughness co-efficient is found to be a critical factor that is dynamic in nature influencing the flow characteristics of a river. The variation of roughness co-efficient based on the riverbed material and morphology affects the fluvial erosion and deposition altering the channel geometry. However, the parameter has been consistently considered as a constant value for the simulation in the numerical models. On the contrary, various experimental studies and analytical models have revealed roughness co-efficient to be one of the sensitive parameter in simulation of flow. Various models were developed for study to analyze the influences of the bed morphology (Roughness coefficient, the shape of the channel, channel slope) on discharge and water level at various locations of the river. It is also proved to be good means to assess the impacts for its capability to do the sensitivity analysis and to predict flood flow and inundated area.

The aim of the present study is to simulate unsteady flow analysis using hydraulic model HEC-RAS for Nethravathi River basin in India for identifying the impact of variability in roughness co-efficient on the river-stage and discharge. Also, it is intended to assess the hydraulic response of the river using flood-routing analysis and to study sensitivity of geometric and computational parameters on model results and stability. A river length of 45 km of the Nethravathi river regime, Karnataka from Uppinangadi and Kumaradhara to Bantwal is considered for the study. HEC-RAS model was used for the simulation of surface water levels and discharge values. Manning's roughness coefficient and river cross sections were defined for the calibration of observed river stage and discharge data. The model is built to examine the hydraulic response in Nethravathi River basin for a calibration period of 2007 - 2009 and validation period of 2010. The simulated model results provided good correlation between observed and simulated discharge and stage respectively. The error function values during validation are found to be marginally lower in

comparison to calibration results. Thus, considering the overall values of the error functions for the gauging station, it is found that the model performs reasonably well for unsteady flow analysis.

The variation of Manning's roughness coefficient was observed to affect the river stage and thereby influencing the associated peak discharges. The coefficients of correlation for the developed rating curves showed the best fit for Manning's $n=0.070$ flood plain. The peak discharge computation accuracy is approximately 80% in the calibration period and 88% in the validation period. The maximum water level computation accuracy is approximately 93.33% in the calibration period and 97.23% in the validation period. Depth of the flood is found to range between 0.1 m to 14.98 m. Velocity of flow along the whole river reach is found to vary between 0.01 m/s to 7.43 m/s. The maximum depth of flow in channel and floodplain is 7.75 m and 3.37 m respectively at downstream gauging station. However, the maximum velocity in the downstream of the river channel is found vary between 0.28 m/s to 1.71 m/s consequently, the river stage and discharge along the cross-section of flow were disturbed resulting in the flooding of river banks and inundation of low lying areas. Flood inundation map shows the spatial variation of the flood in the floodplains of the Nethravathi basin. Flood water flows over the riverbank in the upstream of the Uppinangadi gauging station, near the Nethravathi-Kumaradhara river confluence and at the meandering section in upstream of the Bantwal gauging station.

The Manning's roughness coefficient, normal depth, time step and θ -weighting parameter were considered to test the model sensitivity. The results from the sensitivity analysis showed that the model is very sensitive to the choice of Manning's n . Reducing Manning's n will decrease magnitude of peak and stage, and reduce the total inundation extent. The output is more sensitive to Manning's n than time step, θ -parameter, cross-section spacing and normal depth. This indicates that the choice of friction coefficient can to some extent overshadow the uncertainties related to insufficient geometry data and the numerical solution.

Keywords: Hydraulic Flood Routing; Manning's Roughness; HEC-RAS; Sensitivity Analysis; Stage; Discharge

TABLE OF CONTENTS

| Sl. No | TITLE | Page. No. |
|--------|---|--------------|
| | ABSTRACT | i-ii |
| | TABLE OF CONTENTS | iii-vi |
| | LIST OF FIGURES | vii-x |
| | LIST OF TABLES | Xi |
| | NOMENCLATURE | Xii |
| | ABBREVIATIONS | Xiii |
| | CHAPTER 1: INTRODUCTION | 1-10 |
| 1.1 | GENERAL | 1 |
| 1.2 | FLOW CHARACTERISTICS AND CLASSIFICATION | 2 |
| 1.2.1. | Flow in natural channels | 2 |
| 1.2.2. | Methods of flow measurement | 3 |
| 1.3. | FLOOD ROUTING | 4 |
| 1.4 | RIVER ROUTING MODELS | 4 |
| 1.4.1. | Hydrological routing model | 4 |
| 1.4.2 | Hydraulic routing models | 6 |
| 1.5 | PROBLEM IDENTIFICATION | 7 |
| 1.6 | MOTIVATION OF THE STYDY | 8 |
| | CHAPTER 2: LITERATURE REVIEW | 11-38 |
| 2.1 | GENERAL | 11 |
| 2.2 | HYDRODYNAMIC ROUTING MODELS | 11 |
| 2.2.1. | Effect of bed and side of channel roughness on flow | 12 |
| 2.2.2. | Hydraulic flood routing analysis | 20 |
| 2.2.3. | The sensitivity of hydraulic parameter | 29 |
| 2.3 | SUMMARY OF LITERATURE REVIEW | 37 |
| 2.4 | RESEARCH GAPS | 37 |
| 2.5 | OBJECTIVES | 38 |

| | | |
|--------|---|--------------|
| | CHAPTER 3: METHODOLOGY | 39-50 |
| 3.1 | GENERAL | 39 |
| 3.2 | DESCRIPTION OF THE HYDRAULIC MODEL | 40 |
| 3.2.1. | Numerical modeling using HEC-RAS | 40 |
| 3.3 | UNSTEADY FLOW ROUTING USING HEC-RAS | 41 |
| 3.3.1 | Governing equations of HEC-RAS | 41 |
| 3.3.2 | Solution methodology for Saint Venant equation in HEC-RAS | 42 |
| 3.4 | WATER SURFACE PROFILES | 45 |
| 3.4.1. | Cross section subdivision for Conveyance | 46 |
| 3.4.2. | Friction loss | 46 |
| 3.4.3. | Contraction and Expansion Loss | 47 |
| 3.5 | SENSITIVITY ANALYSIS | 47 |
| 3.5.1. | Parameter Perturbation Method | 47 |
| 3.6 | STATISTICAL PARAMETERS TO VALIDATE THE MODEL PERFORMANCE | 48 |
| | CHAPTER 4: STUDY AREA AND MODEL DEVELOPMENT | 51-68 |
| 4.1 | STUDY AREA | 51 |
| 4.1.1. | Rainfall Pattern | 52 |
| 4.1.2. | Climatology | 53 |
| 4.1.3. | Population and Cities | 53 |
| 4.1.4. | Geology and Soils | 53 |
| 4.1.5 | River drainage features | 54 |
| 4.1.6 | River geomorphology | 54 |
| 4.1.7 | Challenges faced by Nethravathi River | 55 |
| 4.2 | DATA COLLECTION | 55 |
| 4.3 | MODEL DEVELOPMENT AND DISCRETIZATION | 56 |
| 4.3.1 | Geometric data | 56 |
| 4.3.2. | Boundary conditions | 60 |
| 4.4 | STEPS IN BUILDING A HEC-RAS MODEL | 63 |

| | | |
|----------|--|----------------|
| 4.5 | MODEL CALIBRATION AND VALIDATION | 68 |
| | CHAPTER 5: RESULTS AND DISCUSSION | 69-116 |
| 5.1 | GENERAL | 69 |
| 5.2 | SIMULATION FOR UNSTEADY FLOW CHARACTERISTICS | 69 |
| 5.2.1 | Model Calibration | 70 |
| 5.2.2. | Model validation | 76 |
| 5.3 | EFFECT OF ROUGHNESS COEFFICIENT IN NATURAL RIVER | 80 |
| 5.3.1. | Impact of Manning's n on river stage | 80 |
| 5.3.2. | Impact of Manning's n on river stage-discharge rating curve | 83 |
| 5.4 | HYDRAULIC FLOOD ROUTING | 86 |
| 5.4.1. | Model calibration and validation for flood analysis | 87 |
| 5.4.1.1 | Model Calibration for the year 2007 | 87 |
| 5.4.1.2. | Model Calibration for the year 2008 | 91 |
| 5.4.1.3. | Model Calibration for the year 2009 | 94 |
| 5.4.1.4 | Model Calibration for the year 2010 | 97 |
| 5.4.2. | Unsteady flow analysis in Nethravathi river | 99 |
| 5.4.2.1. | Flood Simulation for the year 2007 | 100 |
| 5.4.2.2 | Flood Simulation for the year 2008 | 102 |
| 5.4.2.3 | Flood Simulation for the year 2009 | 104 |
| 5.4.2.4 | Flood Simulation for the year 2010 | 106 |
| 5.4.3. | Flood inundation mapping for flood event of 2008 | 108 |
| 5.5 | SENSITIVITY ANALYSIS | 110 |
| 5.5.1. | Sensitivity analysis for time step | 110 |
| 5.5.2. | Sensitivity analysis for weighting factor (Theta) | 111 |
| 5.5.3. | Sensitivity analysis for normal depth | 112 |
| 5.5.4. | Sensitivity analysis for cross-section spacing (Δx) | 113 |
| 5.5.5. | Sensitivity analysis for Manning's roughness | 114 |
| | CHAPTER 6: SUMMARY AND CONCLUSIONS | 117-120 |
| 6.1 | SUMMARY | 117 |

| | | |
|-----|-----------------------------|----------------|
| 6.2 | CONCLUSIONS | 118 |
| 6.3 | CONTRIBUTIONS | 119 |
| 6.4 | LIMITATIONS OF THE STUDY | 119 |
| 6.5 | SCOPE FOR FUTURE RESEARCH | 120 |
| | REFERENCES | 121-134 |
| | LIST OF PUBLICATIONS | 135 |

LIST OF FIGURES

| Figure No. | Figure Caption | Page No. |
|-------------------|---|-----------------|
| 3.1 | Flowchart of methodology | 39 |
| 3.2 | Typical finite difference cell | 42 |
| 3.3 | Representation of terms in the Energy Equation (Brunner 2016) | 45 |
| 3.4 | HEC-RAS Default Conveyance Subdivision Method (Brunner 2016) | 46 |
| 4.1 | Geographic location of the Nethravathi basin | 51 |
| 4.2 | Rainfall pattern of Nethravathi basin | 52 |
| 4.3 | Schematic of Nethravathi River | 57 |
| 4.4 | The cross-sections of the river reach (a) Kumardhara (b) Uppanangadi and (c) Bantwal. | 58 |
| 4.5 | Bed material near Sarve bridge in Kumaradhara river reach | 58 |
| 4.6 | Bed material near Uppinangadi bridge in Nethravathi river reach | 59 |
| 4.7 | Bed material near Bantwal in Nethravathi river reach | 59 |
| 4.8 | Flow hydrograph Sarve bridge gauging station for the period 2007 to 2010 | 61 |
| 4.9 | Flow hydrograph of Uppinangadi gauging station for the period 2007 to 2010 | 62 |
| 4.10 | Flow hydrograph of Bantwal gauging station for the period 2007 to 2010 | 62 |
| 4.11 | Geometric data | 63 |
| 4.12 | Unsteady flow data | 64 |
| 4.13 | Unsteady Flow Calculation | 65 |
| 4.14 | Results in cross sectional profile | 65 |
| 4.15 | Results in longitudinal sectional profile | 66 |

| | | |
|------|--|----|
| 4.16 | Results in terms of rating curve | 66 |
| 4.17 | Cross sectional output | 67 |
| 4.18 | Inundation mapping as flow depth, velocity and inundated area | 67 |
| 5.1 | Observed vs computed discharge hydrograph for calibration period (2007) | 70 |
| 5.2 | Scatter plot of discharge for the calibration year 2007 | 71 |
| 5.3 | Observed vs computed stage hydrograph for calibration period (2007) | 71 |
| 5.4 | Scatter plot of stage for the calibration year 2007 | 72 |
| 5.5 | Observed vs computed discharge hydrograph for calibration period (2008) | 73 |
| 5.6 | Scatter plot of discharge for the calibration year 2008 | 74 |
| 5.7 | Observed vs computed stage hydrograph for calibration period (2008) | 74 |
| 5.8 | Scatter plot of stage for the calibration year 2008 | 75 |
| 5.9 | Observed vs computed discharge hydrograph for validation period (2009) | 77 |
| 5.10 | Scatter plot of discharge for validation period (2009) | 77 |
| 5.11 | Observed and estimated discharge and stage hydrograph at Bantwal station of validation period (2009) | 78 |
| 5.12 | Scatter plot of the observed and estimated stage for validation period (2009) | 79 |
| 5.13 | Stage hydrograph for different Manning's n values for the year 2007 | 81 |
| 5.14 | Stage hydrograph for different Manning's n values for the year 2008 | 81 |
| 5.15 | Stage hydrograph for different Manning's n values for the year 2009 | 82 |
| 5.16 | Stage-discharge rating curve for different Manning's n for the year 2007 | 83 |

| | | |
|------|--|-----|
| 5.17 | Stage-discharge rating curve for different Manning's n for the year 2008 | 84 |
| 5.18 | Stage-discharge rating curve for different Manning's n for the year 2009 | 85 |
| 5.19 | Cross-section layout of Nethravathi river system | 86 |
| 5.20 | Longitudinal section of water surface elevation (maximum) | 87 |
| 5.21 | Observed and estimated discharge and stage hydrograph for calibration period of 2007 (mixed regime) | 88 |
| 5.22 | Scatter plot of the observed and simulated discharge and stage values during calibration period of 2007(mixed regime) | 90 |
| 5.23 | Observed and estimated discharge and stage hydrograph for calibration period of 2008 (mixed regime) | 91 |
| 5.24 | Scatter plot of the observed and simulated discharge and stage values during the calibration period of 2008 (mixed regime) | 93 |
| 5.25 | Observed and estimated discharge and stage hydrograph for calibration period of 2009 (mixed regime) | 94 |
| 5.26 | Scatter plot of the observed and simulated discharge and stage values during the calibration period of 2009 (mixed regime) | 96 |
| 5.27 | Observed and estimated discharge and stage hydrograph for validation period of 2010 (mixed regime) | 97 |
| 5.28 | Scatter plot of the observed and estimated discharge and stage for validation period 2010 (mixed regime) | 99 |
| 5.29 | Water depth in river channel and floodplain in the year 2007 | 101 |
| 5.30 | Flow velocity in river channel and floodplain in the year 2007 | 101 |
| 5.31 | Water surface elevation along the river reach in the year 2007 | 102 |
| 5.32 | Water depth in river channel and floodplain in the year 2008 | 102 |

| | | |
|------|--|-----|
| 5.33 | Flow velocity in river channel and floodplain in the year 2008 | 103 |
| 5.34 | Water surface elevation along the river reach in the year 2008 | 104 |
| 5.35 | Water depth in river channel and floodplain in the year 2009 | 105 |
| 5.36 | Flow velocity in river channel and floodplain in the year 2009 | 105 |
| 5.37 | Water surface elevation along the river reach in the year 2009 | 106 |
| 5.38 | Water depth in river channel and floodplain in the year 2010 | 107 |
| 5.39 | Flow velocity in river channel and floodplain in the year 2010 | 107 |
| 5.40 | Water surface elevation along the river reach in the year 2010 | 108 |
| 5.41 | Flood inundation map of the Nethravathi river basin | 109 |
| 5.42 | Sensitivity of time step on stage and discharge at downstream gauging station. | 111 |
| 5.43 | Sensitivity of Normal depth on stage at downstream gauging station. | 113 |
| 5.44 | Sensitivity of Manning's n on stage and discharge at downstream gauging station. | 115 |

LIST OF TABLES

| Table No. | Table Caption | Page No. |
|------------------|--|-----------------|
| 4.1 | List of datasets and sources | 55 |
| 4.2 | Considered Manning's values for the study | 57 |
| 5.1 | Model evaluation criteria for calibration period | 76 |
| 5.2 | Model evaluation criteria for validation period | 79 |
| 5.3 | Model Performance | 98 |
| 5.4 | Model output result at downstream gauging station. | 100 |
| 5.5 | sensitivity results obtained at the downstream gauging station | 113 |

NOMENCLATURE

| | |
|----------|---------------------------------------|
| A | Flow Area (m^2) |
| <i>a</i> | Velocity weighting coefficients |
| B | Top width of the channel |
| C | Contraction or expansion coefficients |
| <i>d</i> | Index of agreement |
| D_h | Hydraulic Depth |
| <i>g</i> | Acceleration due to gravity |
| h_{ce} | Contraction or expansion head loss |
| h_e | Energy head loss |
| K | Conveyance of subdivision |
| <i>n</i> | Manning's roughness coefficient |
| Q | Discharge (m^3/s) |
| R | Hydraulic radius |
| S_f | Slope of energy grade line |
| S_b | Channel bottom slope |
| <i>t</i> | Time |
| V | Flow velocity (m/s) |
| <i>x</i> | Distance along the channel length |
| <i>y</i> | Flow depth (m) |

ABBREVIATIONS

| | |
|---------|---|
| 1-D | One-Dimensional |
| 2-D | Two-Dimensional |
| CGWB | Central Ground Water Board |
| CWC | Central Water Commission |
| DEM | Digital Elevation Model |
| GIS | Geographic Information System |
| GOI | Government Of India |
| GSI | Geological Survey Of India |
| HEC-RAS | Hydrologic Engineering Center's - River Analysis System |
| KPWD | Karnataka Public Works Department |
| MAE | Mean Absolute Error |
| MSL | Mean Sea Level |
| NRMSE | Normalized the Root Mean Square Error |
| NSE | Nash-Sutcliffe efficiency |
| RMSE | Root Mean Square Error |
| SOI | Survey Of India |
| SRTM | Shuttle Radar Topography Mission |
| SRTM | Shuttle Radar Topography Mission |
| TIN | Triangulated Irregular Network |
| USGS | United States Geological Survey |
| WSE | Water surface elevation |

CHAPTER 1

INTRODUCTION

1.1. GENERAL

Rivers are the veins of nature which are one of the world's most valuable natural resources and are important to the livelihood in many ways. They are significant in light of the fact that they transport water, provide habitat, support financial exercises and empower transportation. Rivers provide life-continuing supplies of water and significant supplements for living beings around the globe. The essential component of the water cycle structure is served by rivers as drainage channels of surface water. Rivers also perform roles in improving conditions such as flash floods by absorbing excess water. (Ezz 2018).

Civilizations have often flourished beside rivers. This permitted simple access to drinking water, transportation courses and ample nourishment. However, streams flood every once in a while and cause boundless harm, obliteration and death toll. Individuals from isolated cultures still live close to streams, and they draw the vast majority of their resources from the waters. Due to the construction of the dam for storage purposes the dependent communities in the upstream faced issues such as flood inundation, disconnection with mainland etc. during peak inflow. In addition, unexpected precipitation in combination with dam failures in the catchment caused water flow in a river to increase, resulting in floods. (Knebl et al., 2005).

Flooding is the common and most destructive kind of natural disaster, and due to global climate change in recent decades, there has been a substantial increase in the number of recorded floods 7.4% on an average per year. In addition, the rivers have one of the main sources of conflict throughout the world with inadequate sources of water (Cunge and Erlich 1999). The motivation for the study was to understand the meteorological, hydrodynamic and hydrological processes related to flooding in rivers.

1.2. FLOW CHARACTERISTICS AND CLASSIFICATION

In the hydraulic study, flow is differentiated as open channel flow and pipe flow. The stream with a free surface open to the air is called open channel or river. The flow in closed conduit which flows with pressure is defined as pipe flow (Subramanya, 2008).

The river stage and discharge are dynamic due to various factors affecting the flow characteristics in a natural channel.

Steady flow is mentioned as the flow where the depth of water and velocity will not vary regarding the time at a point. Unsteady flow depends on the variation of flow parameters in which stage, velocity, and discharge change with time (Chaudhry 1993). In the channel, a flow might be unfluctuating, however it might be either uniform or non-uniform flow contingent on the flow depth and velocity change by space in consecutive cross-section of the channel. Uniform flow occurs merely when the cross-section is continuous along the waterway. It may only happen in that prismatic channel where cross-section, roughness, and slope in the flow path are constant. Nevertheless, the flow in regular channel or river of inconsistent cross-section called as non-uniform flow. Here the depth and velocity vary in the flow direction.

Subjecting upon the degree of dissimilarity with regard to distance, flows may be categorized as gradually varied flow or rapidly varied flow. The flow depth fluctuates progressively over a long distance in gradually varied flows and in a short distance in rapidly varied flows. These losses may be ignored in the analysis of swiftly varied flows since the distances involved are small (Chaudhry, 1993). In open channel flow, non-uniform flow occurs for its variable properties (Chow, 1959).

1.2.1 Flow in natural channels

The flow appears to be a very complicated phenomenon in case of natural channels such as rivers, due to unsteady and non-uniform flow (Chaturvedi 2000; Li et al., 2004; Matori et al., 2008). The continuous accumulation of unsteady flow at the cross-section of the river may result in flooding due to saturated bed condition and bank storage. The

dynamics of rainfall intensity, modifications of channel geometry, reservoir and sluice operation are significant factors for unsteady flow in a river (Puente et al., 2013).

The various factors affect the flow characteristics in a natural channel in the river stage and discharge which are dynamic in nature. In river and streams, roughness coefficient, flow velocity, river bed materials, bed slope, flow path varies from place to place along with the cross-section of flow. Inundation of low lying areas and flooding are noteworthy variations in the hydraulic characteristics of river flow which is being influenced by erosion and sedimentation of river bed particles across the cross-section of flow.

In open channels, the channel roughness plays a vital role among other hydraulic parameters of the flow. Variations in riverbed morphology affect the rise in depth of flow in rivers. It is dependent upon factors such as river morphology, vegetation cover, meandering and surface roughness. The seasonal fluctuations in river stage and discharge characterize the channel roughness based on fluvial erosion and deposition (Moharana and Khatua 2014).

1.2.2 Methods of flow measurement

Measurements of different hydrodynamic flow properties (e.g. boundary shear stress, discharge, depth and velocity) are often needed to regulate and make effective use of rivers and open channels. These measurements, as usual, accomplished by two methods:

- 1). Direct method - By using measuring devices to measure the characteristics of the fluid with an instrument.
- 2). Indirect method - For indirect measurements, the behaviour and properties of the flow can be predicted by means of numerical models.

Aside from their significant expense, the utilization of measurement instruments in open channels and rivers isn't constantly helpful and in some cases, isn't even possible (for example during flood occasions). In this respect, stable, accurate and reliable models are taken into consideration. Such models are a set of general laws or

mathematical principles and a sequence of assumptions of empirical parameters (Hempel 1963). It represents the properties of the flow, from simple, empirical models (e.g. the Mannings model) to complex models that rely on the numerical solution of the control equations of the turbulent flow's unpredictable motion over the previous decades. The emphasis was placed on improving simple models that rely on the Saint-Venant (1871) one-dimensional flow equations. The main focus of these studies was on simple channel geometries, typically trapezoidal and rectangular cross-areas because these geometries are easy to build and test in the research laboratory. In addition, the findings can be applied to natural rivers, frequently identified by these geometries. The findings of these research studies usually showed that the execution of these simple models is as reliable as complex models.

1.3 FLOOD ROUTING

Flood routing is a prediction of amount and velocity of flood wave at any point in the river channel with respect to time. Channel geometry and morphological characteristics determine the direction of flood waves (Reddy 2005). The other significant purpose is to provide safe designs to protect from floods, to predict whether a flood owns a risk to health and safety, to deliver information about the current quantity of water and the physical characteristics of the region so that satisfactory protection and economic solutions can be provided immediately.

1.4 RIVER ROUTING MODELS

The river routing model consists of two classes namely hydrological routing and hydraulic routing (Arora et al., 2001). Flood routing via distributed system technique is termed as hydraulic routing while hydrologic routing is routing by a lumped system method (Maidment, 1993).

1.4.1 Hydrological routing model

In general, Hydrologic routing is dependent on the conservation of mass and an estimate of the relationship between flow and storage. This directly permits to calculate the outflow hydrograph at the downstream end of the reach (Sanjay et al., 2012). Tools like

hydrological routing models, generally based on linear/non-linear reservoirs, are often used for discharge routing at the regional scale. Usually, it consists of five hydrologic routing methods they are Muskingum-Cunge Routing methods, Lag Routing, Kinematic Wave Routing, Muskingum Routing and Modified Puls Routing. The Muskingum method is one of the most common hydrological routing approaches to predict the flood wave (McCarthy 1938; Nash 1978; Cunge 1969).

The disadvantages of hydrological routing models are the backwater effects during simulation are minimal due to lack of detailed information on a large scale, while changes in river morphology are also neglected at a smaller level. Moreover, the acceleration terms in the hydrological models are negligible with respect to other terms in the equation. The acceleration terms are relatively small for slow-rising flood waves on moderate gradient streams, however this assumption is not applicable for fast rising hydrographs such as those from breaching dam, where the acceleration terms are relatively large (Mockus 1964). In such situation hydraulic routing model can be adopted.

The most of the hydrological models assume either a constant and uniform velocity at a regional scale. This is because it ignores the importance of streamflow on the stage of the river, so it will not be simulated, while it is important for many water resources analysis such as floodplain management, stream-aquifer interactions, average river velocity, flood control operations and overtopping frequency. The variable velocity flow routing algorithms are notable exceptions in large scale, but they describe the river network with its very coarse spatial resolution (Arora and Boer 1999; Schulze et al. 2005).

Hydrological models are simpler compared to hydraulic models. However, they have some limitations of requirements of observed inflow and outflow hydrographs from a reach to determine the routing coefficients. In addition, back-water effects from tides, significant tributary inflow, dams or bridges are not considered in hydrological models.

1.4.2 Hydraulic routing models

Hydraulic routing is based on the conservation of mass and a simplified form of Saint-Venant conservation of momentum equation. The Saint-Venant equations consist of mass and momentum conservation, and it describes the gradually varied and transient flow, in a channel with irregular cross-sections. The hydraulic routing requires the computation of the discharges along the river at every intermediate point, besides the cross-sections in these intermediate points, the hydraulic parameters like roughness coefficient are required for every time step.

Saint-Venant equations are an efficient technique for the simulation of dynamic flow characteristic in a river based on channel geometry and morphology. In hydraulic routing models, the inflow hydrograph at the upstream and downstream of the observed reach is required (Sanjay et al., 2012). This consist of the continuity equation, which defines the balance among input, storage, and output in a section of the river, and a momentum equation, that relay on the change in momentum to the applied forces.

The complete derivation of the basic Saint-Venant equations was noted from past researches (Chow 1959; Cunge et al., 1980; Graff and Altinakar 1996; Strelkoff 1970). As these equations remain valid when downstream backwater effects as they fit to simulate the downstream propagation of kinematic and diffusive waves. The river-reach calibration includes fitting the Manning's roughness coefficients along the river in both main streams and in flood plains. One of the major challenges of hydrodynamic routing models is the lack of accurate data for large-scale applications, which fully reflect spatial variations in channel geometry (e.g. channel form, slope, and length), as it is difficult and very costly to measure on a large scale (Saleh et al., 2013).

Due to both natural processes and human effects, differences in cross-section and bed slopes occur over a wide range of spatial scales (Leopold et al., 1964). The scope of hydraulic routing ranges from for any situation with a rapidly changing water depth such as shallow sloped streambeds, tidal-influenced streams, flash floods, including dam breaks, the benefits of hydraulic routing are higher accuracy for calculated water depths and better representation of various special flow conditions.

The significant advantage of hydraulic routing is the accurate representation of river stage and discharge due to consideration of boundary conditions for river reaches in the study area. The sophisticated approach allows the application of hydraulic routing even for the ungauged and inaccessible portions of the study area with sustainable importance. The hydraulic model accompanied with the data pertaining to any historical flood occurrence is able to estimate and predict the flood discharge and levels for future unforeseen events. With better resolution Digital Elevation Model datasets, the simulated Flood routing model provides accurate flood inundation maps for emergency response and management.

The comprehension and accurate prediction of river flow by hydraulic modelling is essential for flood management. 1D Saint-Venant equations are commonly used in hydraulic modeling such as unsteady flow, discharge routing (Serrano 2016), flood prediction (Alekseevskii et al., 2014), and surface and subsurface runoff (Hughes et al., 2015).

1.5 PROBLEM IDENTIFICATION

River systems need improved hydraulic models in order to better simulate river conditions at different points in time. In natural channels such as river and streams, hydraulic characteristics such as flow velocity, direction, bed slope and material changes from place to place. Consequently, a serious modification of the parameters in the river regime may lead to intense circumstances in river flow. Flooding is one of the extreme conditions in the flow characteristics of a river. Channel roughness co-efficient is a critical factor that is dynamic in nature influencing the flow characteristics of a river. The variation of roughness co-efficient based on the riverbed material and morphology affects the fluvial erosion and deposition altering the channel geometry. However, the parameter has been consistently considered as a constant value for the simulation in the numerical models. However, various experimental studies and analytical models have revealed roughness co-efficient to be one of the sensitive parameters (Boulomytis et al., 2017; Kuta et al., 2010; Barati et al., 2012; Vojtek et al., 2019). Various models were developed for the study to analyze the influences of the bed morphology (Roughness coefficient, the shape of the channel, channel slope) on

discharge and water level at various location in the river. It is also proved to be good means to assess the impacts for its capability to do the sensitivity analysis and to predict flood flow and associated inundated area.

In natural channel, unsteady flow occurs due to the changes in discharge and depths. Also, unsteady flow in a natural channel like a river is a very complicated phenomenon to predict and understand. A simple numerical model utilized in the present study can help the researchers to comprehend the flow behaviour and identify the associated flow characteristics. The study highlights the significance of hydro-geological heterogeneity in a catchment and encourages the possibility to incorporate complex hydraulic properties in a numerical model. The flood inundation map was intended to be one of the main basis to formulate appropriate flood management plan to assist the Authorities in handling any possible flood events in the future. The flood inundation map developed for the Nethravathi River basin would help in the assessment and management of flood risk.

The aim of the present study is to simulate unsteady flow analysis using a hydraulic model for Nethravathi River basin in India for identifying the impact of variability in roughness co-efficient on the river-stage and discharge, intend to assess the hydraulic response of the river using flood-routing analysis and to study the sensitivity of geometric and computational parameters on model results and stability.

1.6 MOTIVATION OF THE STUDY

For the purpose of progressive development of watershed, thorough understanding of the river characteristics is essential. Factors such as geomorphology, geometry, morphometry affect the hydraulic response of the river in a basin. However, the natural flow of river in the basin is subjected to various kinds of flow such as steady, unsteady flow, etc. In the past, flood routing has been an exercise of predicting the impact of steady flow characteristics in a river basin. Less attempt has been made to study the impact of simple yet critical parameter such as surface roughness of the natural channel on the unsteady flow behaviour of river.

Commonly, the Manning's roughness co-efficient (n) have always been treated as constant parameter for a channel in a basin. In contrast, Manning's roughness co-efficient varies for river cross-section from origin to different phases of river flow until it reaches the ocean/sea. The hydraulic properties such as river flow depth and velocity are dynamic due to the varying landscapes of river flow as discussed above.

The motivation for the present study has been the negligence of the consideration of the variation in channel roughness under unsteady flow condition in the hydraulic models. Till now the variation in channel geometry has been the considerate for flood routing under steady flow conditions. The study area Nethravathi basin origins at Western Ghats of Karnataka and flow down with a steep gradient along the rocky boulders of the valley. With accumulated flow velocity Nethravathi river reaches the wide coarse of gravel bed after the descend from the hills. The flow characteristics of the Nethravathi river makes it unique and significant feature for the present study based on the geographical virtue. An effort is made in the present study to evaluate/calculate the hydraulic response of Nethravathi river at different cross-section of its flow after the descend from the hills expanding into the wide floodplain. This study helps in understanding the flow for various roughness coefficient of the bed material. This study also focuses on selecting sensitive parameter for flow analysis.

CHAPTER 2

LITERATURE REVIEW

2.1. GENERAL

In the present study, the literature review is carried out to establish the background study undertaken in the present research. The articles published based on the analytical, numerical models and experimental studies of open channel flow are considered. Many researchers have attempted to find better methods for solving the complex case of unsteady flow. The flood routing analysis using HEC-RAS is discussed in this section with emphasis on sensitivity analysis and effect of roughness co-efficient.

2.2. HYDRODYNAMIC ROUTING MODELS

In the past researchers have utilized different numerical methods to solve hydraulic equations in flood routing analysis. However, these methods appear to be complex in the case of unsteady flow. Among them, few cases are easy to understand and predict the flood wave by using simulation process. In computational fluid dynamics, hydraulic flood routing problem can be solved by the dynamic wave equation. Saint-Venant (1871) proposed a 1-dimensional equation of motion, termed as dynamic wave equation for the simulation of unsteady, non-uniform flow. At present, flood routing subjected to dynamic change in the hydrological/hydraulic parameters involved is a challenging area for research.

The flow parameters evaluated by using momentum equation are dimensionless (Woolhiser and Liggett 1967). Flood routing problem was addressed by using Preissman four-point implicit finite-difference scheme for channel and floodplains (Rashid and Chaudhry 1995). Methods to study the characteristics of flow were applied for solving the 1-D shallow water equation, which is mostly used in the explicit method (Elhanty and Copeland 2007).

Flood hydraulic routing models is appropriate, to assess the effect of channel irregularities, change in cross-sectional geometry, bed slope and roughness (Graff and Altinakar 1996).

Flood inundation maps and risk zonation maps are important to reduce the damages incurred by the flood along the river channel. Structural and nonstructural methods are requisite for planning and management of floodplain areas and optimizing the land usage policies to reduce flood risk. Numerical modeling is an efficient and cost-effective technique for the simulation of dynamic behaviour of river discharge during flood situations. (ShahiriParsa et al., 2016).

2.2.1. Effect of bed and side of channel roughness on flow

The roughness coefficient varies along the river channel based on flow characteristics. Hence, estimation of discharge and depth of flow is essential depending upon the roughness coefficient, surface condition and channel geometry (Moharana and Khatua 2014).

Jia and Wang (1999) The 2-Dimensional hydrodynamic, sediment transport model, Center for Computational Hydroscience and Engineering-2 dimensional (CCHE2D) was developed with the integration of channel-depth. Channel morphological changes were calculated by considering the secondary flow and the effects of bed slope in curved channels. Physical model data was validated by simulating with morphological development of meandering streams with instream structuring, which yielded satisfactory results. Feasibility studies were carried out in order to demonstrate their applicability for hydraulic engineering and design studies on stream stabilization and ecological efficiency.

Ramesh et al. (2000) applied the optimization model to estimate roughness coefficient in open-channel flow. Measured data of flow depths and discharges at different locations and times were used as input data to the model. The Sequential Quadratic Programming Algorithm was used to solve the optimization model. The study explored the potential to apply the proposed technique for estimating the roughness coefficient in open channels.

Ding et al. (2004) developed a numerical model based on shallow water equation for identifying Manning's roughness coefficients. The methodology was applied to determine the optimal values of the spatially distributed parameters, which gave the least overall discrepancies between simulations and measurements. Series of systematic studies were carried out to identify the roughness coefficient in both hypothetical open channel and natural stream. It was found that the limited-memory quasi-Newton method has the advantages of a higher rate of convergence, numerical stability and computational efficiency. Although the identification of Manning's n was chosen as an example, the identification methods can be applied to numerical simulations of various flow problems.

Chagas (2005) developed a hydrodynamic model capable to realize simulations to analyze the behaviour of the depth of water when a flood wave comes into the channel as functions of time. This model was developed to verify the reach of the depth of the channel under the influence of a dynamic wave, for different bed slope and roughness coefficient. The results showed that the hydraulic parameters play an important role in the propagation of a flood wave.

Zarrati et al. (2005) developed a depth-averaged model for predicting water surface profiles for meandering channels and applied it to three meandering channels (two simple and one compound) data. The model was found well enough to predict the water surface profile and velocity distribution for simple channels, and the main channel of the compound meandering channel.

Knight et al. (2007) proposed a depth-averaged flow equation for the forces acting on the natural water body with Newton's second law as part of the secondary flow rectangular compound path. In addition to bed friction, the research method was considered for the transverse variance of the depth-averaged velocity involving the effect of lateral momentum and secondary flow exchange. This research also introduced a distinct type of internal wall boundary conditions between the rectangular main channel and the associated floodplain.

Bong and Mah (2008) carried out an experimental study on a small-scale irregular compound channel with rough floodplain and validated for prediction of discharge of various numerical methods for the prediction of discharge. Weighted channel method was used to check the validity of the horizontal division method and the vertical division method for predicting the discharge. For wider floodplain in the non-symmetrical compound channel, the horizontal division method gave an accurate prediction of discharge. Whereas in narrower floodplains, vertical division method verified to be more accurate.

Zarrati et al. (2008) determined semi-analytical equations for the distribution of shear stress in straight open channels with rectangular, trapezoidal, and compound cross-sectional areas. These equations based on improved stream-wise vorticity condition that incorporated secondary Reynolds stress. Reynolds stresses were demonstrated and their distinctive terms were assessed based on experimental data conducted by different researchers. Substitution of these terms into the rearranged vorticity equation yielded the relative shear stress distribution equation along the lateral cross-sections of various channels.

Bao and Zhao (2011) simulated a flood prediction model for the channel flow in plain rivers based on dynamic wave theory. Roughness updating technique was developed using the Kalman filter method to update Manning's roughness coefficient at each time step. Channel shapes as rectangles, triangles, and parabolas was simplified and the relationships between hydraulic radius and water depths for plain rivers were established. To check the performance and rationality of the developed flood routing model, the original hydraulic model was compared to the model developed for the Huaihe channel from Wangjiaba to Lutaizi stations. Results showed good agreement with the observed stage hydrographs of the stage hydrographs determined by means of an advanced flood routing model with a modified Manning roughness coefficient.

Rezaei and Knight (2011) studied the composite channel non-prismatic floodplain with various converging angles in overbank flow condition. Estimation of local velocity distributions, boundary shear stress distributions and depth-averaged velocity at a different relative depth of flow were conducted along the converging flume portion.

Forces were analyzed using the momentum balance method to act on the fluid in the main channel and for the entire cross-section. It has been estimated and compared with the prismatic cases apparent shear forces on the vertical interface between the main channel and flood plain for the compound channel with a non-prismatic flood plain.

Khatua et al. (2012) presented a modified equation for the measurement of compound channel boundary shear stress. The concept of momentum transfer was considered to derive the method of one dimensional approach for analyzing the relation between stage and discharge. The natural channels validated by the proposed method obtained satisfactory results.

Hameed and ali (2013) applied HEC-RAS unsteady flow model to Hilla river (upstream Hilla city) to predict the value of Manning's coefficient through the calibration procedure. The data were taken for the period from 20 August 2008 to 12 September 2008 and divided equally into two sets; the first set is for calibration purpose; i.e., estimation of (n) and the rest for verification which is the process of testing the model with actual data to establish its predictive accuracy. It was found that the value of Manning's roughness coefficient (n) for Hilla river which showed good agreement between observed and computed hydrographs is (0.027).

Parhi (2013) attempted to calibrate and validate the model using Manning's roughness value in the Mahanadi River in Odisha (India). The floods for the years 2001 and 2003 have been considered for calibration of Manning's "n" value. The calibrated model was simulated for the flood prediction in the year 2006. Nash and Sutcliffe efficiency test was used to check the performance of the HEC-RAS model. The study results concluded that the optimum Manning's "n" value for Khairmal to Barmul reach of Mahanadi River is 0.029. It is shown also, that only 5.43% of the observed flood data of 2006 showed an error for peak flood discharge and time to reach peak values, measured using Manning's n 0.029.

Saleh et al. (2013) studied the impact of bed morphology (Roughness coefficient, the shape of the channel, channel slope) on discharge and water level by using the hydraulic model at a regional scale in various geometry scenario. Lateral inflows were taken by

hydrological model and river morphology. For calibration of observed discharges and stages, high-resolution cross-sections were used. In certain geometrical scenarios, the hydraulic model prediction wasn't satisfactory. The accuracy of predicted water level and maximum water depth simulated by Hydraulic model depended on the accurate representation of channel geometry and bed slopes. Varied scenarios indicated, as compared to the cross-sectional shape of the channel, that longitudinal of the bed level profile to have more effect on the simulation of the water level.

Abu-Aly et al. (2014) developed two-dimensional hydrodynamic model U.S. Bureau of Reclamation finite-volume code, SRH-2D for 28.3 km of a gravel and cobble-bed river reach, with and without spatially distributed vegetation roughness and flows ranging from 0.2 to 20 times bank full discharge. Study was analyzed to gain insight into the scale-dependent and stage-dependent effects of vegetation on depths, velocities and flow patterns. Both stage- and scale-dependent is the magnitude of the sensitivity of model effects. When compared to the constant roughness model, the mean depth velocity reduced by 0.6 m/s (30%) and the mean water depth was increased to 0.8 m (25%) with an overall maximum discharge of 3126.18 m³/s. The flux was affected by vegetation, which increases the difference between the middle and the bank velocities. It also diverted from heavily vegetated areas flowing downstream. The river discharge increases, overall roughness increases.

Al Faruque et al. (2014) carried out experimental study on the effect of bed-roughness coefficient and Reynolds number at outer and inner surface for mean velocity condition. The permeable, impermeable, smooth, rough, sand bed and distributed bed roughness values and two different Reynolds number ($R_e = 47,500$ and 31,000) were studied. However, the results failed to agree with that of different Reynolds number and for all different bed surfaces for mean velocity condition. Consequently, the maximum velocity for all flow conditions was observed to be matching w.r.t. the free surface extent. The maximum velocity condition appeared to be dependent on both roughness coefficient and Reynolds number.

Moharana and Khatua (2014) applied soft computing techniques to predict the roughness coefficient for meandering open channel flow. An experimental

investigation was carried out by varying roughness coefficient with flow depth, aspect-ratio and slope. From the result, it was concluded that the adaptive neuro fuzzy inference system (ANFIS) model was appropriate and effective method to predict the nonlinear relationship between the roughness coefficient and the non-dimensional factors affecting it.

Pal and Ghoshal (2014) investigated the influence of bed roughness, flow velocity and suspension height in a laboratory flume. The grain-size distribution in suspension over five sediment beds having different values of bed roughness at three different flow velocities were considered.

Al Faruque and Balachandar (2015) studied the effect of roughness coefficient on the stream-wise turbulence intensity throughout the flow depth. The distributed roughness was observed to have the greatest effect followed by the sand bed and the continuous bed roughness. Compared to the smooth bed, the stream-wise turbulence intensity observed to be reduced but the vertical turbulence intensity increased near the bed location due to the continuous bed roughness.

Keupers et al. (2015) developed two hydrodynamic models to investigate the time-varying river bed roughness due to plant growth. The models were applied to the Grote Nete river catchment in Belgium. The simulated model yielded accurate river water-levels and discharge values by considering the vegetation in the bed roughness. The increase in the accuracy of simulations of water levels balanced the increase in model complexity.

Awad (2016) developed an HEC-RAS model to choose suitable Manning coefficient for calculating water surface profiles. For Al-Rumaith River, a steady flow HEC-RAS model is utilized to predict the value of the Manning coefficient through calibration. The flows for the year 2014 was considered for calibrating the model. The results found a good agreement between the computed and observed surface water profiles when considered the value of Manning's roughness coefficient $n=0.023$ and $n=0.04$ for main channel and floodplain.

Mitra and Saikia (2016) carried out open channel experimental study for three-bed materials, the original bed surface of the channel, PVC and grass carpet. Roughness coefficients Manning's "n" and Darcy's "f" were determined for constant slope and three different discharges. Hydraulic parameters such as depth, velocity and Froude's no. were also compared. The original bed surface with a combination of different material resulted in fluctuation of Manning's "n" whereas very uniform for grass carpet and PVC bed material.

Ebissa (2017) estimated open channel flow parameters using Genetic Algorithm (GA) optimization technique for different bed materials of Gradual Varied Flow (GVF). The model was studied for three-bed materials (i.e, $d_{50}=20\text{mm}$, $d_{50}=6\text{mm}$ and lined concrete) for the specified downstream head and discharge rate. The model was considered to optimally reduce the difference between the observed and the measured GVF profiles at the preselected discrete section. The study results illustrated the optimal range for fitting parameter varies from 1.42 to 1.48 as the bed material becomes finer. The actual recorded value varied from the documented value i.e. 1.5. The optimal estimates of Manning's n of three different bed conditions of experimental channel appeared higher than the corresponding range.

Boulomytis et al. (2017) calculated the Manning roughness coefficient in Juqueriquere River Basin using HECRAS model calibrated using field observation data. Model prediction was found to be appropriate for the measured n values of the HEC-RAS were within the range of 0.004–0.008 at the Claro Gauging Station. The findings of this study showed that the methods of estimation and calibration matched satisfactorily, with absolute mean deviations in the sections studied below 10%.

Mohammed and Zainab (2018) estimated manning's roughness coefficient for Tigris River using HEC-RAS model calibrated for Manning's value range of 0.021-0.034. The river reach Stage and discharge data were measured in the field during 2016-2017. The range of water surface elevation found to be 10.300 m to 12.511 m and flow discharge range from $202.7 \text{ m}^3/\text{sec}$ to $355.280 \text{ m}^3/\text{sec}$. The calibration results gave acceptable values of Manning n of 0.026 for Kut Barrage downstream, reflecting the mean value of the results. The Manning's n for the study reach during 2017 found to be 0.034.

Ardıçhoğlu and Kuriqi (2019) developed hydraulic model to calibrate the Manning's n roughness coefficient using HEC-RAS in the Kizilirmak River, Turkey. Six different flow regimes based on the mean daily flow data between 2005 and 2010, were analyzed for the calibration of Manning's n value. The water surface profiles for various Mannings were slightly smaller than those indicating that the roughness coefficient n under-estimated by the model. The results showed that in intermittent flows, the higher Manning's n values should be taken into consideration. There was a polynomial correlation between roughness and Froude numbers. Eventually, a linear relation was formed between the estimated and measured Manning n coefficient of roughness. The average difference between the water surface heights measured and estimated six measurements was 3.96%. Mean roughness coefficients for six measures at Barsama station found to be 0.045 with the HEC-RAS model. The determined roughness values with HEC-RAS were used to calculate the water profile accurately.

Liu et al. (2019) studied the performance of hydraulic models 1D and 2D, LISFLOOD-FP sub-grid, HEC-RAS 1D, HEC-RAS 2D, and LISFLOOD-FP diffusive, w.r.t. the sensitivity towards surface roughness and their model structure characterization. Model was calibrated for four study reaches with different river geometry and roughness characterization. Overall, 2D models showed slightly better results when compared to 1D model's performance. In the floodplain, the uniform surface characterization improved the model results when compared with that of distributed roughness.

Wang and Zhang (2019) compared the efficiency and applicability of different vegetation roughness methods with that of the 1D hydraulic model. HEC-RAS model was implemented with dense riparian vegetation to predict the river stage of the San Joaquin River. The Freeman et al. method overestimated the Manning's n value for flow depths greater than its 1.5 m among the eleven methods of vegetation roughness. Whittaker et al. consideration of reconfiguration of versatile vegetation provided slightly more precise river stage estimation than all other methods. The methods that modeled vegetation as a rigid cylinder gave identical and reasonable river stage predictions. The San Joaquin River HEC-RAS model combined with dynamic roughness, predicted significantly better output for flood flows that exceeded the average reference flow. The results showed that computation of 1-D hydraulic

simulation was preferred for the riparian vegetation with un-submerged areas managed with trees and plants.

2.2.2. Hydraulic flood routing analysis

The incessant process of unsteady flow in the rivers can result in flooding. Unsteady flow in a river due to dynamics of rainfall discharge, modifications of channel geometry, and reservoirs and sluices operation are significant effects on river discharge (Wang et al., 2014). The comprehension and accurate prediction of river flow by hydraulic modeling are essential. Changes in riverbed morphology influence the increase in depth of flow in rivers.

Zeinyvand (2001) demarcated flood zones for part of the Broudjerd Seilakhor River in Iran with specific return periods using HEC-RAS. The research was conducted at 32 cross-sections and characteristics of the flood plains were studied using the hydrologic data obtained from different sources. Flood routing in various stretches were carried out using the Muskingham method for different return periods.

Horritt and Bates (2002) calibrated the 60 km reach of Severn river, United Kingdom using 1D and 2D hydraulic models. The models was simulated using inundation area and measured discharge at the downstream. The result showed that both the HEC-RAS and TELEMAC-2D models predicted well flood inundated area.

Knebl et al. (2005) developed an integrated framework for regional-scale flood modeling using NEXRAD Level III rainfall, GIS, HEC-RAS. The model was calibrated using the hydraulic model (HEC-RAS) that unsteady-state flow through river channel network based on the Hydrologic Center's hydrologic Modeling System (HEC-HMS) derived hydrographs. In this study, a GIS tool named Map to Map was incorporated to create a local scale that extends up to the regional scale as a prototype for the model application.

Rivera et al. (2007) conducted a study on the Aguna River basin of Honduras, Central America to identify the flood predominant zones due to high-intensity rainfall event. The SWAT model was used to estimate annual flood peak values with the hydro-

climatic database, detailed DEM, land use/land cover map and soil map of the basin. The discharge values were used along with the DEM to predict the flood hazard areas in the Aguna River basin floodplains. The procedure was designed using the HEC-RAS model. Finally, the results were classified as the areas with the high, moderate and low-risk zone areas for a specific flooding event.

Vijay et al. (2007) developed a hydrodynamic RiverCAD model for the stretch of 23 km in the Yamuna floodplain of Delhi region from Wazirabad barrage in the upstream to downstream Okhla barrage. The developed model was used to simulate and visualize flood scenarios for different designated flood flows under complex riverbed geometry with several bridges and barrages. The standard flood frequency analysis techniques used to estimate flood flows for the varies return periods based on observed flow data for the period of 1963 to 2003. The simulation results were compared and the model was calibrated with water surface elevation records of the previous floods at various barrage and bridge locations. Simulation results enabled prediction of maximum water levels, submergence scenarios and land availability under different designated flood flow for riverbed assessment, development and management.

Cook (2008) compared one-dimensional HEC-RAS with two-dimensional FESWMS (Finite Element Surface Water Modeling System) model to map flood inundation. The study revealed that the HEC-RAS model linearly interpolates the flood plain boundary between cross-sections and then defines the floodplain by subtracting the topographic data from the water surface elevations which results in a discontinuous floodplain. Also for calibrating purpose in HEC-RAS only one parameter was used i.e., Manning's "n" value. But in case of FESWMS, both Manning's "n" value, as well as eddy viscosity, was used as a calibrating parameter.

Patro et al. (2009) developed a coupled MIKE FLOOD 1D-2D hydrodynamic model to simulate the flooding depth and flood inundation extent in the delta region of Mahanadi River basin, India. Field stage and discharge data of monsoon period for the year 2002 of various gauging stations were obtained for calibration and validated with monsoon period of the year 2001 data from the same gauging stations. SRTM DEM

was used to extract bathymetry of the study area. 2-Dimensional flood inundation was prepared for the study area by coupling MIKE 11 and MIKE 21 models to form the MIKE FLOOD model. For the year 2001 flood inundation was simulated. The simulated flood inundation using MIKE FLOOD showed reasonable agreement with the observed flood inundation obtained from the IRS-1D WiFS image.

Manandhar (2010) performed flood plain analysis and risk assessment of Lothar Khola catchment. 1-D Model HEC-RAS along with HEC-GeoRAS and GIS was used for the analysis. Model was successfully simulated for steady-state boundary conditions defined at both upstream and downstream to generate maps.

Kadam and Sen (2012) used a hydrodynamic model for flood simulation of the Ajoy River, in West Bengal. MIKE-11 model was calibrated and validated with gauged station data. Two monsoon months of the year 2000 was used to calculate flood inundated area and compared with Dartmouth Flood Observatory's flood inundation extent map.

Kalita and Sarma (2012) estimated the arrival time and height of flood waves at any downstream section of river flow using numerical schemes derived from non-linear partial differential equations. Lax diffusive scheme, and Beam and Warming scheme were compared them with MIKE-21C model results in the study. The results in terms of surface profiles at a different time and velocity vectors for both the schemes were plotted, and it was observed that both the schemes showed similar results.

Sanjay and Ravindra (2012) analyzed the water level in the upper reaches of the Krishna and Koyna rivers. The flood routing studied by using one-dimensional numerical analysis software HEC-RAS and compared with observed discharge data at Karad and Sangli. The flood data used to measure the flood sensitivity of Sangli, due to release of Koyna and Dhom dam floodwater. A sensitivity analysis was carried out for three different scenarios of release from Koyna Dam only, Dhom dam release only and both dams release. Results indicated that flood situations at Sangli depend mainly on the release of water from the dam at Koyna.

Soleymani and Delphi (2012) compared different flood routing models including wave models and numerical models for Maroon river, Iran. The wave models kinematic, diffusive and dynamic wave were compared using laboratory data. Several numerical solutions for basic equations were developed by using Visual Basic and computer codes. To verify the applicability of developed models in the field, observations data such as hydrological, hydraulic and geometrical data for the Maroon River were considered. The results showed that the method of characteristics is more accurate than other models.

Hasani (2013) prepared Flood Plain Zoning (FPZ) using HEC-RAS hydraulic model. The study area considered was Zaringol River of Golestan province in Northern Iran. In the study, topo sheets of scale 1:10000 were used and the geometric data were prepared in order to extract cross-sections for around 24 kms length of the river reach. The model was simulated for hydraulic calculations carried out for the periods: 2, 5, 10, 50 and 100 years. The critical zones subjected to flooding were determined and various preventive measures were recommended to reduce the damages.

Nut and Plermkamon (2013) used SWAT and HEC-RAS model to predict the flood in the Nam Pong watershed, the northeast region of Thailand. In the study, the estimation of flood damage was simulated using the HEC-RAS model and the runoff was simulated by the SWAT model for 10-year rainfall records (2000-2010). Gumbel's method was used to analyze the flood frequencies with various return periods. The simulation revealed that the percent of damage was 20%, 23.2%, 27.8%, 34.3% and 38.5% for return periods of 5, 10, 25, 50 and 100 years respectively. The flood maps were prepared according to the simulation result using the software ArcGIS.

Kardavani and Qalehe (2013) used the HEC-RAS model for hydraulic calculations of Ay-Doghmarsh River flooding. Flood zone mapping of floods with 5yrs, 10yrs, 20yrs, 50yrs and 100yrs return period was done in this case. The topo sheets were used to extract the geometry of the river at the scale of 1:1000 into the HEC-RAS model for simulation. Flood maps were obtained for various return periods by simulating the HEC-RAS results with field observation data.

Duvvuri and Narasimhan (2013) coupled a hydrologic model with a hydraulic model using GIS platform to predict flood. ASTER DEM data was used for the Thamiraparani River Basin along with gridded precipitation, temperature, land use and soil data. A distributed hydrologic model, SWAT was used to quantify the surface runoff in a watershed. Whereas, L.P.Type-III distribution was used to calculating flood peaks with different return periods. The surface runoff and peak flood data were used as an input to calculate water spread area for various return periods. The respective flood depth and extent were mapped under the steady-state condition.

Belicci (2014) prepared a flood risk map of Baraolt river, located in centre Romania by using HEC-RAS. Along the length of the river 11km and with 36 cross-sections, the area plan with location of cross-sections, cross-section topographical data, roughness of riverbed, flood discharge hydrographs were considered. The flood risk map was prepared for maximum discharge w.r.t. the maximum water level in each cross-section of the flooded area.

Kute et al. (2014) applied HEC-RAS model in order to suggest mitigation measures of flooding due to heavy rain or dam break at River Godavari flowing through Nashik city. In the study, flood discharged during 1969 from Gangapur dam which is constructed on upstream of Nashik city is considered for modelling. For the given discharge, the submergence at the given section was modeled presenting the different levels of flood. After simulating the model for various return periods, the flood profile for the worst flood intensity was found out and its aid in adopting appropriate flood disaster mitigation measures.

Abdelbasset et al. (2015) developed a hydraulic model to calculate the water surface level for some flood event occurred in downstream of Al Wahda dam. The flood event of December 19, 2009, to January 15, 2010, was selected to simulate the hydraulic behaviours in the river reach. Model was calibrated and validated with the observed data at the downstream gauging station. The output result showed that the preparatory management for rainy seasons has significantly attenuated the extent of flooding during the flood event.

Samantaray et al. (2015) developed a hydrodynamic model for the flood-prone area of the delta region of Mahanadi river basin in India. Flood inundation map simulated by using MIKE FLOOD for optimal rice allocation model of Mahanadi river. The results showed that, in comparison to standard rice cultivars throughout the study area, the average yearly projected net benefit of the optimum rice allocation model for the study area was increased by Rs. 178,545 million.

Traore et al. (2015) computed the flow characteristics to analyze the hydraulic behaviour of the system using HEC-RAS. The total length of the river is divided into 78 cross-sections perpendicular to flow directions to identify the large and narrow section of river and estimate the floodplain. Few of these flow characteristics such as the volume, total surface area was found to be decreased from upstream to downstream. Flow velocities were found to be substantially higher in the main channel than in the floodway. The study provided an opportunity to identify important elements of irrigated agriculture land for investment plans.

Atallah et al. (2016) applied Runge-Kutta Discontinuous Galerkin (RKDG) finite element scheme based hydraulic model with limited field data. Semi-arid flash flood was forecasted by using unsteady flow hydraulic model. The results showed good agreement between the measured and simulated data. The model was found suitable to determine the flood hydrograph at the outlet of the Wadi Mekerra, Algeria watershed.

ShahiriParsa et al. (2016) applied one-dimensional model HEC-RAS and two-dimensional model CCHE2D to simulate the flood zoning in the Sungai Maka district in Kelantan state of Malaysia. The results of both the models were approximately similar in utmost sections, however most differences were found in the shape of the river.

Ullah et al. (2016) forecasted flood inundation for different return periods using integrated HEC-RAS and HEC-Geo RAS model. The model was simulated and calibrated for flood 2010 event. The correlation coefficient of the observed and estimated water surface is 0.999 and 0.996 for calibration and validation respectively.

Ding et al. (2017) developed a numerical model based on the coupling of implicit and explicit solution algorithms of Shallow Water Equations (SWEs). The accuracy of the numerical model was validated for both steady and unsteady flow using the hydrological data of two large rivers in the reach of Yangtze River, China. It was found that the unsteady flow showed much more complex in water level and discharge behaviours than the steady flow. Computed stage-discharge rating curves at all observation stations demonstrated multi-value loop patterns because of the presence of additional water surface gradient. This numerical model proved to be robust for simulating complex flows in very long rivers up to 400km.

Ferreira et al. (2017) applied Lax diffusive scheme to simulate the hydrodynamic model based on Saint Venant Equation. The model results were compared with hypothesis of trapezoidal cross-sections with uniform velocity varying over the longitudinal direction. The observed and simulated hydrographs obtained from HEC-RAS model and hypothetical trapezoidal cross-sectional study found to be satisfactory.

Ingale and Shetkar (2017) calculated water surface elevation for various return period and flood discharges using HEC-RAS model. Steady flow and unsteady flow condition were considered for the simulation of water surface elevation.

Logah et al. (2017) developed a hydraulic model to simulate surface water elevation along the Lower Volta River reach for specified discharge hydrographs. The cross-sectional profiles at selected river sections were mapped and used in the hydraulic model. In addition, suspended and bed-load sediment were analyzed to determine the current sediment load and the potential to carry more sediment. The results indicated that if dam discharge exceeds 2300 m³/s the large areas of downstream including its flood plains would be inundated. Suspended sediment transport was found to be very low in the Lower Volta River. The geomorphology of the river can be expected to change considerably with time, particularly for sustained high releases from the Akosombo and Kpong dams due to the predominant soil type and sandy soil in the river banks and river bed.

Ezz, H. (2018) estimated the extent of the maximum flash flood for Assiut plateau area, near Durunka village, using integrated GIS, SCS model, and HEC-RAS. Water depths and velocities occurred from the flash flood were predicted for the ungauged catchments of the study area. The model results showed that the maximum water depth is 4.01 m and the highest velocity is 11.75 m/s. The model result helped the decision-makers to minimize the flood hazards and protecting the proposed road.

Khalfallah and Saidi (2018) prepared a flood inundation map using HEC-RAS and HEC-GeoRAS for the flood occurred in February March 2015 in the Medjerda basin. Hyfran was used to calculate flood and return a period estimation of rainfall. The model result showed a good correlation between observed parameters with those of simulated. Model result predicted a flood of the river exceeding 240 m³/s revealing that HEC-RAS is a significant tool for understanding flood events.

Parhi et al. (2018) simulated HEC-RAS model to find the peak flood levels at different locations between Hirakud dam and Naraj of Mahanadi River reach. In addition, Gumbel's distribution method was used to calculate an extreme value for 10, 25, 50 and 100 years return period. The research carried out for 36 cross-sections of 310 km of river length by considering 25 years return period floods (45067 m³/s) for the analysis. Model results showed that out of 36 cross-sections, the 23 sections, required increasing height of embankment from a minimum of 0.11 m to a maximum of 10.63 m in the left bank side. Similarly, for right bank embankment heightening was required from 0.09 m to a maximum of 9.94 m to protect the inundation of the low-lying areas of Mahanadi delta.

Gori et al. (2019) studied the future development of 100-year floodplain in Houston watershed. Distributed hydrologic model and coupled 1D/2D unsteady hydraulic model was used for future floodplain estimation. The result indicated that the 100-year floodplain might expand up to 12.5% across the watershed.

Marko et al. (2019) developed two-dimensional flood inundation model in urbanized areas Wadi Qows located in Jeddah City, Saudi. The WMS and HEC-RAS models were used for a hydraulic simulation based on channel geometry. A resampling method was

used to produce a higher resolution from DEM 90 X 90 m to 10 X 10 m grid cell sizes. The results showed that a higher resolution leads to increasing the average flood depth and decreasing the flood extent. The integration of WMS, HEC-RAS and GIS proved to be an appropriate technique for flood modelling in rural, mountainous and urban areas.

Pinos and Timbe (2019) developed a 2-D hydraulic model in the Santa Barbara River catchment for flood inundation mapping. The model's performance was estimated based on the water surface elevation and flood extent, in terms of the mean absolute difference and measure of fit.

Pinos et al. (2019) compared the performance of 1D hydraulic models with HEC-RAS, MIKE 11, and Flood Modeler models to estimate flood levels of a mountain river. The study considered a 5 km reach of Santa Bárbara River to conduct the valuation of models by steady-state conditions through two different scenarios (Cross-section extracted by LiDAR and DEM). The evaluated models revealed similar results when using cross-section extracted by LiDAR, (NSE were between 0.94 and 0.99). The goodness of fit decreased when using cross-section extracted from DEM, with an average NSE of 0.98 (HEC-RAS), 0.88 (Flood Modeller) and 0.85 (MIKE 11) when compared with observed data. The results showed that the HEC-RAS model provided similar results for the two scenarios as compared to the other two models.

Jacob et al. (2019) developed an L-moment-based regional flood frequency analysis hydrodynamic model with a non-dimensional analysis of flood hydrographs to generate flood risk assessment for the lower Bharathapuzha basin. The model was calibrated with the limited data available discharge and water level and extracted river cross-sections from widely available SRTM DEM for the year 1992. Flood inundation extent for the year 2002 was simulated by a coupled 1D-2D flood inundation model. The magnitude of flooding was validated with the optical data from the IRS-1D WiFS sensor. To assess the flood hazard, the calibrated and validated flood model and the estimated regional flood frequency were used. The result concluded that the MIKE FLOOD model is reasonably satisfactory in simulating the flood inundation extent.

Yalcin (2019) developed a hydraulic model to investigate the effects of flooding events with high, medium and low probability. The high-resolution terrain and land use data were produced by processing the aerial images acquired by the unmanned aerial vehicle (UAV) flights over the flood risk zone to simulate the movement of water more accurately. The absence of representative stream gauging stations inside or near the region, the synthetic unit hydrograph methods were used to estimate the flood hydrographs. The resultant flood hazard maps addressed cautionary in terms of demonstrating the effects of possible floods that were unexpected to come from such an intermittent stream basin.

Patel (2020) successfully applied GIS-based rainfall-runoff model and HEC-RAS model during the flood event of 2017 of the Banas river, Gujarat, India for flood management plans.

2.2.3. The sensitivity of hydraulic parameter

Significant advances are being made in reliability and probabilistic methods and their use in hydraulic and hydrologic engineering is rapidly increasing. If the uncertainties that underlie any of these methods cannot be properly defined, the results of the reliability analysis are inaccurate. In the past, Johnson (1996) quantified uncertainties of various hydraulic parameter in terms of coefficients of variation and associated distributions.

Wohl (1998) carried out uncertainty analysis for Manning's n-values. The values of n were selected for study reach using Jarrett's (1984) equation for high-gradient channels, Limerinos's (1970) equation for natural alluvial channels, visual estimation of n-values was performed at each site using Barnes (1967) as a guideline and the Cowan (1956) method for estimation of n. The n-values were varied by $\pm 10\%$ and $\pm 25\%$. The percentage change in discharge associated with varying n-values is proportional to roughness and inversely proportional to channel slope and to width/depth ratio. The result showed a maximum change of 20% in discharge when the channel with a gradient less than or equal to 0.01 varying n by $\pm 25\%$. The results indicate that uncertainties in discharge estimation resulting from the roughness coefficient.

Pappenberger et al. (2005) performed uncertainty analysis using generalised likelihood uncertainty estimation (GLUE) method. Selected Manning roughness coefficient ranged between 0.001 and 0.9 to check the performance of the model. Also investigated weighting coefficient variation influence on the numerical scheme. The results showed that choosing the weighting parameter for the implicit scheme has no impact on model results output. The effects of varying the roughness of the range suggested that even with extreme values, many parameter sets will perform equally well. However, it depended upon boundary conditions and the model region. The results concluded that an analysis of uncertainty can be used to generate flood maps with complex probability.

Casas et al. (2006) investigated the effects of flood using one-dimensional (1-D), hydraulic model from topographic data sources. Results found that, flooded area and flood level estimated were less accurate by using contour-based digital terrain model (DTM). However, the GPS-based DTM proved to be more realistic estimation of the flooded area and water surface elevation. In terms of the flooded area and the water surface elevation, the LiDAR model gave the acceptable results relative to the reference data. The results found that LiDAR, in particular in large areas, is the most economical technique for developing a DEM with reasonable accuracy.

Yu and Lane (2006) studied the impact of re-scaling strategy on the output of the LISFLOOD-FP model results. Using the standard re-scaling strategies (i.e. nearest-neighbour interpolation, bilinear interpolation, mean and cubic spline convolution), the DEMs used in the study were re-scaled from 2 m (original resolution) to 4, 8 and 16 m. The study concluded that there was not much difference of the model outputs associated with the re-scaling strategy and found inconsistent results from the re-scaled DEMs. Furthermore, the study revealed that, high-resolution DEMs needed to be coupled with advanced inundation process to obtain effective predictions of flood inundation extent.

Schumann et al. (2008) demonstrated the effects of DEMs on deriving the water stage and inundation area. Three DEMs were used in a study area in Luxembourg, using three different resolutions from three sources (lidar, contour and SRTM DEM). The results showed that the lidar DEM obtained the water stages with the lowest RMSE, preceded

by the DEM contour and lastly by the SRTM using HEC-RAS model to simulate the flood propagation. However, topographical uncertainty affected the simulated flood level when simulating elevations of the water's surface are transferred to flood maps.

Castellarin et al. (2009) developed a 1-D hydrodynamic model to test the optimal cross-sectional spacing for two case studies in the United Kingdom and Italy. The main purpose of the analysis was to determine the efficiency of the 1-D model by following certain of Samuels' (1990) Guidelines and Equations. The inaccuracy of the model was found to increase as the spacing between the cross-sections increased in terms of mean absolute error (MAE) for both selected rivers. The results showed that spatial resolution has less effect on the accuracy of the 1D hydraulic model.

Cook and Merwade (2009) developed 1-D hydraulic modelling for two rivers reaches in the USA and simulated the flood extent. However, the effects of the hydraulic structure are neglected. The results indicated that the increase or decrease of the inundation area was not only influenced by the number of cross-sections used, but also by the cross-section width itself.

Di Baldassarre and Montanari (2009) determined that the estimated flow of river may lead up to 40 % errors in flood conditions due to application of rating curves. Such errors were found in hydraulic modeling due to uncertainty in the calculation of design flood profiles and flood maps. In addition, the uncertainties with the flow data emerged not only from the evaluation of flow data but also from the probabilistic approaches used for the estimation of flood design.

Kim et al. (2010) determined the Manning roughness coefficient using field measurements of discharge and water level for gravel bed stream. Results showed that the roughness coefficient continued to decrease with the increase in discharge and water depth, and appeared to remain constant above a certain range. The roughness coefficient determined when compared with that of field measurement indicated that, the measured values provided the approximate roughness coefficients for a relatively large discharge, due to the variance in the estimates where there is apparently very high uncertainty. On average, a 20% increase of the roughness coefficient caused a 7% increase in the water

depth and an 8% decrease in velocity with 15% increase in the water depth and an equivalent decrease in velocity for certain cross-sections in the study reach. A 10% failure in the calculation of discharge may lead to more than 10% uncertainty in the estimation of roughness, but corresponding uncertainty in the measured water depth and velocity is reduced to about 5%. In comparison, the need for roughness coefficient calculation is verified by field measurement.

Kuta et al. (2010) carried out hydraulic simulation for urban stream channel, Red Hill Creek of Ontario in Canada. The simulations were conducted using the HEC-RAS model to determine the sensitivity of the model predictions to field data precision, data density and estimation techniques, as well as accuracy of the model. The results showed that the variability in Manning's n roughness estimates had considerable impact on model accuracy and, for overbank flow events.

Barati (2011) utilized Nelder-Mead simplex (NMS) algorithm to estimate nonlinear Muskingum model parameters. The output of this algorithm was compiled together with a historical example with other documented parameter estimation techniques. The experimental results revealed that the NMS algorithm to be effective in the estimation of the nonlinear Muskingum model parameters. The algorithm was easy to program and very simple to find the optimal solution. Although the initial estimate of this technique involved an initial guess, 84.8% of cases obtained the optimal or near-optimum results from a sensitivity analysis of their initial parameter values.

Nassar (2011) applied the CCHE2D model to simulate the unsteady flow for Elbogdady reach, Nile River. Multi-Parametric Sensitivity Analysis (MPSA) was used to determine the relative importance of the different empirical parameters controlling the unsteady flow. Wu and Wang (1999) and Van Rijn (1984) bed roughness formulas were used to determining the roughness coefficient. The results from the multi-parametric sensitivity analysis showed that the coefficient of bed roughness in the Nile River is more sensitive. Therefore, Van Rijn's empirical method (1984) was more effective in estimating bed roughness.

Akbari and Barati (2012) developed a mathematical model to check the sensitivity of flood routing parameters using implicit numerical approach. In three unmanaged catchments of the Persian Gulf region, a sensitivity analysis of flood routing parameters was investigated through field measurement, statistical and mathematical procedures. The results indicated that the importance rankings of various parameters on output results are peak inflow, roughness coefficient, bed slope, bed width, river length, side slope, weighting factor and base flow. The results also showed that the effects of input parameter errors on the output results, such as the peak inflow on the peak outflow and volume of flooding, the river length on the time to peak, the roughness coefficient on the velocity, and the peak inflow, roughness coefficient and bed width on depth.

Akbari et al. (2012) simulated an unsteady non-uniform flow model for flow-sediments and compared to past research including HEC-series models. Uncertain value of flow-sediment transport equation parameters and errors were studied in existing coupled flow-sediment models. Sensitive nonlinear flow – sediment concepts simplified in linear models were considered, and non-uniform sediment-laden flooding flows were considered in loose boundaries. Numerical analytical findings were compared with field observations relying on the accuracy of the model developed. The results showed significant effects on a solution and other parameters, such as bed width, bed slope, and side slope, weighting factors, reach length, and baseflow on model performance, of the peak inflow hydrograph and roughness variation. Also, the sensitivity of the established computer model was also examined to grid sizes, and the results showed that the peak outflow increased by the space step while the time step decreased.

Barati et al. (2012) developed a dynamic wave model for flood routing in natural rivers using graphical multi-parametric sensitivity analysis (GMPSA). The results showed that the effects of input parameter errors on the output results to be more significant in special situations, such as lower Manning's roughness coefficient value and a steeper bed slope on the characteristics of a design hydrograph, higher skewness factor value and time to peak on the channel characteristics, higher Manning's roughness coefficient value and the bed slope on the space step, and lower Manning's roughness coefficient value and a steeper bed slope on the time step and weighting factor calculated peak

outflows and grid intervals increased the peak outflow in space and decrease in time. When the Manning roughness coefficient was increased with mild bed slope, the lag criterion was found to be decreased and the attenuating criterion to be increased.

Moya Quiroga et al. (2013) developed an HEC-RAS hydraulic model for the Timis-Bega basin in Romania. SRTM DEM sampling of Monte Carlo was found to be significant on the flood area mapping uncertainties.

Yan et al. (2013) compared the LiDAR and SRTM DEM hydraulic model, taking into account the uncertainty between parameter and inflow. Apart from the DEM inaccuracy, an uncertainty analysis was performed. The result indicated that the variation between the SRTM-based model and the LiDAR-based model to be significant within the accuracy related to large-scale floods.

Papaioannou et al. (2017) analyzed the different types of hydraulic model to check the sensitivity of different resolution of DEM for flood inundation modelling and floodplain mapping process at ungauged watersheds. Typically, digitized contours from 1:5000-scale topographic maps, topographic land survey data and unprocessed and processed TLS data were used for the extraction of the river and riparian areas. One-dimensional hydraulic models, two-dimensional hydraulic models and combinations of coupled hydraulic models were applied to investigate the sensitivity. Flood inundation maps were generated for each modelling approach and landscape configuration at the lower part of Xerias River reach and compared for calculating the sensitivity of input data and model structure uncertainty. Results showed that the sensitivity of floodplain modelling on the DEM spatial resolution and the hydraulic modelling approach.

Lamichhane and Sharma (2018) developed a hydraulic model to identify the error associated with input data, including various Manning's roughness and resolutions of elevation datasets for floodplain mapping and computation of travel time. LiDAR data incorporated into survey data is cautious perdition and coarser elevation data sets provided positive inundation area (32.56–44.52%) and travel time (1.03–15.01%) variations. When the results of the LiDAR integrated with survey data were compared with 10-m DEM integrated with survey data, the minimum differences were 3.55–

7.16% and 0.50–4.33% respectively in the inundation area and travel time. The effect of Manning's roughness was found to be more crucial in predicting flood inundated area and flood travel time computation, particularly in channel sections. The results concluded that a LiDAR data in the floodplain and 10-m DEM in the channel combined with survey data would be suitable for a flood warning system. For the lower value of the Manning's roughness, the flooded area decreased by 8.97%

Mokhtar et al. (2018) investigated the uncertainties of hydraulic parameters using sensitivity analysis with Monte Carlo simulation method to generate random data combinations. In the study, HEC-RAS model was developed using calculated discharge based on the three variables, and Manning's n for differentiated existing floodwater bodies and normal water extent using TerraSAR-X data. Combined variable uncertainty was measured with probability indicators like Nash – Sutcliffe efficiency, mean absolute error, F-statistic, and root mean square error.

Oubennaceur et al. (2018) used point estimate method (PEM) for the analysis of the uncertainty of a hydraulic two-dimensional model. In the 46 km reach from Richelieu River in Canada, and uncertainty study was carried out to simulate water depth. Manning's coefficient, topography and flow rate were considered for uncertainties input parameter variables. For mean water depth, standard deviations were calculated for the considered flow rates of 759, 824, 936, 1113 m^3/s with the mean standard deviation of 27 cm. The mean and standard deviation values of water depth was accurately calculated using PEM method. The results showed the maximum standard deviation was found in upstream of the Richelieu River using the PEM method with a rough estimate of the uncertainty.

Vojtek et al. (2019) evaluated the input parameter sensitivity of hydrological model EBA4SUB and one-dimensional hydraulic model HEC-RAS for various combinations of input parameters of simulated flood volume and flood area. Hydrological modeling results showed huge variation in the design peak discharges that have a strong influence on the model flood volume and flood area. The cross-section spacing and Manning's roughness was considered for sensitivity analysis in the hydraulic model. The result showed that, for the cross-section spacing, the difference in flood volume and flood

area between the 5-m and 80-m cross-section spacing with respect to the reference, normal roughness values is 49.4% and 21.1% for flood area, while for flood volume it is 18.9% and 13.3%. The sensitivity of flood volume and flood area to the roughness parameter was 1.5–2 times greater than the sensitivity to the cross-section parameter. The results concluded that the input parameters for hydraulic modeling is sensitive.

Xu et al. (2019) analyzed the runoff parameter sensitivity using the Stormwater Management Management Model (SWMM) and calculated the optimum parameters. To check the impact of degree of single parameter effects on the simulation results, the sensitivity of the selected parameters was determined using Morris sieve approach. One parameter was changed at a fixed step, with the other parameters to remain unchanged. Results showed that the shrub parameters have a greater sensitivity than those for the lawn to runoff and peak flow. The relative errors were within $\pm 9.5\%$ of runoff and dynamic mean runoff (60 min) for lawn and shrub. The peak flow error was between -21 and 16.6% .

Jahandideh-Tehrani et al. (2020) developed hydrodynamic river model for Nerang River, South East Queensland, Australia. The MIKE HYDRO model was calibrated using Manning's roughness coefficient for flood periods. The observed and simulated stage values were used to estimate performance indices. Results showed acceptable agreement between the observed and simulated stage value. The sensitivity of boundary conditions was investigated based on adding stochastic terms (random noise) to the time series of boundary conditions. For both downstream and upstream boundaries, the differences in the simulated results were separately estimated under 5%, 10% and 15% perturbation. Sensitivity analysis showed that downstream boundary conditions were more prone in middle parts of the River, as maximum water levels may reach 8%, 12% and 15% under 5%, 10% and 15% variation in downstream boundary condition respectively.

2.3. SUMMARY OF LITERATURE REVIEW

From the review of literature, it is apparent that the implicit finite difference scheme is the most commonly used procedure for solving the one-dimensional de Saint-Venant equation, by using the Hydraulic Model River Analysis System HEC-RAS.

Many attempts have been made to study, understand and predict the flood in natural channel or river using analytical and numerical methods. Analytical methods prove to be a good approach for understanding the flood flow in channels. Numerical models are found to be a suitable approach for the characterization of flow at regional/catchment scale.

Both numerical models and analytical methods were found to be competitive to assess impacts of bed morphology (Roughness coefficient, the shape of the channel, channel slope) on discharge and water level in rivers. Numerical models are proved to be good means to assess the impacts for its capability to do the sensitivity analysis and to predict flood flow.

There are several models developed in this domain have been the focus of research from several decades. There is a need to understand river behavior when unexpected precipitation, drainage modifications of the catchment, dam failures, etc. will occur. Numerical modeling is one of the best tools for study to analyze the influences of the bed morphology on discharge and water level at various location in the river.

2.4. RESEARCH GAPS

1. Less studies were carried out for analyzing the hydraulic response of the Nethravathi river due to variation in roughness co-efficient across the natural channel.
2. Fewer research has focused on the influence of unsteady flow over downstream boundary conditions based on variation in the channel hydraulic properties.
3. Scarce studies have considered the unsteady flow condition for river especially for the reach length scale of a river during the flood routing simulation.

4. Sensitivity analysis of parameter influencing the unsteady flow characteristics of the river was found to be inadequate.

2.5. OBJECTIVES

The proposed work is intended to use HEC-RAS, one-dimensional flow model to simulate unsteady flow state condition in a natural channel. In this study, a detailed hydraulic routing with varied bed conductivity is attempted, with special reference to the Nethravathi basin. The study proposes the hydraulic flood routing without considering the lateral flow and to understand the characteristics of unsteady flow. Also, in this study, parameter perturbation method for few hydraulic routing parameters is considered for the sensitivity analysis. Overall, the present study is taken up with the following objectives:

1. A numerical study on the effect of roughness coefficient on discharge and stage in natural river.
2. To study the hydraulic response in the Nethravathi river regime by flood routing analysis for unsteady flow.
3. Sensitivity analysis of hydraulics routing parameters.

METHODOLOGY

3.1 GENERAL

In the present work, the hydraulic model has been used to know the effect of roughness co-efficient on stage and discharge along the length of the river regime and also to develop the flood plain mapping. Figure 3.1 shows the overall flow process of methodology carried out in the present study.

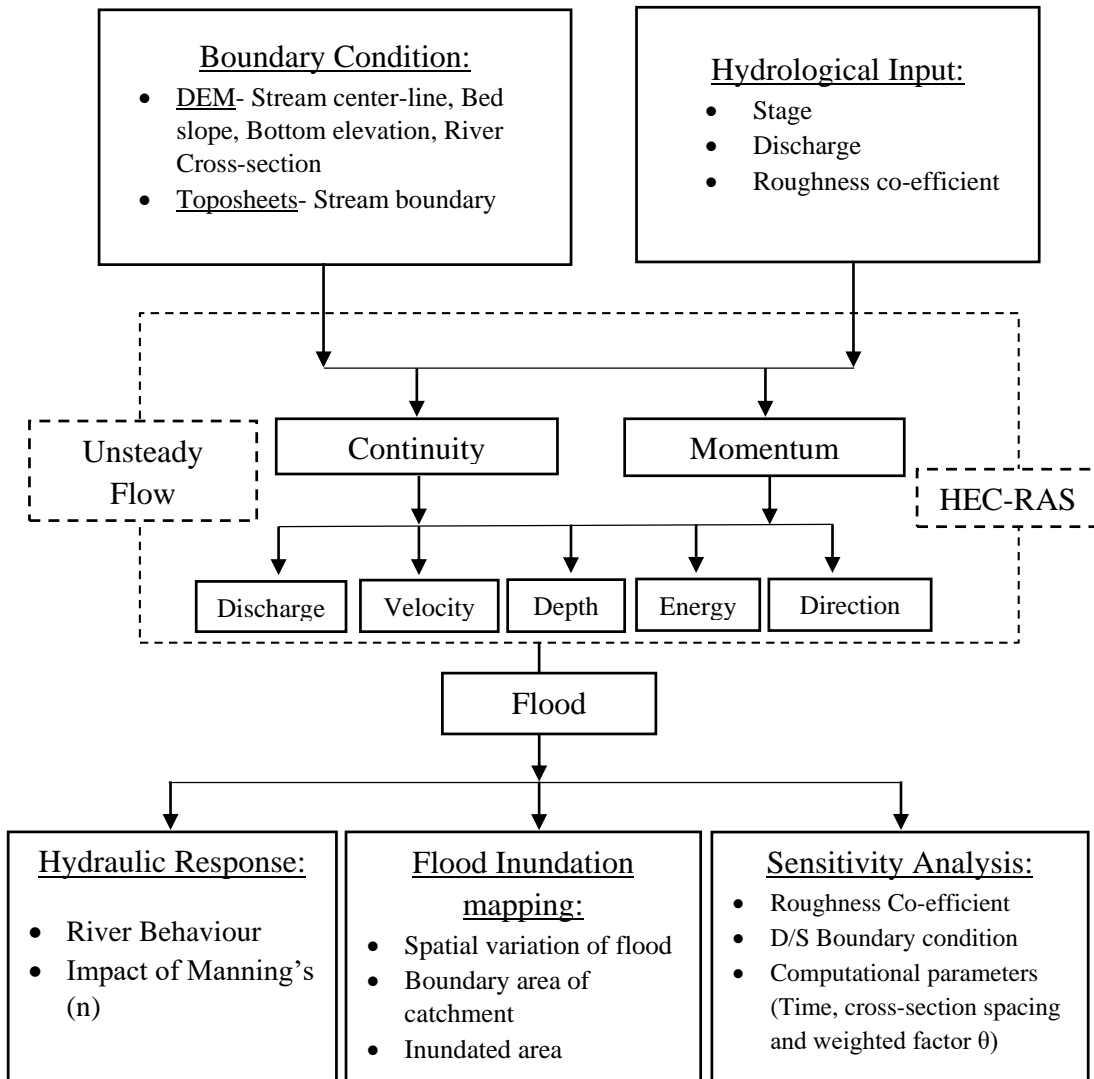


Figure 3.1 Flowchart of methodology

3.2 DESCRIPTION OF THE HYDRAULIC MODEL

The numerical study proposes to use Saint-Venant equation using a one-dimensional flow model. To identify the discharge and water depth in river channel use of hydraulic and hydrological parameters such as morphological data, hydrograph (flow and stage), rating curve, normal depth and remote sensing data (DEM) are used. These hydraulic and hydrological parameters will help to understand the behaviour of the river that indeed helps to analyse the flow characteristics in the open channel. The major contribution of the study is to establish the relationship between hydraulic parameters and flow characteristics. Initially, to understand the flow characteristics the roughness coefficient is used along the riverbed. As the roughness coefficient varies along the natural channel, it makes necessary to study the relationship based upon the change in the morphological characteristics. This evaluation will help to understand the behaviour of Natural River at time of heavy precipitation and overflow of water. Further, other hydraulic and hydrological parameters are used to measure the magnitude of the flood characteristic. As along the natural channel, the flood characteristics also varies with the cross-sectional geometry and other characteristics.

3.2.1 Numerical modeling using HEC-RAS

Hydrologic Engineering Center's – River Analysis System (HEC-RAS) is a software which solves the mass and momentum equations using implicit finite difference approximations and Preissman's second-order scheme. HEC-RAS is a hydraulic simulation model for calculating water surface profiles for natural and man-made channels. The model has one-dimensional steady and unsteady flow analysis options. It also has components for movable boundary sediment transport computations and water quality analysis. Also, HEC-RAS can be effectively coupled with other tools to generate the flood inundation maps by considering both depth and velocity.

HEC-RAS has the capability to yield results for various flows such as super-critical, sub-critical and mixed flow regimes. The model can be simulated for straight stretches of a river or the rivers having the dendritic systems. In order to run the HEC-RAS model, various input parameters such as geometric data and boundary conditions are to

be prescribed. In the present case, the geometric file is prepared using the HEC-GeoRAS for the river stretches considered.

HEC-RAS assumes that the energy head is constant across the cross-section and the velocity vector is perpendicular to the cross-section. As such, care should be taken so that the flow through selected cross-section reach meets these criteria. Before simulating the model, certain initial conditions have to be defined such as normal depth, discharge at the inlet, Manning's "n" value, expansion and contraction values, etc., After entering all the boundary conditions, HEC-RAS is performed for unsteady-state conditions. Boundary conditions are necessary to define discharge and water depth at the system endpoints, i.e., upstream and downstream.

HEC-GeoRAS is the geospatial extension used in the study to define initial and boundary conditions of the study area using GIS format. It helps to create the essential input data for hydraulic parameters at a cross-section. The GIS data include cross-section geometry, channel network connectivity, reach lengths, stream junction information and energy loss coefficients. Cross-sections are needed at representative locations throughout the reach and at locations where changes in discharge, slope, shape or roughness occur.

3.3 UNSTEADY FLOW ROUTING USING HECRAS

3.3.1 Governing equations of HEC-RAS

For an unsteady state flow of water, the basic governing equations which is followed by HEC-RAS model is the principle of conservation of mass and momentum which are developed by A.J.C Barre de Saint Venant (1871), hence they are commonly known as St. Venant equations. In the differential form, the equation of continuity for unsteady flow in a reach with no lateral flow is given by:

$$\text{Continuity equation} \quad \frac{\partial y}{\partial t} + D_h \frac{\partial V}{\partial x} + V \frac{dy}{dx} = 0 \quad (3.1)$$

$$\text{Momentum equation} \quad \frac{\partial y}{\partial t} + V \frac{\partial V}{\partial x} + g \left(\frac{dy}{dx} - S_b + S_f \right) = 0 \quad (3.2)$$

Where: V is the flow velocity; y is the flow depth; $D_h = A/B$ is hydraulic depth; A is flow area, B is a top width of the channel; S_b is the channel bottom slope, S_f is the slope of energy grade line; x is the distance along the channel length; t is time and g is the acceleration due to gravity.

3.3.2 Solution methodology for Saint Venant equation in HEC-RAS

The most successful and accepted procedure for solving the one-dimensional unsteady flow equation (Saint Venant equation) is the four-point implicit scheme also known as the box scheme. Under the scheme, methods of solution are as follows,

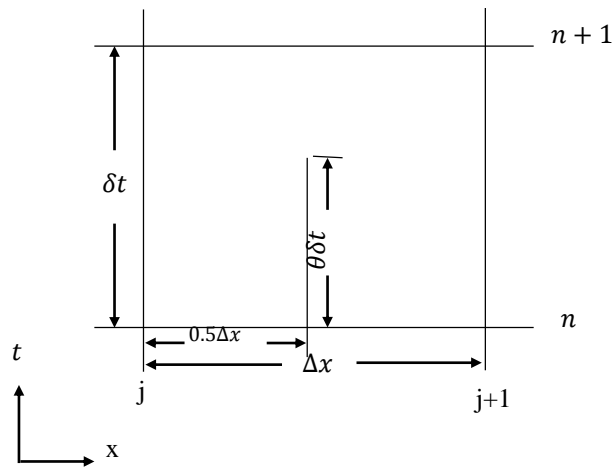


Figure 3.2 Typical finite difference cell

$$f_i = f_i^j \quad (3.3)$$

$$\Delta f_i^j = f_{i+1}^{j+1} - f_i^j$$

$$\text{or } f_i^{j+1} = f_i^j + \Delta f_i^j \quad (3.4)$$

Size of grid taken as (i, j) ; where i =space interval, j = time interval

General implicit finite difference scheme forms are

1. Time derivative

$$\frac{\partial f}{\partial t} \approx \frac{\Delta f}{\Delta t} = \frac{0.5(\Delta f_{i+1} + \Delta f_i)}{\Delta t} \quad (3.5)$$

2. Space derivative

$$\frac{\partial f}{\partial x} \approx \frac{\Delta f}{\Delta x} = \frac{(f_{i+1} - f_i) + \theta(\Delta f_{i+1} - \Delta f_i)}{\Delta x} \quad (3.6)$$

3. Function value

$$f = 0.5(f_{i+1} + f_i) + 0.5\theta(\Delta f_{i+1} + \Delta f_i) \quad (3.7)$$

f , refers to both V and y in the partial derivatives and f stands for S_f and V as a coefficient.

A. Continuity Equation

$$\frac{\partial A}{\partial t} + \frac{\partial S}{\partial t} + \frac{\partial Q}{\partial x} - q_l = 0 \quad (3.8)$$

The above equation can be written for channel or floodplain:

$$\frac{\partial Q_c}{\partial x_c} + \frac{\partial A_c}{\partial t} = q_f \quad (3.9)$$

$$\frac{\partial Q_f}{\partial x_f} + \frac{\partial A_f}{\partial t} + \frac{\partial S}{\partial t} = q_c + q_l \quad (3.10)$$

Where the subscripts c and f refer to the channel and flood plain, respectively

q_l is the lateral inflow per unit length of floodplain, q_c and q_l are the exchange of water between the channel and floodplain.

$$\frac{\partial Q_c}{\partial x_c} + \frac{\partial A_c}{\partial t} = q_f \quad (3.11)$$

$$\frac{\partial Q_f}{\partial x_f} + \frac{\partial A_f}{\partial t} + \frac{\partial S}{\partial t} = q_c + q_l \quad (3.12)$$

The exchange of mass is equal but not opposite in sign such that

$$\Delta x_c q_c = -\Delta x_f q_f \quad (3.13)$$

B. Momentum Equation

The equation states that the rate of change in momentum is equal to the external forces acting on the system. For single channel,

$$(3.14)$$

The above equation can be written for the channel and floodplain as,

$$\frac{\partial Q_c}{\partial t} + \frac{\partial(V_c Q_c)}{\partial x} + gA_c \left(\frac{\partial Z}{\partial x_c} + S_{f_c} \right) = M_f \quad (3.15)$$

$$\frac{\partial Q_f}{\partial t} + \frac{\partial(V_f Q_f)}{\partial x} + gA_f \left(\frac{\partial Z}{\partial x_f} + S_{f_f} \right) = M_c \quad (3.16)$$

Where M_c and M_f are the momentum fluxes per unit distance exchange between the channel and floodplain respectively.

In the present study, HEC-RAS is used to route an inflowing flood hydrograph through the river channel with following assumptions for Saint Venant equation:

- Flow is one-dimensional
- Hydrostatic pressure prevails and vertical accelerations are negligible
- Streamline curvature is small.
- Bottom slope of the channel is small.
- Manning's equation is used to describe resistance effects
- The fluid is incompressible

3.4 WATER SURFACE PROFILES

Water surface profiles are computed from one cross-section to the next by solving the Energy equation which is an iterative procedure called the standard step method. Figure 3.3 shown the terms of the energy equation.

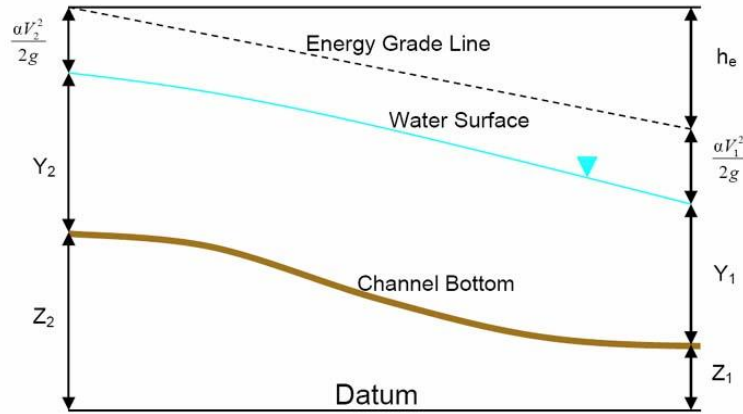


Figure 3.3 Representation of terms in the Energy Equation (Brunner 2016)

The energy equation is as follows:

$$Z_2 + Y_2 + \frac{a_2 V_2^2}{2g} = Z_1 + Y_1 + \frac{a_1 V_1^2}{2g} + h_e \quad (3.17)$$

Where: Z_1, Z_2 = elevation of the main channel invert, Y_1, Y_2 = depth of water at cross-sections V_1, V_2 = average velocities, a_1, a_2 = velocity weighting (energy correction) coefficients

g = gravitational acceleration, h_e = energy head loss

The equation for the energy head loss is as follows:

$$h_e = L \bar{S}_f + C \left| \frac{a_2 V_2^2}{2g} - \frac{a_1 V_1^2}{2g} \right| \quad (3.18)$$

Where: L = discharge weighted reach length, \bar{S}_f = representative friction slope between two sections, C = expansion or contraction loss coefficient

The discharge weighted reach length, L , is calculated as:

$$L = \frac{L_{lob} \bar{Q}_{lob} + L_{ch} \bar{Q}_{ch} + L_{rob} \bar{Q}_{rob}}{\bar{Q}_{lob} + \bar{Q}_{ch} + \bar{Q}_{rob}} \quad (3.19)$$

Where: L_{lob}, L_{ch}, L_{rob} = cross section reach lengths specified for flow in the left overbank, main channel, and right over bank, respectively

$\bar{Q}_{lob}, \bar{Q}_{ch}, \bar{Q}_{rob}$ = arithmetic average of the flows between sections for the left overbank, main channel, and right over bank, respectively.

3.4.1 Cross section subdivision for Conveyance

To evaluate the overall conveyance and the velocity coefficient for a cross-section, the flow must be subdivided into units for which the velocity is distributed uniformly. The method used in HEC-RAS is to subdivide flow into overbank areas using the n-value breakpoints input cross-section (locations where n-values change) as the basis for subdivision as shown in figure 3.4. Conveyance is calculated within each subdivision from the following form of Manning's equation:

$$Q = KS_f^{1/2} \quad (3.20)$$

$$K = \frac{1}{n} AR^{2/3} \quad (3.21)$$

where: K = conveyance for subdivision n = Manning's roughness coefficient for subdivision, A = flow area for subdivision, R = hydraulic radius for subdivision, S_f = slope of the energy grade line

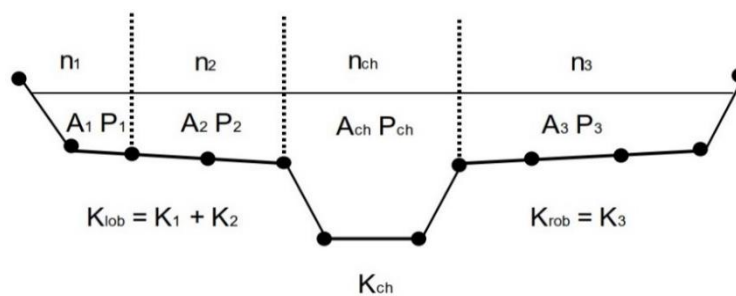


Figure 3.4 HEC-RAS Default Conveyance Subdivision Method (Brunner 2016)

3.4.2 Friction loss

The friction slope (slope of the energy grade line) at each cross-section is computed using equation 3.21

$$S_f = \left(\frac{Q}{K} \right)^2 \quad (3.22)$$

3.4.3 Contraction and Expansion Loss

Contraction and expansion losses in HEC-RAS are evaluated by the following equation:

$$h_{ce} = C \left| \frac{a_1 V_1^2}{2g} - \frac{a_2 V_2^2}{2g} \right| \quad (3.23)$$

h_{ce} = contraction or expansion head loss (m)

C = contraction or expansion coefficient

3.5 SENSITIVITY ANALYSIS

Sensitivity analysis is carried out to determine the effect of hydraulic parameters on the natural flow characteristics. It predicts the outcome of causing flood during the higher precipitation level or overflow of water. The HEC-RAS model uses, channel geometry, upstream and downstream boundary conditions and roughness coefficients to compute a water-surface profile.

3.5.1 Parameter Perturbation Method

Parameter perturbation method is based on perturbing i.e., varying each parameter at a time, involved in the simulation. If there are N parameters involved in the simulation, then the governing equations of the model are solved for $(N+1)$ iterations. The sensitive parameters are identified by using sensitivity co-efficient that determined from the perturbation of suitable parameters on trial and error basis (Yeh 1986).

In this study, a sensitivity analysis was carried out for the 1D HEC-RAS model to determine the impact of some geometric and computational parameters on model results and stability. The parameters that were investigated in the sensitivity analysis are Manning's roughness coefficient, downstream boundary condition (Normal depth), computational time step and θ -weighting parameter.

3.6 STATISTICAL PARAMETERS TO VALIDATE THE MODEL PERFORMANCE

The model performance is assessed by following five statistical measures:

The Nash-Sutcliffe efficiency (NSE) is an identical statistic measure that determines the relative magnitude of the residual variance ("noise") compared to the variance of measured data (Nash and Sutcliffe, 1970). For model evaluations, NSE is recommended, as the best target feature to represent the overall fit of a hydrograph is found (Moriasi et al., 2007). Typically, this shows the wellness of the 1:1 data observed and simulated. Their values differ from- ∞ to 1, and the values between 0 and 1 are appropriate.

The NSE value of 1 is rare and considered as a perfect value for an ideal model. NSE is calculated by using the following equation.

$$NSE = 1 - \left[\frac{\sum_i^N (O_i - P_i)^2}{\sum_i^N (O_i - \bar{O})^2} \right] \quad (3.24)$$

Coefficient of determination R^2 measures the fitness of observed and simulated data. R^2 varies from 0 to 1, indicating 1 as a perfect fitness of data.

$$R^2 = \left(\frac{\sum_{i=1}^N (O_i - \bar{O})(P_i - \bar{P})}{\sqrt{\sum_{i=1}^N (O_i - \bar{O})^2} \sqrt{\sum_{i=1}^N (P_i - \bar{P})^2}} \right)^2 \quad (3.25)$$

The Root Mean Square Error (RMSE) has the same unit as actual and predicted data. The error between measured and predicted values should always below,

$$RMSE = \sqrt{\frac{\sum_{i=1}^N (O_i - P_i)^2}{N}} \quad (3.26)$$

Normalized the Root Mean Square Error (NRSME) was used in the current study as a measure of the accuracy of the estimating stage and discharge, where lower NRMSE values would indicate higher accuracy.

$$NRMSE = \frac{RMSE}{\bar{o}} \quad (3.27)$$

The Mean Absolute Error(MAE) is the average of all absolute errors

$$MAE = \frac{1}{N} \sum_{i=1}^N |O_i - P_i| \quad (3.28)$$

The index of agreement (d) is given by (Willmott et al. 1985)

$$d = \left(\frac{\sum_{i=1}^N (O_i - P_i)^2}{\sum_{i=1}^N (|P_i - \bar{o}| + |O_i - \bar{o}|)^2} \right)^2, \quad 0 \leq d \leq 1 \quad (3.29)$$

In Equation 3.24 to 3.29,

P_i = the model predicted the value of the output variable

O_i = observed value of the output variable

\bar{O} = mean of observed value

\bar{P} = mean of predicted value

N = total number of reference data points

STUDY AREA AND MODEL DEVELOPMENT

4.1 STUDY AREA

Nethravathi River is a west-flowing river of Karnataka originating at Bangarabaliga gudda located at Western Ghats at an elevation of 1686 m. The river descends fast from the hills into steep valleys up to the foot of the Ghats and flows to join the Arabian Sea. The basin is spread over an area of 3314.43 km² lying between 12°30' to 13°15' north latitudes and 74°45' to 75°45' east longitudes as shown in Figure 4.1.

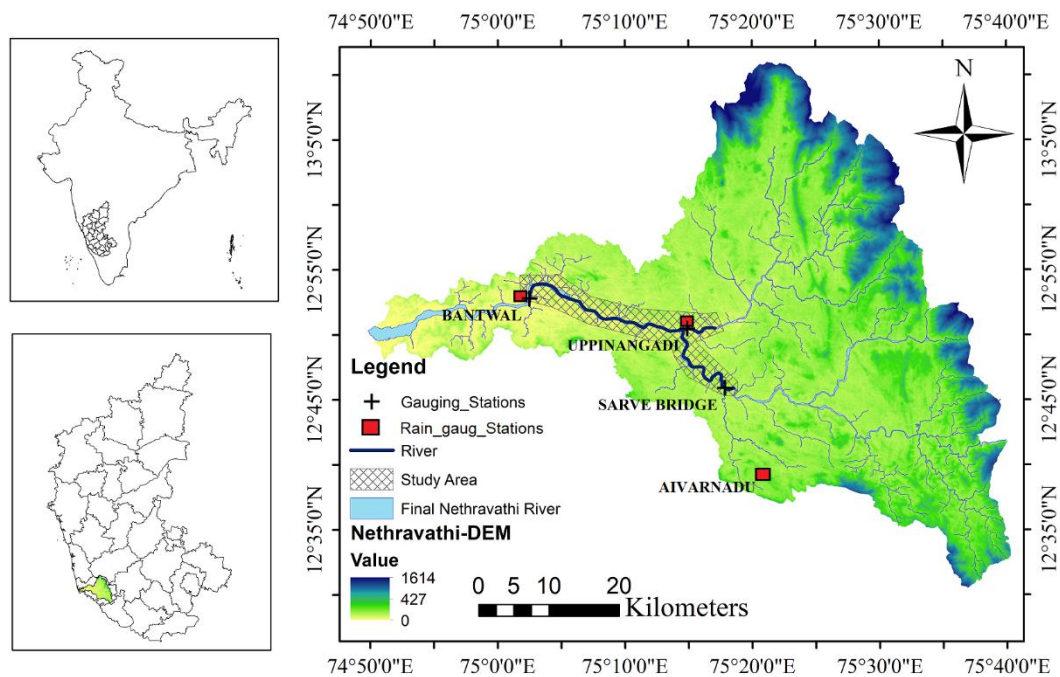


Figure 4.1 Geographic location of the Nethravathi basin

Nethravathi River originates at Bangrabalige valley, Yelaneeru Ghat in Kudremukh in Chikkamagaluru district of Karnataka, India. It merges with the Kumaradhara River at Uppinangadi before flowing to the Arabian Sea, south of Mangalore city. The total length of the river is 106 km.

4.1.1. Rainfall Pattern

The annual rainfall over the area varies between 1500 mm and 8000 mm. Rainfall in the Western Ghats occurs during three separate seasons, Pre-monsoon (March to May), South-west monsoon (June to September), and North-east monsoon (October to December). These three seasons respectively contribute about 4%, 90% and 6% of the total annual rainfall (Putty and Prasad 2000).

The average annual rainfall at Nethravathi Basin over the decade 2003-2013 is 3,922.5 mm. The standard deviation of rainfall over the decade was 383 mm. A maximum rainfall of 4,427.8 mm was experienced in the year 2009-2010. A major variation in rainfall has not be experienced over the decade. Even though the region receives an average annual rainfall of about 3,930 mm, it has non-uniform distribution with most of the rainfall confining to a few months of a year. In view of this, the region suffers from a prolonged dry period during February to May. The rainfall pattern for the study area based on the rain gauge data is presented in the Figure 4.2.

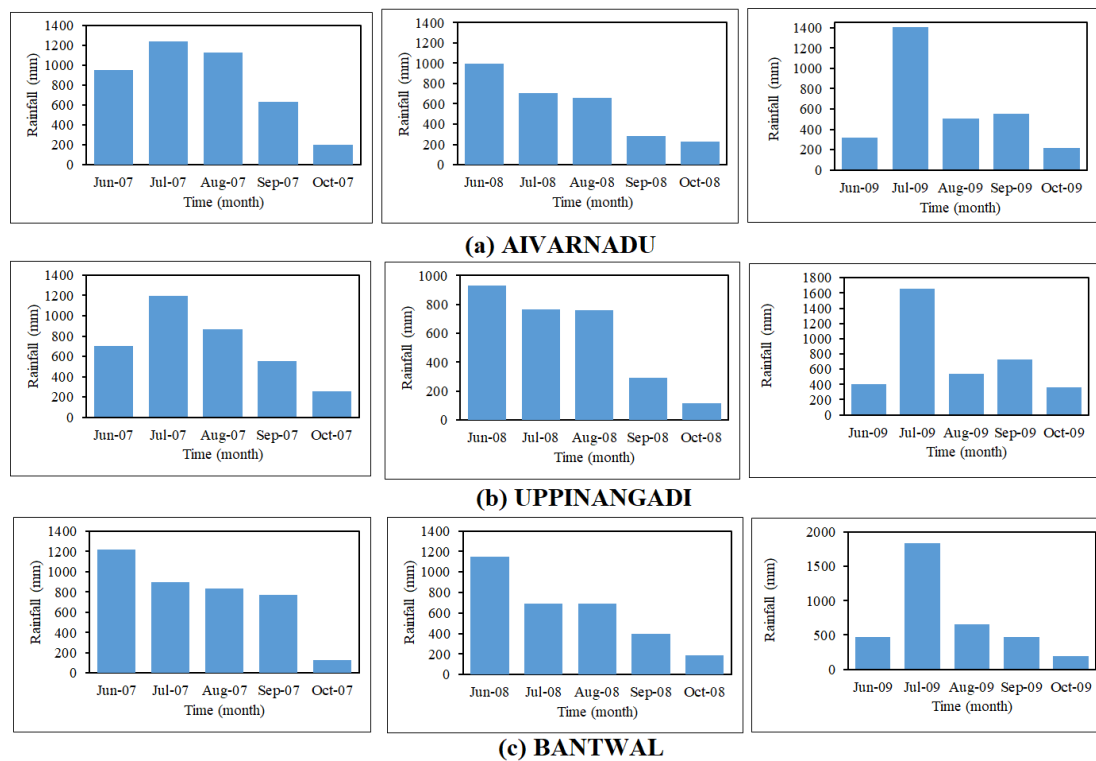


Figure 4.2 Rainfall pattern of Nethravathi basin

4.1.2. Climatology

The study area is marked by high intensity rainfall during monsoon, suppressive weather conditions in hot season and humidity throughout the year. The weather is cooler in the upstream part of the study area i.e., along the Western Ghats, compared to the coastal areas. The South-West monsoon period is relatively cooler with the daily mean temperature around 20°C. Whereas in the summer months of March to May, the daily mean temperature is around 35°C. The weather is humid throughout the year especially during South-West monsoon season since the mean humidity is always more than 85%. The sky is covered with dense clouds on most of the days and winds are strong mainly in the South Westerly direction during South-West monsoon period. Whereas, the number of such heavy clouded days is less during the post monsoon season. Otherwise, the area experiences a typical maritime climate, since it lies on the West Coast of India.

4.1.3. Population and Cities

It has been estimated that more than 40 Lakhs people are dependent on the waters of the Nethravathi river to meet their daily requirements and more than 10 Lakhs people are resided along the river side. Some of the prominent towns on the Nethravathi riverbanks are Belthangady, Dharmasthala, Uppinangady, Bantwal, Panemangalore, and Mangalore.

4.1.4. Geology and Soils

Migmatite Tonalitic Gneiss are the major rocks underlying in the basin, which are of Archean age and termed as one of the oldest rock formations in peninsular India. Metabasalt with thin iron stone formations are found in the upstream and thick patches of Charnockite (Orthopyroxene Granite) are noticed across the catchment.

Laterites are found to overlay on the preliminary rock formations. Laterites are formed due to weathering and leaching process because of heavy rainfall with alternating wet and dry periods. Due to intense leaching in the rainy season, a thin clay layer is formed below the porous laterites. The clay layer is about a meter or two

meter in thickness. The thickness of the laterites gradually decreases towards the coast. Thin alluvial sand covers these laterites. Alluvial, sandy and clayey-skeletal soils are observed in the coastal belt whereas fine, fine-loamy, loamy-skeletal soils are found in the top-surface of upstream hilly areas, forest, vegetation and river plain of the basin (Putty and Prasad 2000).

4.1.5. River drainage features

The area has adequate rainfall giving birth to numerous streams flowing through the Western Ghats, in small meandering channels within narrow steep valley. Streams descend down the Ghats and expand their channel at the wide valley floors. The cross-section and bed slopes are varying significantly in Nethravathi river due to natural process and human influences. Consequently, various sections of river fluvial channels are found to be decreased due to erosion and sand-mining activities in the river alluvial plain. However, the riverbed is noticed to be increasingly widened at different locations shifting of accumulated sediments.

4.1.6. River geomorphology

The riverbed comprises of paleo-river sediments (sand, gravels and pebbles) over irregular gneissic rock and boulders as observed across bridges and river banks. The floodplain of the river is covered with riparian vegetation and sand deposits are found along the meandering loops of island segments. The sand deposits in the river bed range from coarser sand particles with gravel at the confluences and finer sand particles near the river mouth. The decrease in riparian vegetation as well as variation in the river-morphological parameters tends to be the cause of dynamic changes in the hydraulic characteristics of the river's fluvial channel (Kumar et al., 2010).

The flood plain of the considered 45 km length of Nethravathi river consists of land use patterns such as agriculture land, built-up area and land cover patterns such as natural vegetation. The Manning's n for above mentioned land use and land cover classes were from representative values provided by Barnes (1967) and Chow (1959).

4.1.7. Challenges faced by Nethravathi River

Nethravathi River is important source of providing clean water for the Bantwal and Mangalore city. To ensure adequate water supply, especially during summer season, there are two vented dams which were built in this basin. The Nethravathi River Basin has been subjected to repetitive flooding during its history. Most of the severe floods occurred during the southwest monsoon period, which brought large volume of runoff to the Nethravathi River. The considered river reach of the Nethravathi basin is a vital part of the Nethravathi-Kumaradhara confluence posing challenge for the management of flood or surface water availability.

4.2. DATA COLLECTION

Table 4.1 summarizes the datasets and their common sources.

Table 4.1 List of datasets and sources

| Sl. No. | Data Type | Data Source |
|----------------|---|---|
| 1 | Terrain data (Digital Elevation Model data-SRTM) 30m resolution | USGS and Bhuvan websites |
| 2 | Toposheets of scale 1:50000 | Survey of India (SOI) |
| 3 | Morphological data (River geometry) | Extracted from DEM Central Water Commission (CWC) and Karnataka Public Works Department (KPWD) |
| 4 | Gauge and discharge data of rivers/streams | Central Water Commission (CWC) and Karnataka Public Works Department (KPWD) |

4.3. MODEL DEVELOPMENT AND DISCRETIZATION

In the present study, a hydraulic model is developed to represent the unsteady flow characteristics and flood routing in Nethravathi river basin, using HEC-RAS model.

The hydraulic modelling in HEC-RAS starts with data management. In this phase, geographic features in the real world are represented as through GIS operations of spatial registration and geo-referencing. This process optimizes the information calibration and collation processes and also preserve the intrinsic properties of the studied geographic feature in the real world. The GIS processes were completed within RAS Mapper in HEC-RAS 5.0. The finite difference model grid utilized for flood inundation mapping (RAS Mapper) is of 30m resolution interpolated using DEM data for river cross-section of 2 km for a length of 45 km. different time steps starting from 5 secs to 1hr, was attempted and it was found that 5 min is optimal and that is adopted in the present study.

4.3.1. Geometric data

Geometric data consists spatial geometrical inputs of the river network, DEM of the watershed, river system schematic, cross-section river geometry, channel and floodplain surface roughness.

a) River system schematic

The geometric data is developed by using HEC-GeoRAS and imported to HEC-RAS. The river system schematic imported by using Geometric data window. The analysis is done for the river based on reach by reach, starting from upstream till downstream. Figure 4.3 shows the schematic of the Nethravathi River system.

b) River cross section data

River cross section from the survey and extracted from DEM used as main geometric data for executing the hydraulic model. In the geometric window, a river network was created by adding 80 cross sectional data linked to each other from upstream to downstream. The 3 cross-sectional details namely Kumaradhara, Uppinangadi and Bantwal (Figure 4.1) are shown in Figure 4.4.

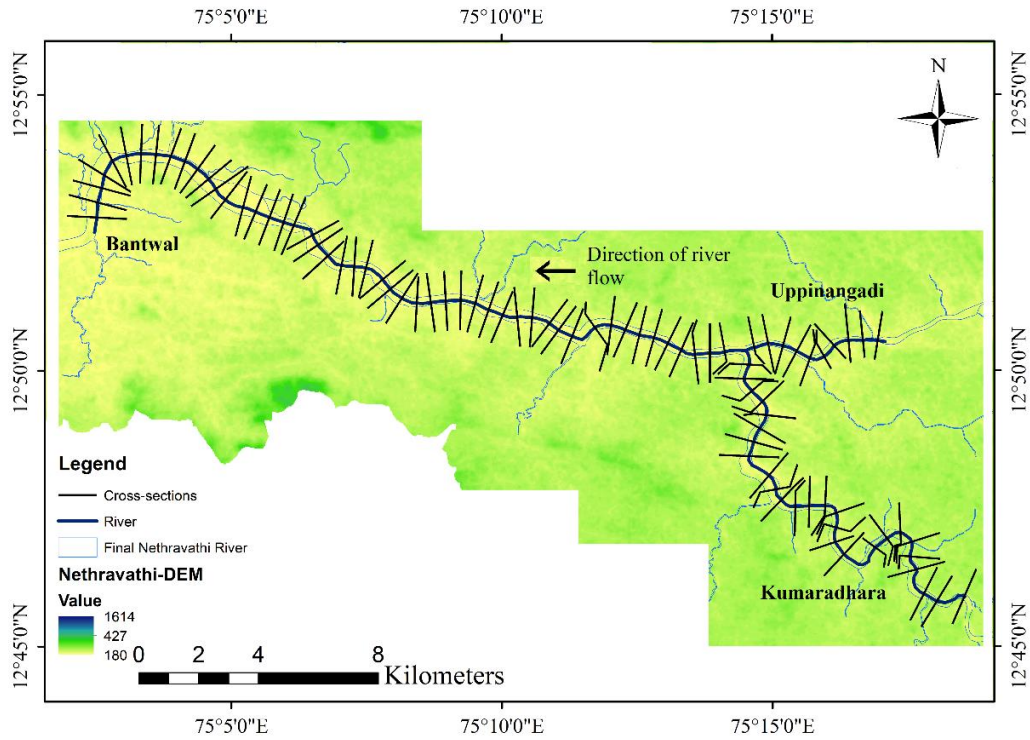


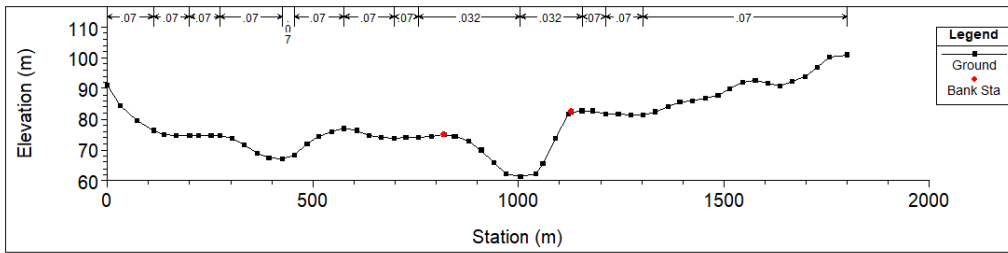
Figure. 4.3 Schematic of Nethravathi River

c) Roughness coefficient

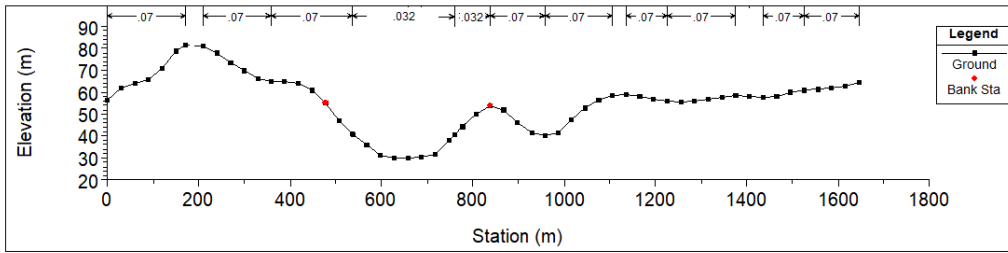
The river profiles were defined with Manning’s roughness coefficient (n), that describes the resistance to flow. Roughness characteristics of natural channels were assigned for Nethravathi river reach based on bed material, soil and channel characteristics as suggested by Barnes (1967) and Chow (1959) are represented in Table 4.2.

Table 4.2 Considered Manning’s values for the study (Chow, 1959)

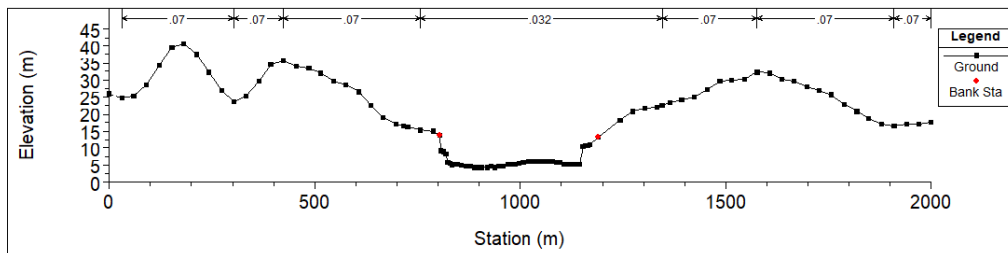
| Sl. NO | Type of Channel and Flood plain | Minimum | Normal | Maximum |
|--------|--|---------|--------|---------|
| 1 | Main Channel:- clean, straight, full stage | 0.025 | 0.030 | 0.033 |
| 2 | Main Channel:- weeds and stones | 0.035 | 0.045 | 0.050 |
| 3 | Floodplain:- Cultivated areas | 0.020 | 0.035 | 0.050 |
| 4 | Floodplain:- light brush and trees | 0.040 | 0.060 | 0.080 |
| 5 | Floodplain:- few own trees, little undergrowth, flood stage below branches | 0.070 | 0.080 | 0.100 |



(a)



(b)



(c)

Figure 4.4 The cross-sections of the river reach (a) Kumardhara (b) Uppanangadi and (c) Bantwal

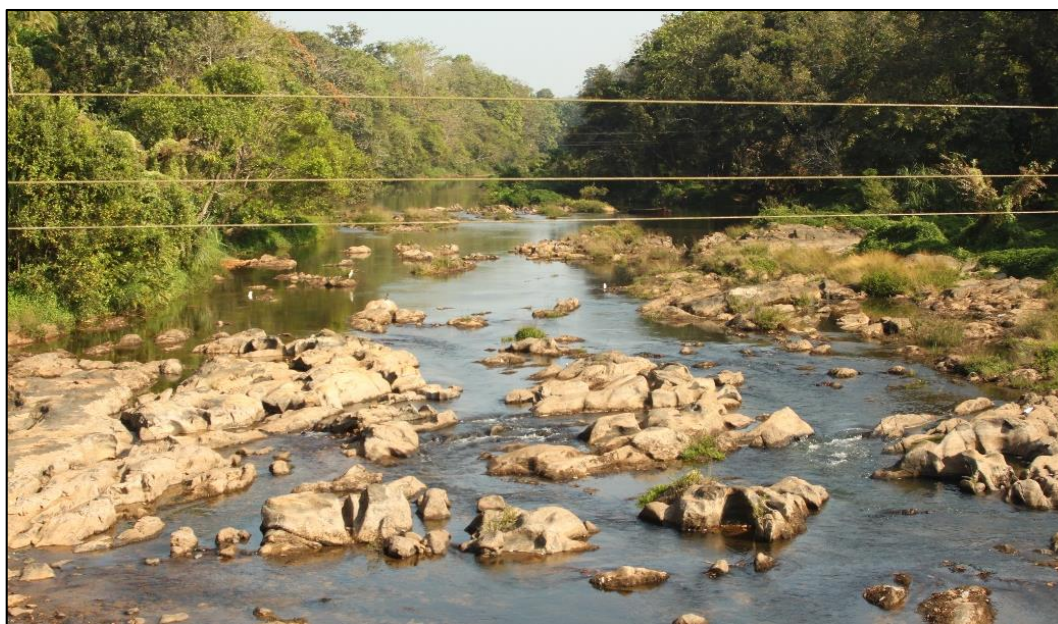


Figure 4.5 Bed material near Sarve bridge in Kumaradhara river reach

In the Figure 4.5, the river cross-section is observed to be deposited with coarse grained soil exposed with rocky strata and vegetation over the river bed as well as river bank. For the above case, the Manning's n value is considered as 0.035 to 0.05 based on Barnes (1967) and Chow (1959).



Figure 4.6 Bed material near Uppinangadi bridge in Nethravathi river reach

From the Figure 4.6, it can be observed that the river cross-section of along the Uppinangadi bridge consists of fine to medium grained soil over the river bed and continuous vegetation aligned in the river bed and river bank. The Manning's n value for the above circumstance is considered as 0.03 to 0.04 based on Barnes (1967) and Chow (1959).



Figure 4.7 Bed material near Bantwal in Nethravathi river reach

In the Figure 4.7, the wide cross-section of Nethravathi river at Bantwal is found to be fine sand deposited throughout the river bed. The Manning's n value is considered as 0.02 to 0.03 based on Barnes (1967) and Chow (1959).

Consequently, the roughness co-efficient has been varied from 0.030-0.070 in the calibration of hydraulic model throughout the Nethravathi river reach.

d) Expansion and Contraction Coefficient

The expansion and contraction coefficient were assigned manually into the HEC-RAS cross section data editor. From physical observation of the reach, the transition flow is gradual so the default value of expansion coefficient 0.3 and contraction coefficient 0.1 was used for the analysis

4.3.2. Boundary conditions

a) Initial condition

Flow data are imported into HEC-RAS to define boundary condition in order to model the real historical event. The flow hydrograph at Uppinangadi and Sarve bridge and normal depth (0.001) at Bantwal were considered as initial boundary conditions. Initially, the Manning's 'n' is considered about 0.03 - 0.07 based on riverbed material and channel characteristics. The initial flow for all Manning's n corresponds to non-uniform flow. The coefficients of contraction and expansion considered are 0.1 and 0.3, respectively, where the change in river cross section is small, and the flow is subcritical. The expansion and contraction values were used to evaluate the energy loss in the river flow.

b) Upstream - downstream boundary conditions

In this study, recorded upstream stream flow data at Uppinangadi and Sarve bridge for 2007 to 2010 flood event were assigned as the upstream boundary condition to the river model and normal depth was set as the downstream boundary condition to perform unsteady flow calculation. The final simulation process was to compute the unsteady flow model in the 'Run' windows. During the computation, 1D model HEC-RAS characterized the flow as unsteady, with the flow moving in a downstream direction

(1D) and the provided cross section as the whole characterization of the river environment. The extreme high discharge event simulations were performed and the outputs were analyzed. In the present study, upstream boundary conditions were defined using flow hydrographs obtained from KPWD at the upstream locations of Kumaradhara river and Uppinangadi as presented in Figure 4.8 and Figure 4.9. The downstream boundary conditions were defined using normal depth and flow hydrographs obtained from CWC at downstream location Bantwal as presented in Figure 4.10.

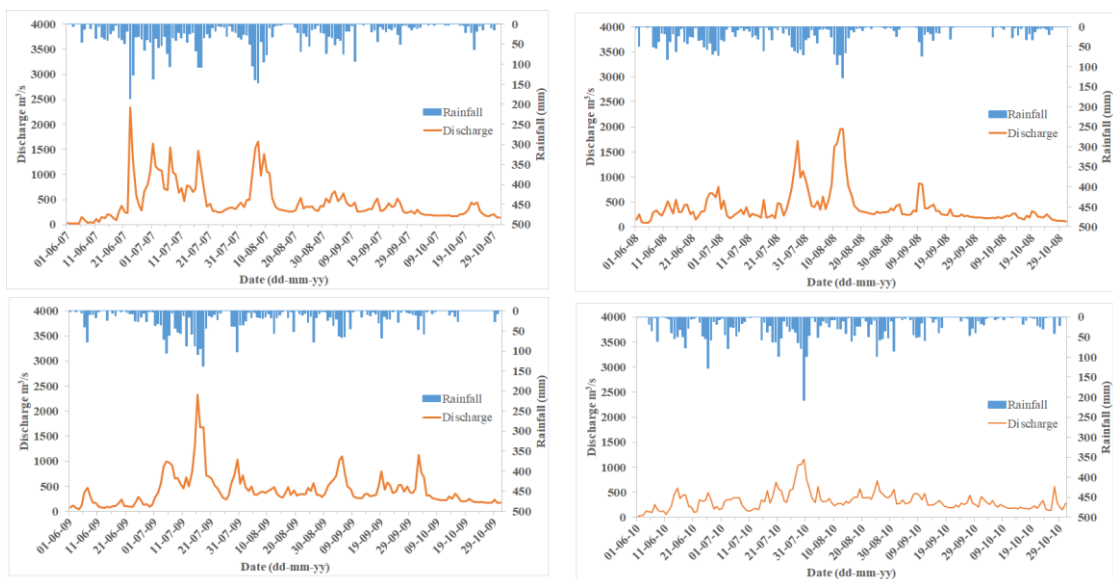


Figure 4.8 Flow hydrograph Sarve bridge gauging station for the period 2007 to 2010

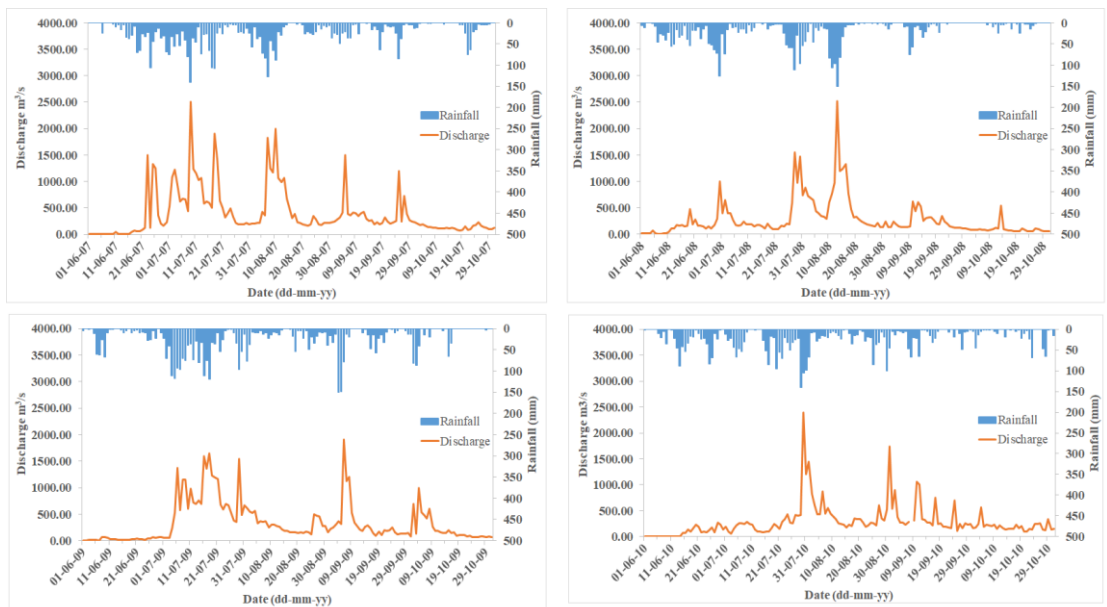


Figure 4.9 Flow hydrograph of Uppinangadi gauging station for the period 2007 to 2010

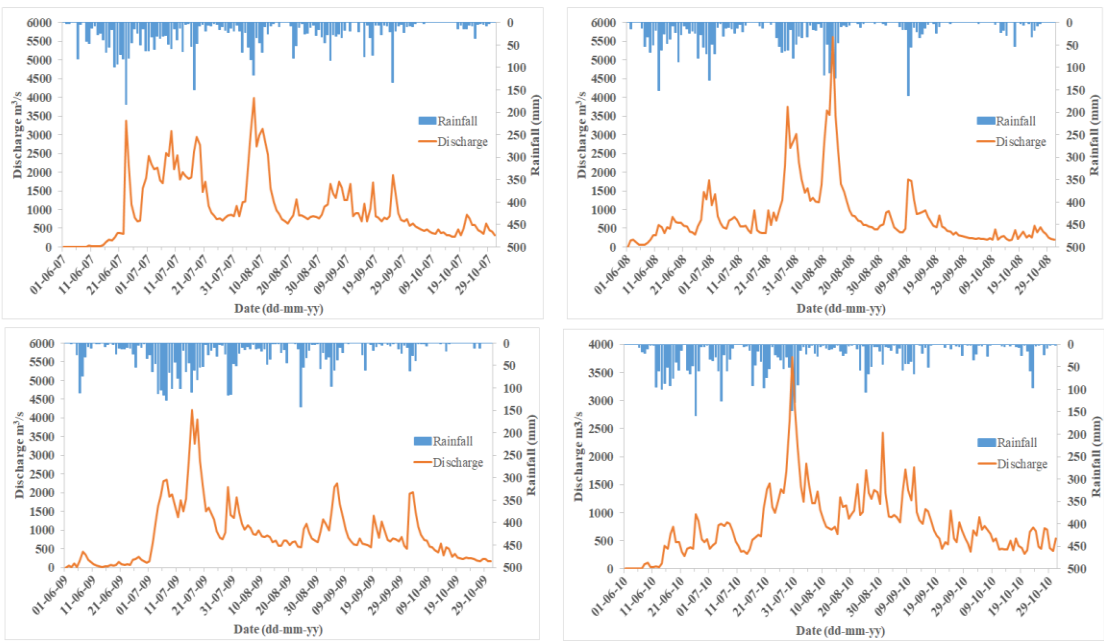


Figure 4.10 Flow hydrograph of Bantwal gauging station for the period 2007 to 2010

4.4. STEPS IN BUILDING A HEC-RAS MODEL

(i) Importing and Editing Geometric Data

In HEC-RAS, a new model is created to build the model and units using Geometry data as presented in Figure 4.11. The main component considered is the channel geometry. To analyse stream flow, HEC-RAS represents a stream channel and floodplain as a series of cross-sections along the channel. The geometry data describe the cross-section include the river station/cross-section, lateral and elevation coordinates for each terrain point, Manning's roughness coefficients (n), reach lengths between adjacent cross-section, left and right bank station, and channel contraction and expansion coefficients.

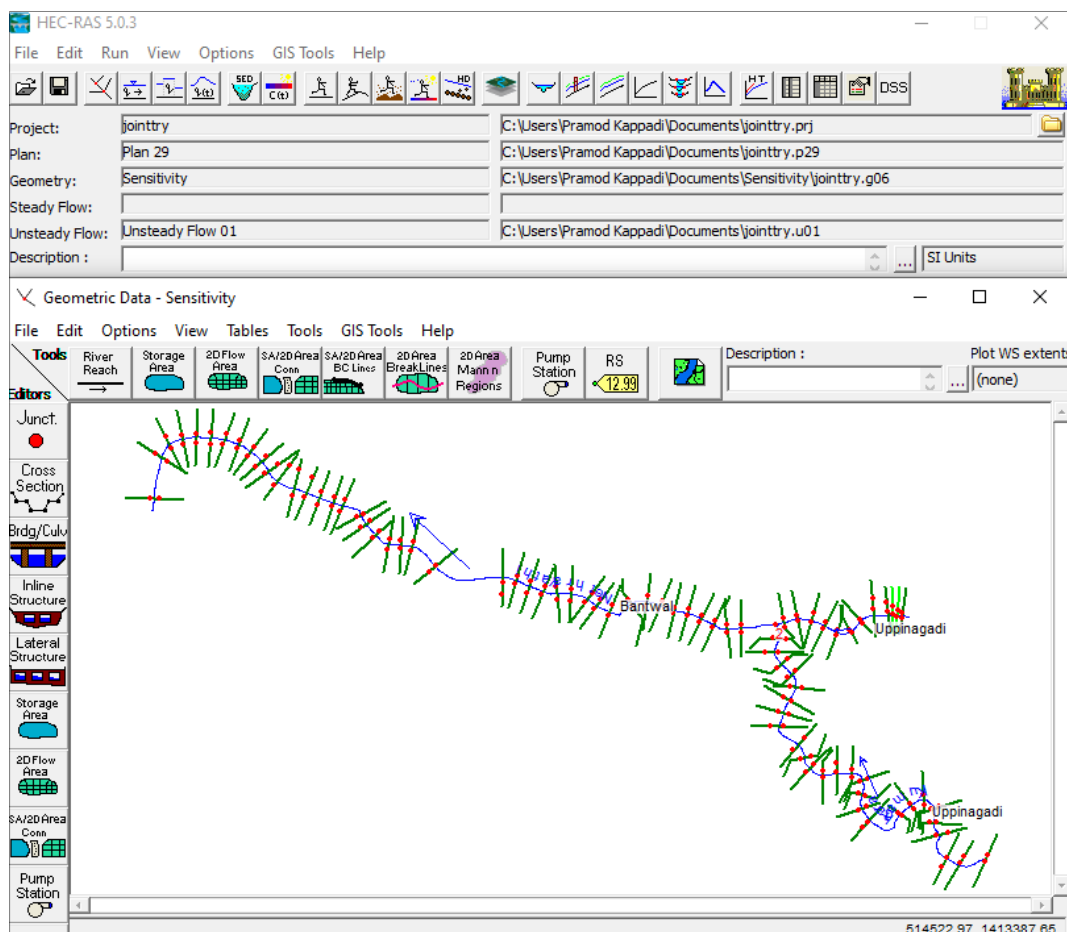


Figure 4.11 Geometric data

(ii) Importing and Editing Flow Data

The flow hydrograph and Normal depth data is imported as boundary condition in HEC-RAS model. At the upstream discharge hydrograph is assigned and Normal depth at downstream for simulating the unsteady flow data as presented in the Figure 4.12.

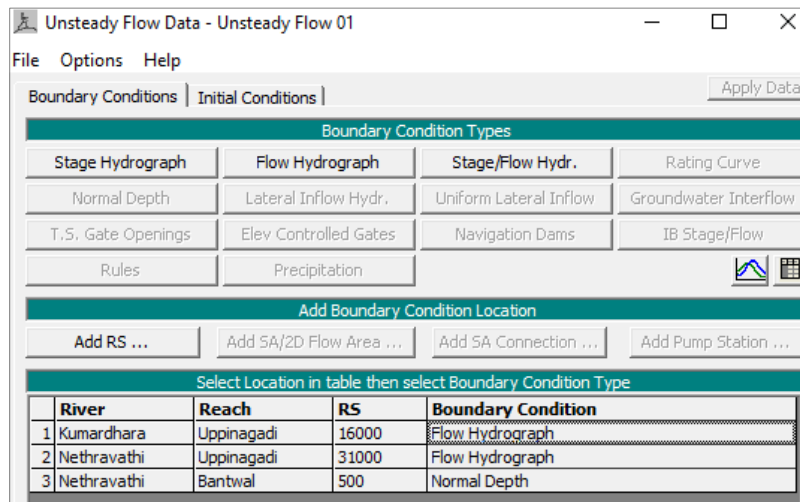


Figure 4.12 Unsteady flow data

(iii) Performing Unsteady Flow Calculation.

Once all of the geometry and unsteady flow data have been entered the begin performing the unsteady flow calculations as presented in the Figure 4.13. There are three components used in performing an unsteady flow analysis within HEC-RAS. These components are: a geometric data pre-processor, the unsteady flow simulator, and an output post-processor.

(iv) Checking and running the simulation

Prior to the unsteady simulation, the steady simulation is used to rectify the mistakes/errors if any are made during the preparation of the model. HEC-RAS model is run for the simulation after removing all the errors and warnings.

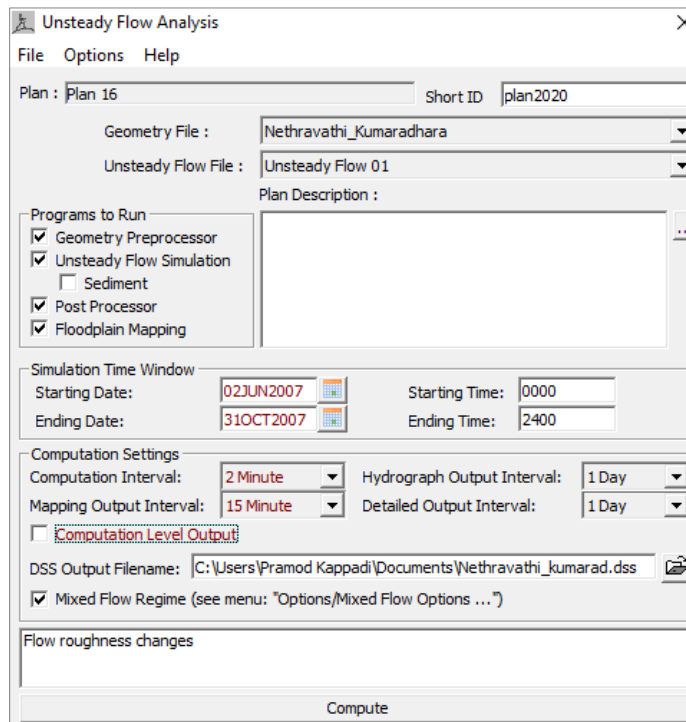


Figure 4.13 Unsteady Flow Calculation

(v) Viewing the results

There are several methods available with which to view HEC-RAS output, including cross-section profiles (Figure 4.14 & 4.15), perspective plots (Figure 4.16), and data tables (Figure 4.17) for all time steps from the simulated model. The HEC-RAS result consists of discharge and stage values.

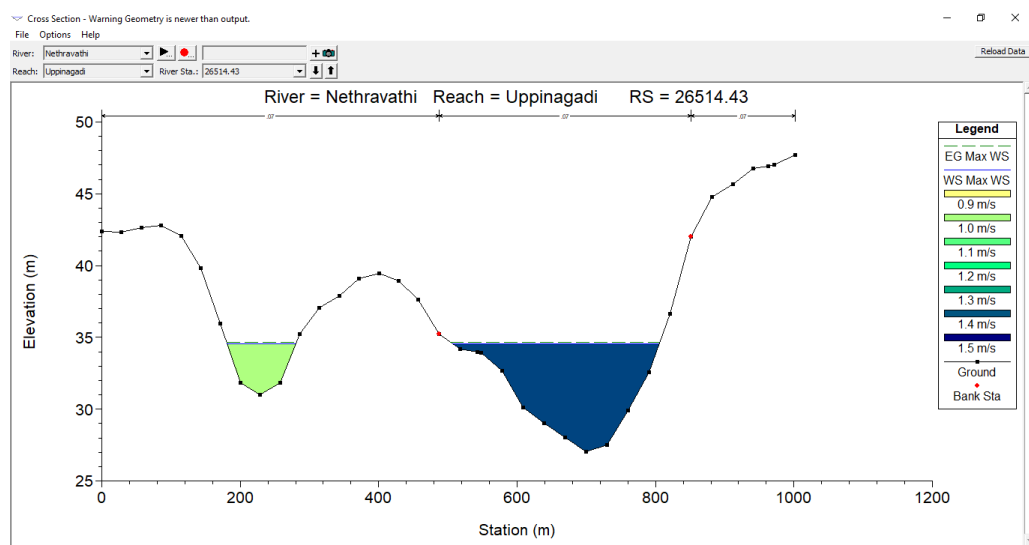


Figure 4.14 Results in cross sectional profile

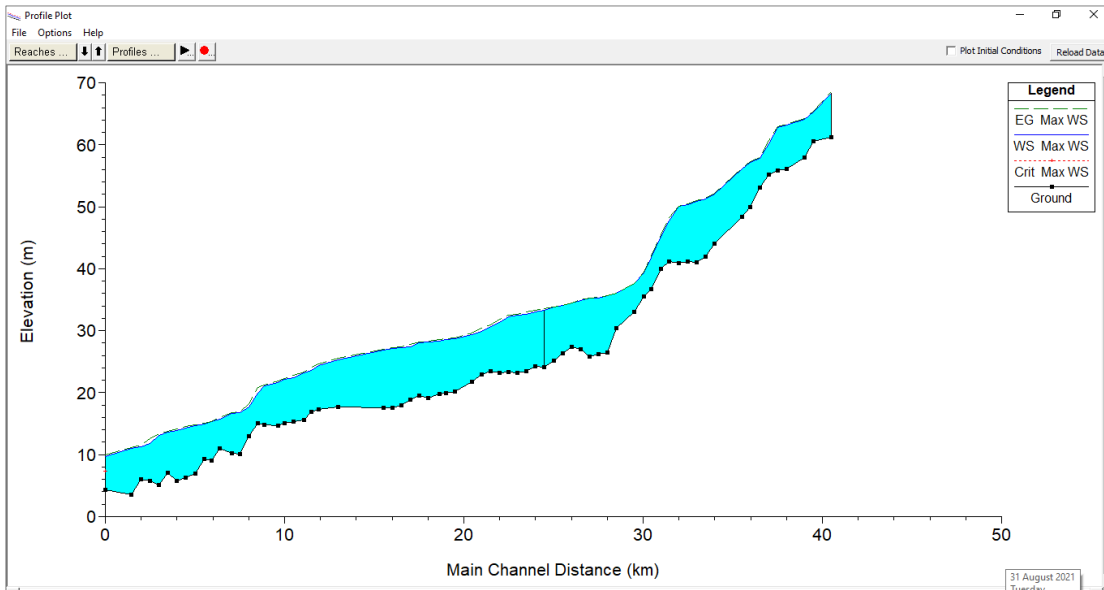


Figure 4.15 Results in longitudinal sectional profile

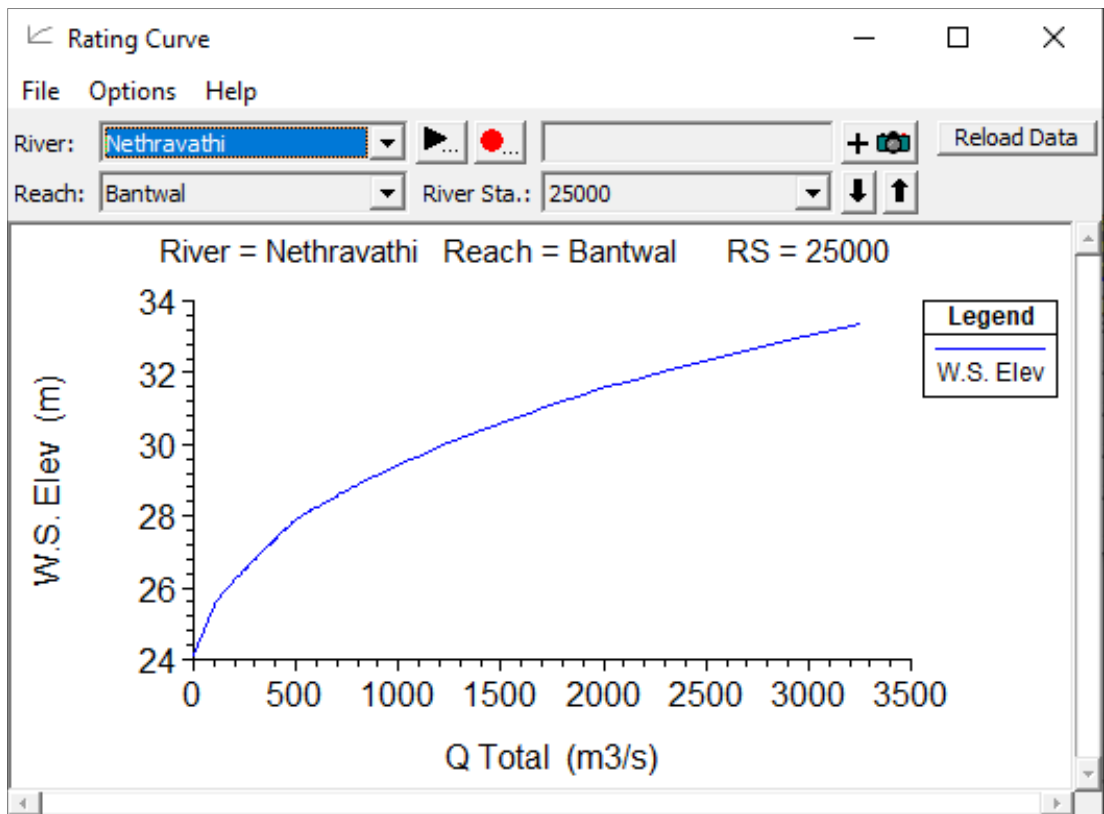


Figure 4.16 Results in terms of rating curve

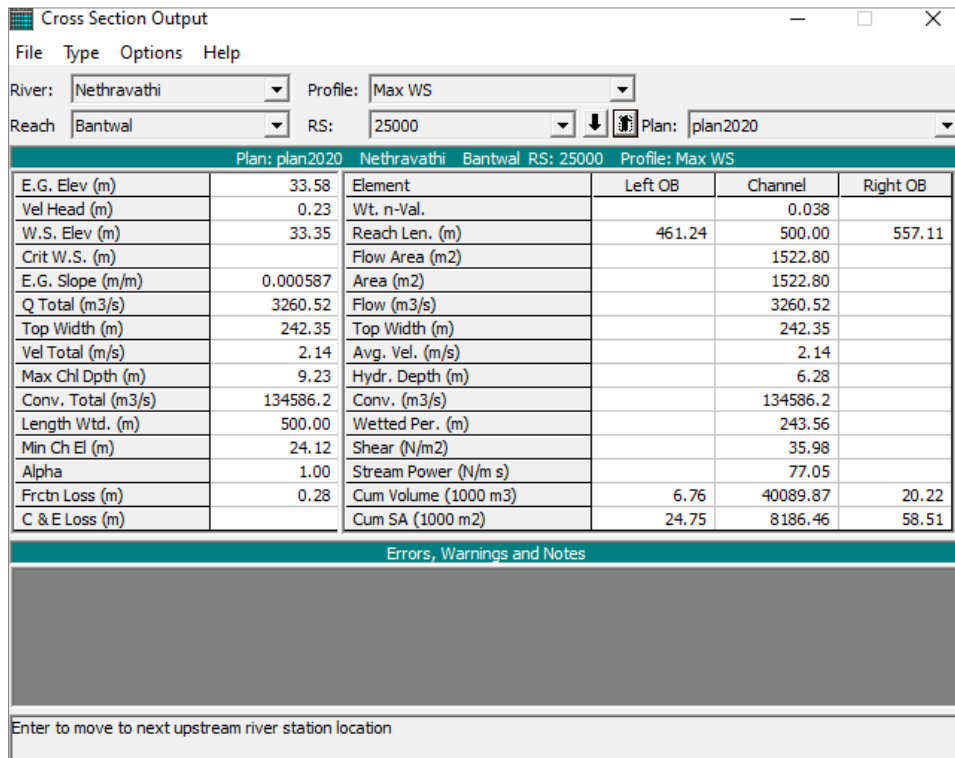


Figure 4.17 Cross sectional output

(vi) Inundation mapping

The visualization of inundated areas has been performed in the RAS Mapper for flow depth, velocity and inundated area as presented in the Figure 4.18. From this interface it is possible to store some results.

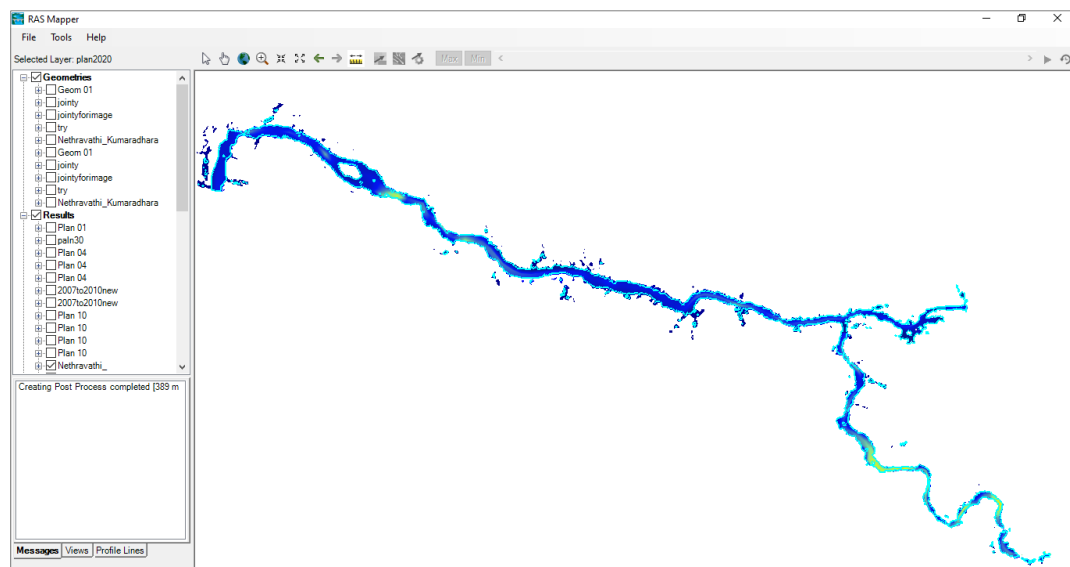


Figure 4.18 Inundation mapping as flow depth, velocity and inundated area

4.5. MODEL CALIBRATION AND VALIDATION

Model calibration is the process of adjusting model parameter values until model results match historical data. The process can be completed using engineering judgement by repeatedly adjusting parameters and computing and inspecting the goodness-of-fit between the computed and observed hydrographs. Significant efficiency can be realized with an automated procedure. The quantitative measure of the goodness-of-fit is the objective function. An objective function measures the degree of variation between computed and observed hydrographs. Parameter values are adjusted by the search, the hydrograph and objective function for the target element are recomputed. The process is repeated until the value of the objective function reaches the minimum to the best possible extent.

During calibration, model input parameters are systematically changed to match field data within satisfactory condition. Model calibration is carried out to simulate flow discharge and stage by analyzing set of parameters, boundary conditions and factors that influence unsteady flow.

The model was calibrated under unsteady-state condition for monsoon months of June to October 2007 to 2009. In the calibration task, the Manning's n values are varied by trial and error method until, a good match between computed and observed flow hydrograph is achieved. The observed flow discharge available from Central Water Commission (CWC) and Karnataka Public Works Department (KPWD). The developed hydraulic model was validated for the monsoon months of June to October 2010. Calculated flow discharge at the downstream boundary for flood events was fitted to the observed discharge to validate the simulation. In this study, the calibration values of Manning's n that gave the best agreement between observed and simulated results were equal to 0.032 for the main channel and 0.07 for the floodplain.

CHAPTER 5

RESULTS AND DISCUSSION

5.1 GENERAL

In the present study, a hydraulic model is developed for unsteady flow simulation using HEC-RAS. The study focused on the simulation of stage and discharge in the study area using hydrodynamic modeling, effect of roughness coefficient in natural river, flood inundation mapping of the study area and sensitivity parameter of hydraulic model. The model is calibrated and validated using observed discharge and stage data. The results are discussed in the following sections.

5.2 SIMULATION FOR UNSTEADY FLOW CHARACTERISTICS

Manning's roughness coefficients "n" of the riverbed and banks were considered as the calibration parameters during the calibration of HEC-RAS model. In the HEC-RAS model, the global value of "n" refers to the Manning's roughness coefficient for the entire river system of the study area unless local values are specified which override the global value. Manning's roughness coefficients were noted from Patro et al. (2009a), Patro et al.(2009b), Samantaray et al. (2015), and Jena et al. (2016). The values of roughness coefficient for study reach are found to be in the range of 0.030–0.07 (Chow 1959). The daily discharge is set as an upstream boundary condition and normal depth (friction slope=0.001) as a downstream boundary condition. The process of calibration was initiated with a single n value of 0.03 for the river reach. During the process of calibration, the n values for Nethravathi rivers were adjusted to obtain a close agreement between the observed and computed discharge and stage at Bantwal gauging station in the river reach. The HEC-RAS model is calibrated for the monsoon and post monsoon period of the year 2007 and 2008 from 1st June to 31 October. During calibration, the process of adjusting the global and local values of "n" is continued until the observed and the computed discharge and stage values are in close agreement. The calibrated HEC-RAS model is validated for the monsoon and post monsoon period

from 1st June to 31st October of the year 2009. The validation of the model is carried out for the Bantwal gauging station which used during calibration.

5.2.1. Model Calibration

The observed and computed discharge hydrographs which are calibrated for the year 2007 at Bantwal gauging station are presented in the Figure 5.1.

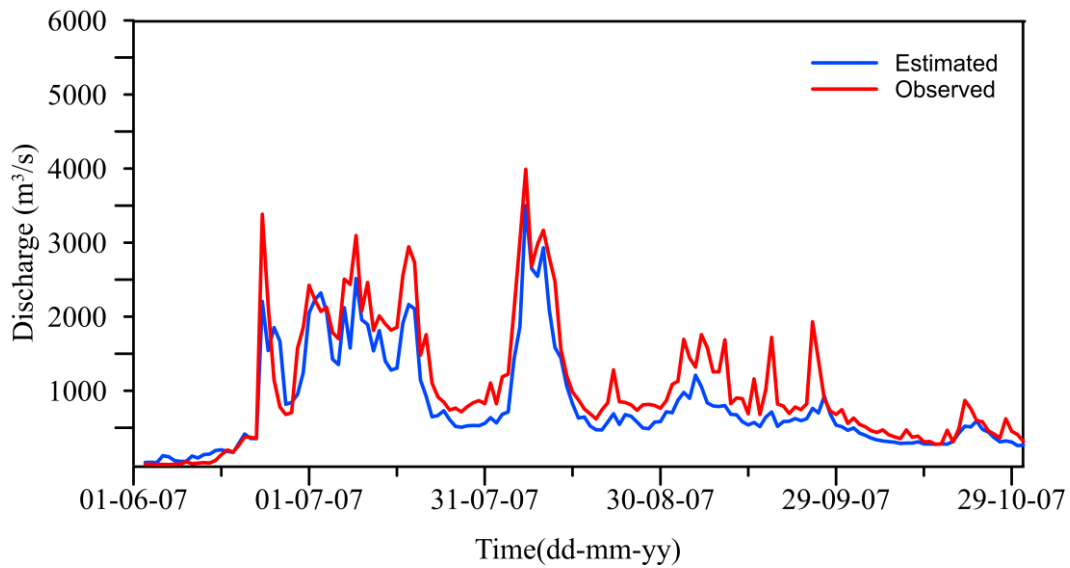


Figure 5.1 Observed vs computed discharge hydrograph for calibration period (2007) at Bantwal gauging station

From the Figure 5.1, it is observed that the observed and computed discharge hydrographs are reasonably matching except at the peak flow. Accordingly, the following observations are made. The simulated discharges are lower than those observed in most periods. This is due to the existence of canals and small branches reaching the Nethravathi River at different locations; these branches and canals have not been considered in the present research. The simulated discharge is overestimated when the flow is less than 500 m³/sec and underestimated when the flow is more than 500 m³/sec for calibration year 2007. The model result showed good consensus between computed and observed flow discharge. The computation accuracy of peak discharge is about 81% for the year 2007. Figure 5.2 shows the scatter plot with 1:1 line of the observed and simulated discharge after calibration year 2007. From the Figure 5.2, it is observed that, the model correlation is acceptable with co-efficient values close to 0.910

in the calibration year 2007. This shows that the calibration of hydraulic model is reasonably well applicable for analyzing streamflow.

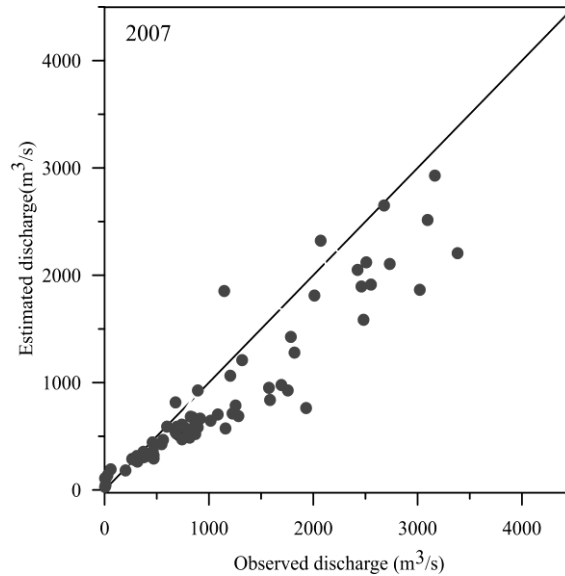


Figure 5.2 Scatter plot of discharge for the calibration year 2007 at Bantwal gauging station

The observed and computed stage hydrographs which are calibrated for the year 2007 at Bantwal gauging station are presented in the Figure 5.3.

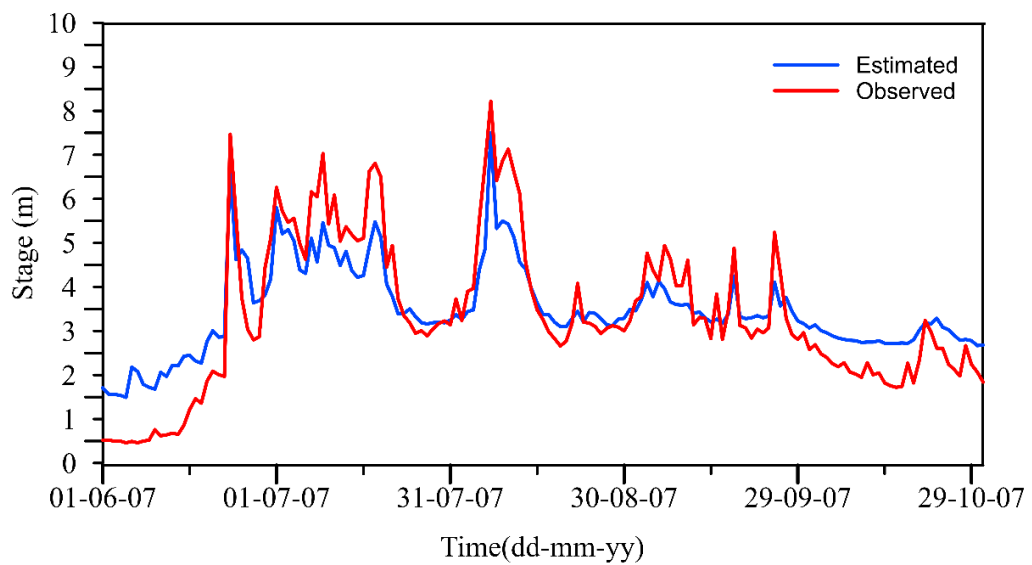


Figure 5.3 Observed vs computed stage hydrograph for calibration period (2007) at Bantwal gauging station

From the Figure 5.3, a clear overall agreement between observed and simulated stage can be seen during the low to medium flow conditions. The following analysis is made subsequently. As can be seen in Figure 5.3, the highest peak stage was underestimated by approximately 0.72 m. It is worth noting that the number of data containing high flows was significantly lower than medium to low stage. Consequently, scarce peak water level data was available for model calibration, which led to less efficient performance of the model over extreme events. Additionally, the measurement of gauging stations might not measure the water level accurately over the flooding events. Therefore, such difference between observed and simulated peak might be also the result of poor and uncalibrated measurements. The variation in peak stage value for the Nethravathi river show a good agreement between the observed and computed peak stage.

Figure 5.4 shows the best fit for observed and computed stage in the calibration year 2007 at Bantwal gauging station.

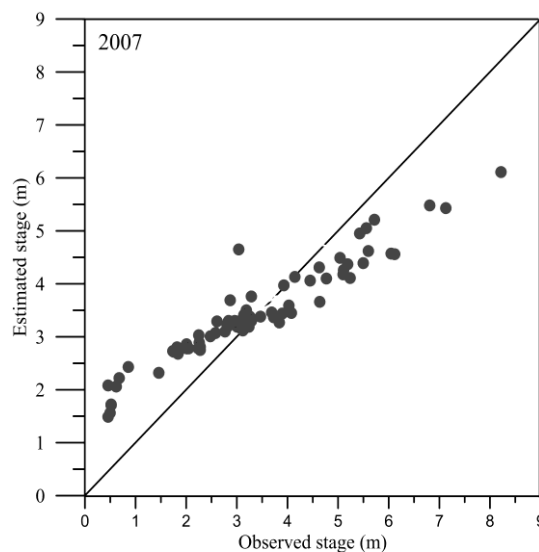


Figure 5.4 Scatter plot of stage for the calibration year 2007 at Bantwal gauging station

The simulation results for the calibration are compared with the observed stage and are presented in Figure 5.4 which shows the correlation of observed and simulated stage. The simulated results give R^2 statistics of 0.892 which show higher correlation between observed and simulated stage. The performance of the model during calibration is evaluated using four error functions presented in Table 5.1.

The observed and computed discharge hydrographs which are calibrated for the year 2008 at Bantwal gauging station are presented in the Figure 5.5.

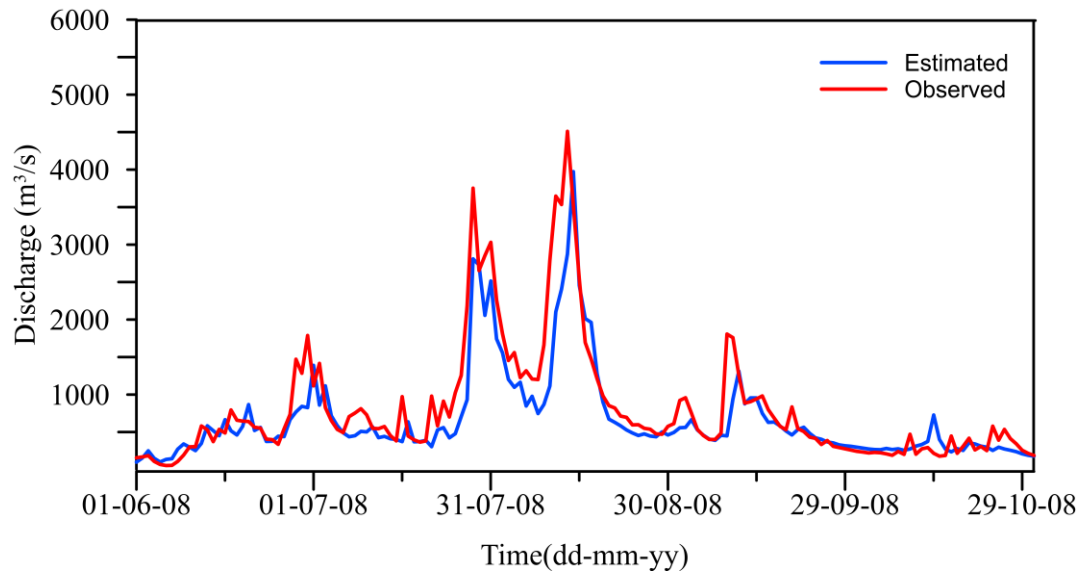


Figure 5.5 Observed vs computed discharge hydrograph for calibration period (2008) at Bantwal gauging station

From the Figure 5.5, it is observed that the observed and computed discharge hydrographs are reasonably matching except at the peak flow. Accordingly, the following observations are made. The simulated discharges are lower than those observed in most periods. For same reason as explained in above section the simulated discharge is under-estimated when the flow is less than $650 \text{ m}^3/\text{sec}$ and overestimated when the flow is more than $650 \text{ m}^3/\text{sec}$ for calibration year 2008. The model result showed good consensus between computed and observed flow discharge. The computation accuracy of peak discharge is about 88% for the year 2008.

Figure 5.6 shows the best fit for observed and computed discharge in the calibration year 2008 at Bantwal gauging station.

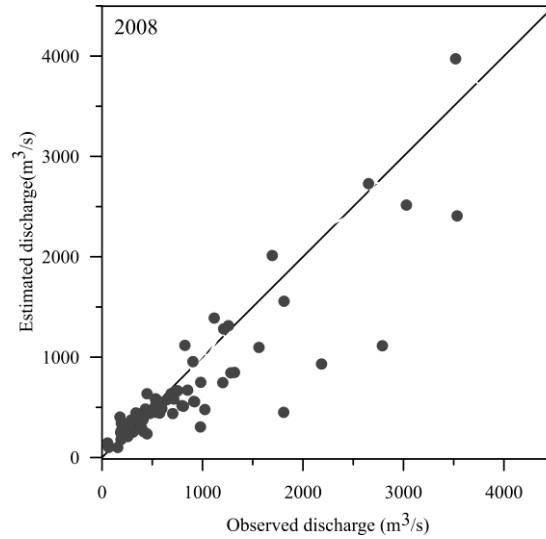


Figure 5.6 Scatter plot of discharge for the calibration year 2008 at Bantwal gauging station

From the Figure 5.6, it is observed that, the model correlation is acceptable with coefficient values close to 0.917 in the calibration year 2008. This shows that the calibration of hydraulic model is reasonably well applicable for analyzing streamflow.

The observed and computed stage hydrographs which are calibrated for the year 2008 at Bantwal gauging station are presented in the Figure 5.7.

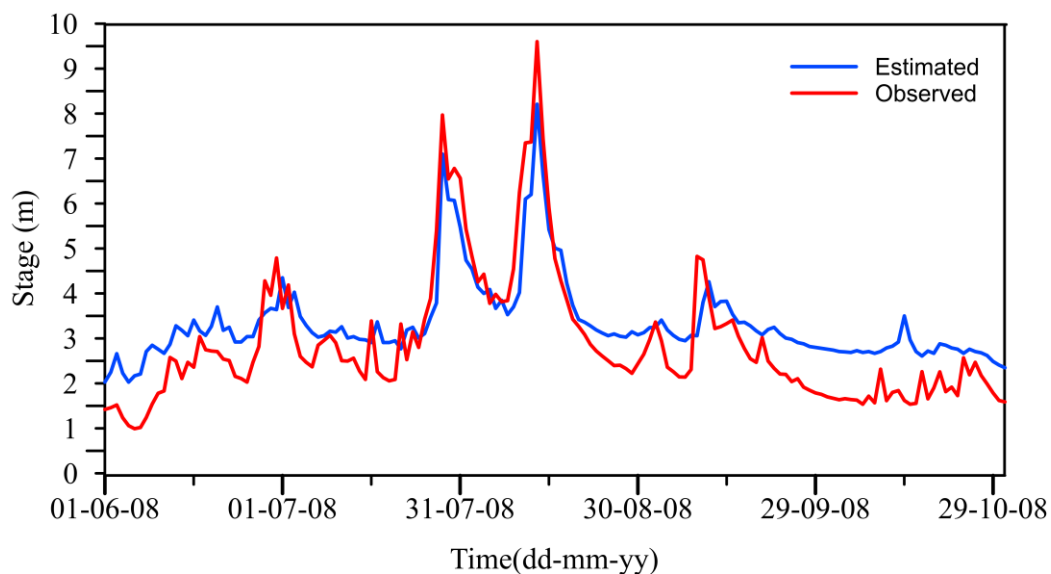


Figure 5.7 Observed vs computed stage hydrograph for calibration period (2008) at Bantwal gauging station

From the Figure 5.7, a clear overall agreement between observed and simulated stage can be seen during the low to medium flow conditions. The following analysis is made subsequently. As can be seen in Figure 5.7, the highest peak stage was underestimated by approximately 0.6 m. It is worth noting that the number of data containing high flows was significantly lower than medium to low flow. Consequently, scarce peak water level data was available model calibration, which led to less efficient performance of the model over extreme events. Additionally, the measurement of gauging stations might not measure the water level accurately over the flooding events. Therefore, such difference between observed and simulated peak might be also the result of poor and uncelebrated measurements. The variation in peak stage value for the Nethravathi river show a good agreement between the observed and computed peak stage. Thus, the peak stage value which are of utmost importance in the present flood inundation study are preserved during the calibration process.

Figure 5.8 shows the best fit for observed and computed stage in the calibration year 2008 at Bantwal gauging station

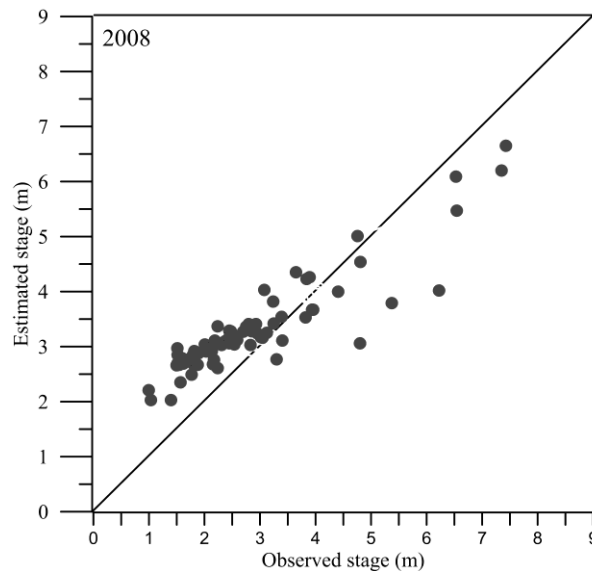


Figure 5.8 Scatter plot of stage for the calibration year 2008 at Bantwal gauging station

The simulation results for the calibration are compared with the observed stage and are presented in Figure 5.8 which shows the correlation of observed and simulated stage. The simulated results give R^2 statistics of 0.923 which show higher correlation between

observed and simulated stage. The performance of the model during calibration is evaluated using four error functions presented in Table 5.1.

In the present study, roughness factor is defined for hydraulic model depending upon the peak discharge. The roughness factor is suitably varied in the model, yet the value might be limited for initial offset and end point of monsoon. During calibration, roughness factors are varied by trial and error method for the Nethravathi river reach cross-section. Consequently, prediction of hydraulic model might have stream-lined for average depth and flood conditions rather than minimum depth for the variation in roughness factors. This is due to the limitation of present study in the characterization of roughness coefficient in the river bed and flood plain.

Table 5.1. Model evaluation criteria for calibration period

| Perform Indices | Calibration period | | | |
|--|--------------------|-------------------------------|-----------|-------------------------------|
| | 2007 | | 2008 | |
| | Stage (m) | Discharge (m ³ /s) | Stage (m) | Discharge (m ³ /s) |
| Coefficient of Determination (R ²) | 0.892 | 0.910 | 0.923 | 0.917 |
| Nash-Sutcliffe efficiency (NSE) | 0.840 | 0.830 | 0.879 | 0.858 |
| index of agreement (d) | 0.891 | 0.859 | 0.971 | 0.920 |
| Normalized Root Mean Squared Error (NRMSE) | 0.197 | 0.489 | 0.158 | 0.476 |
| Mean Absolute Error(MAE) | 0.213 | 0.401 | 0.123 | 0.317 |

5.2.2. Model validation

After the model calibration, the model was validated using the daily discharge and stage values at Bantwal gauging station. Figure 5.9 indicates the compared discharge values of the observation and simulation at Bantwal station during the validation period.

It is apparent that both discharge values fit very well. The peak discharge computation accuracy is approximately 80% for validation period 2009.

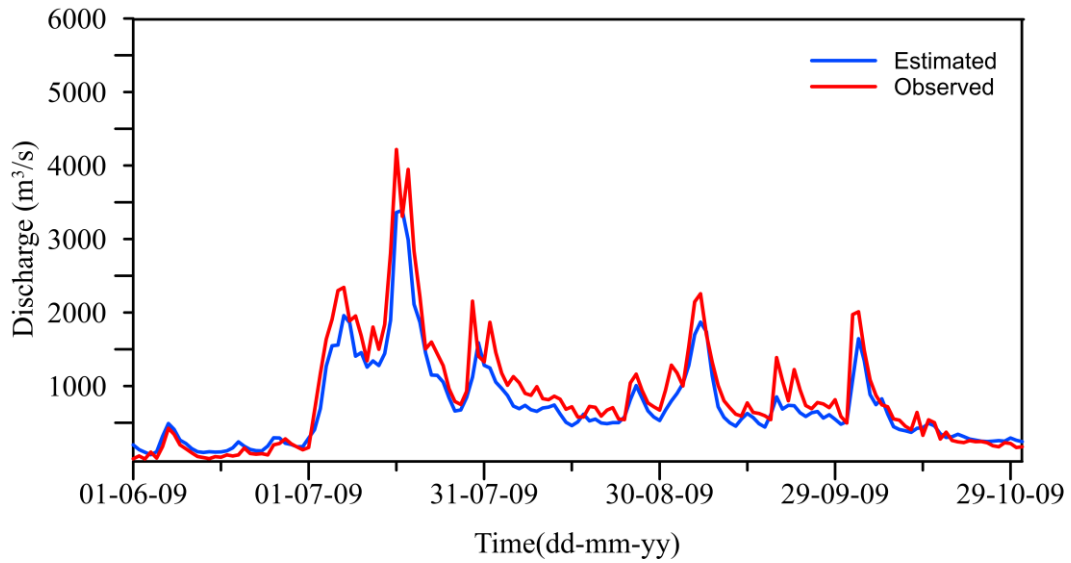


Figure 5.9 Observed vs computed discharge hydrograph for validation period (2009) at Bantwal gauging station

Figure 5.10 shows the best fit for observed and computed discharge in the validation year 2009 at Bantwal gauging station.

From the Figure 5.10, it is observed that, the model correlation is acceptable with coefficient values close to 0.840 in the validation period 2009. This shows that the calibration of hydraulic model is reasonably well applicable for analyzing streamflow.

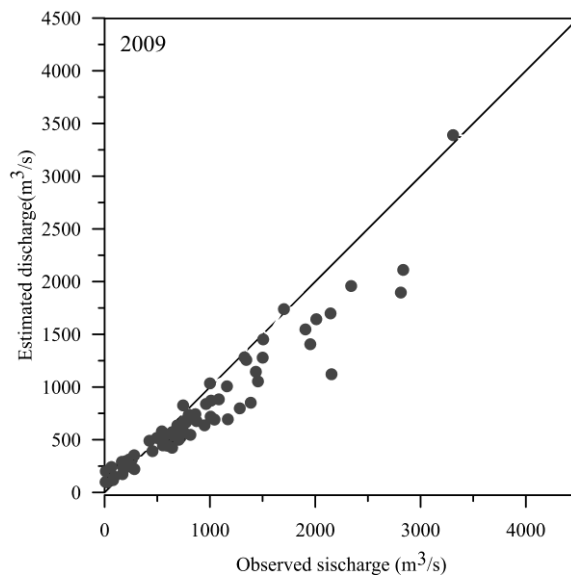


Figure 5.10 Scatter plot of discharge for validation period (2009) at Bantwal gauging station

The observed and computed stage hydrographs which are calibrated for the year 2008 at Bantwal gauging station are presented in the Figure 5.11.

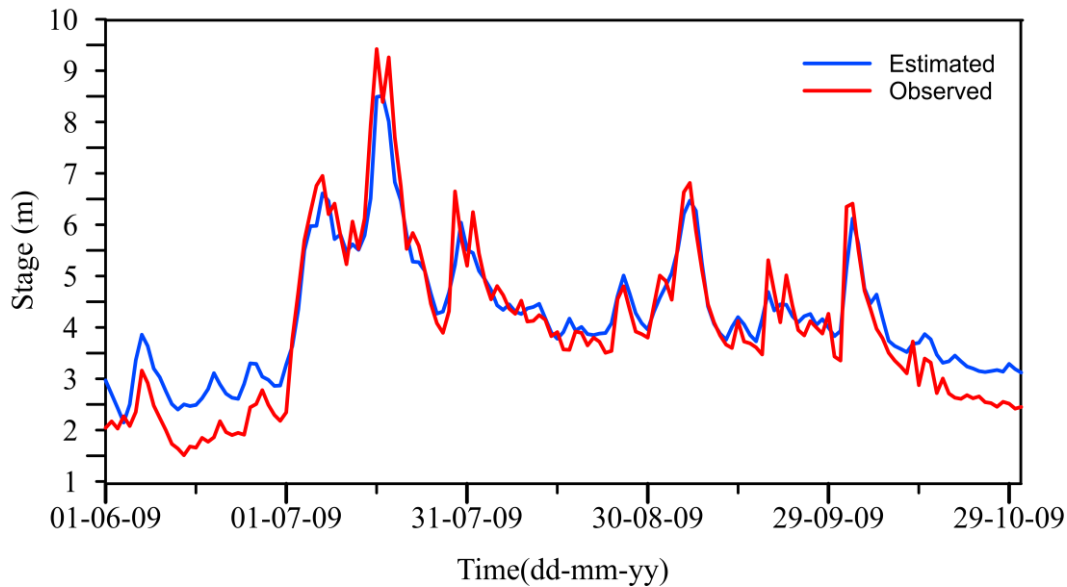


Figure 5.11 Observed and estimated discharge and stage hydrograph at Bantwal station of validation period (2009) at Bantwal gauging station

Figure 5.11 indicates the compared stage values of the observation and simulation at Bantwal station during the validation period. A clear overall agreement is seen between observed and simulated stage values. The following analysis is made subsequently. As can be seen in Figure 5.11, the highest peak stage was underestimated by approximately 0.72 m. The simulated stage is over-estimated when the water level is less than 3.5m and under-estimated when the flow is more than 8.5m for validation period 2009.

In the upstream section of study area, the average minimum depth was found to be 5 m and average maximum depth of the river is found to be 6 m. Peak stage was observed to decline after each rainfall event/storm due to rainfall distribution over the area and river bed variation in longitudinal slope. The steep inclined river bed with irregular vegetation and boulders along the river influences the river stage average depth of river to diminish after the peak discharge. In the downstream section of study area, the average minimum depth was found to be 8 m and average maximum depth was found to be around 10 m.

Figure 5.12 shows the best fit for observed and computed stage in the validation period 2009 at Bantwal gauging station.

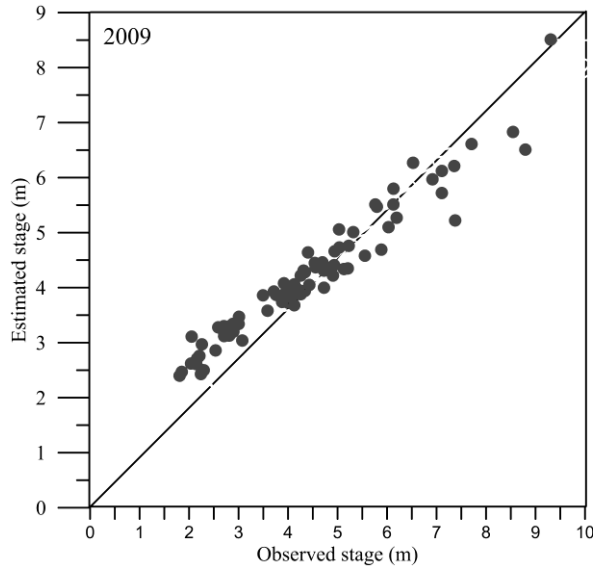


Figure 5.12 Scatter plot of the observed and estimated stage for validation period (2009) at Bantwal gauging station

The simulation results for the validation are compared with the observed stage and are presented in Figure 5.12 which shows the correlation of observed and simulated stage. The simulated results give R^2 statistics of 0.918 which show best correlation between observed and simulated stage. The performance of the model during validation period is evaluated using five error functions presented in Table 5.2.

Table 5.2. Model evaluation criteria for validation period

| Perform Indices | Validation period (2009) | |
|--|--------------------------|-----------------------|
| | Stage (m) | Discharge (m^3/s) |
| Coefficient of Determination (R^2) | 0.843 | 0.840 |
| Nash-Sutcliffe efficiency (NSE) | 0.789 | 0.704 |
| index of agreement (d) | 0.969 | 0.945 |
| Normalized Root Mean Squared Error (NRMSE) | 0.171 | 0.357 |
| Mean Absolute Error(MAE) | 0.160 | 0.300 |

The error function values during validation are found to be marginally lower in comparison to calibration results. There is a very close agreement of the estimated and observed stage value, both during calibration as well as validation. Thus, considering the overall values of the error functions it is found that the model performs reasonably well during validation.

Therefore, the calibrated and validated HEC-RAS model was used to determine the effect of roughness coefficient on discharge and stage of flow. Based on the calibrated model, discharge and stage at any cross-section along the length of the river can be predicted separately with the adoption of this hydraulic modelling approach.

5.3 EFFECT OF ROUGHNESS COEFFICIENT IN NATURAL RIVER

In the study, effect of the roughness coefficient on discharge and stage are carried out. However, it was found that the effect of roughness co-efficient on discharge is negligible compared to river-stage values. The stage hydrograph at Bantwal station for the year 2007, 2008 and 2009 for different Manning's n obtained from HEC-RAS model are shown in Figure 5.13 to Figure 5.15. The initial flow for the all Manning's n corresponds to non-uniform flow with discharge $100 \text{ m}^3/\text{sec}$. Also, the friction slope is computed using Manning's equation with different roughness coefficient which is used at a downstream boundary condition. Varied n from 0.03 to 0.07 with an increment $\Delta n = 0.01$.

5.3.1 Impact of Manning's n on river stage

Computed stage hydrograph for different Manning's n 0.030 to 0.070 values for the year 2007 is shown in Figure 5.13.

From Figure 5.13, it can be noted that there is a significant effect on stage with respect to roughness coefficient for the year 2007. Increase in roughness coefficient from $n = 0.03$ to $n = 0.04$ leads to an 17.75% increase in depth of flow, from $n = 0.04$ to $n = 0.05$ leads to a 6.80% increase in depth of flow, from $n = 0.05$ to $n = 0.06$ leads to an 8.44% increase in depth of flow and from $n = 0.06$ to $n = 0.07$ leads to a 7.77% increase in

depth of flow. The computed peak stages are 4.62m, 5.44m, 5.81m, 6.30m, and 6.79m when $n = 0.03$, $n=0.040$, $n=0.050$, $n=0.060$, and $n=0.070$ respectively.

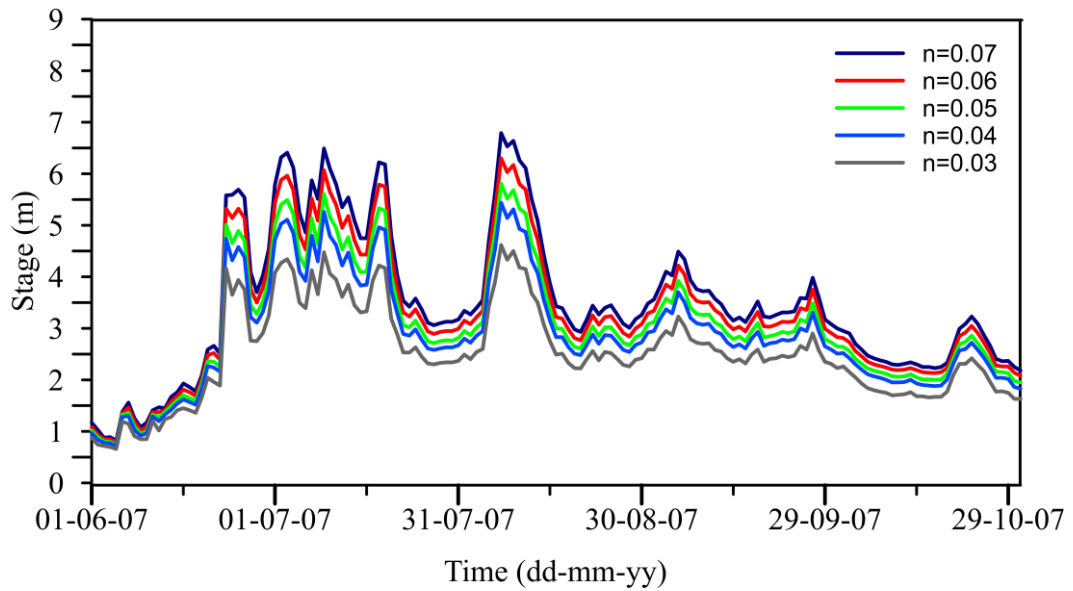


Figure 5.13 Stage hydrograph for different Manning's n values for the year 2007

Computed stage hydrograph for different Manning's n 0.030 to 0.070 values for the year 2008 is shown in Figure 5.14.

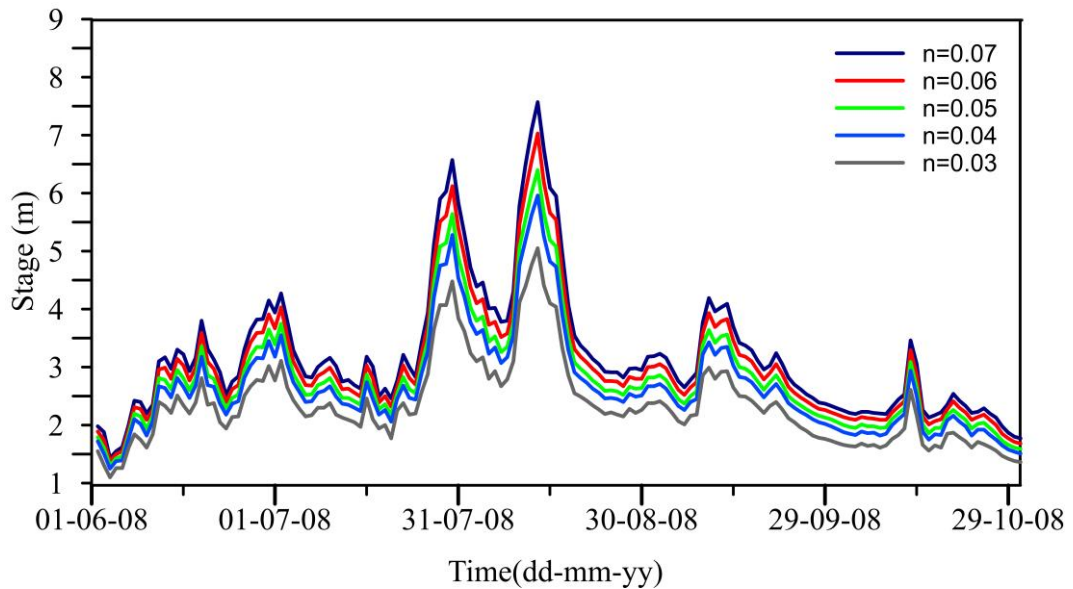


Figure 5.14 Stage hydrograph for different Manning's n values for the year 2008

From Figure 5.14, it can be noted that there is a significant effect on stage with respect to roughness coefficient for the year 2008. Increase in roughness coefficient from $n = 0.03$ to $n = 0.04$ leads to an 18.02% increase in depth of flow, from $n = 0.04$ to $n = 0.05$ leads to a 7.38% increase in depth of flow, from $n = 0.05$ to $n = 0.06$ leads to an 9.85% increase in depth of flow and from $n = 0.06$ to $n = 0.07$ leads to a 7.68% increase in depth of flow. The computed peak stages are 5.05m, 5.96m, 6.40m, 7.03m and 7.57m when $n = 0.03$, $n=0.040$, $n=0.050$, $n=0.060$, and $n=0.070$ respectively.

Computed stage hydrograph for different Manning's n 0.030 to 0.070 values for the year 2009 is shown in Figure 5.15.

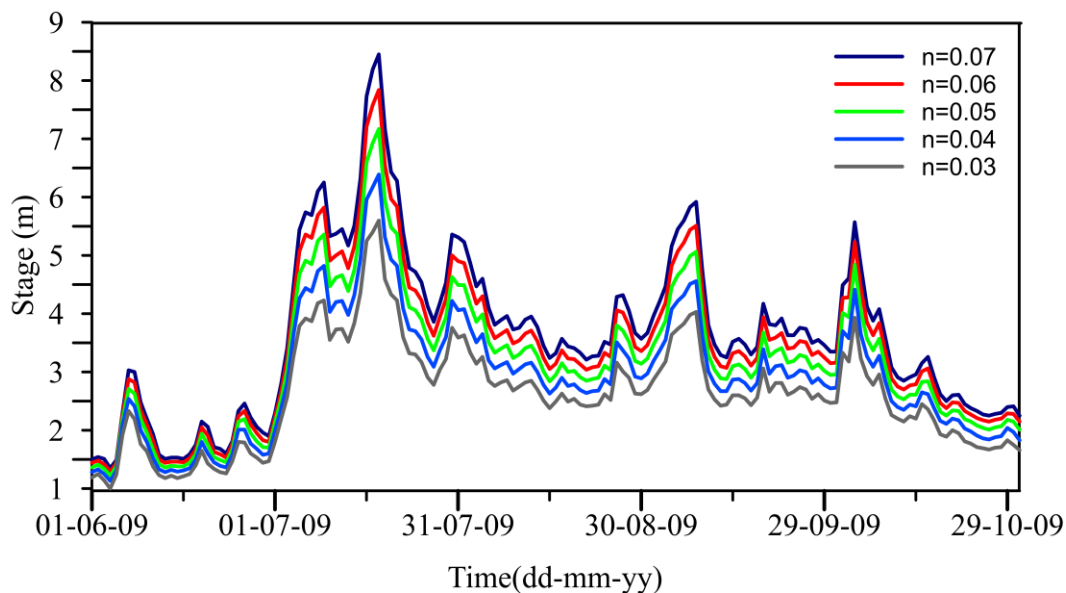


Figure 5.15 Stage hydrograph for different Manning's n values for the year 2009

From Figure 5.15, it can be noted that there is a significant effect on stage with respect to roughness coefficient for the year 2009. Increase in roughness coefficient from $n = 0.03$ to $n = 0.04$ leads to an 14.11% increase in depth of flow, from $n = 0.04$ to $n = 0.05$ leads to a 12.20% increase in depth of flow, from $n = 0.05$ to $n = 0.06$ leads to an 9.35% increase in depth of flow and from $n = 0.06$ to $n = 0.07$ leads to a 7.78% increase in depth of flow. The computed peak stages are 5.60m, 6.39m, 7.17m, 7.84m and 8.45m when $n = 0.03$, $n=0.040$, $n=0.050$, $n=0.060$, and $n=0.070$ respectively. The Manning's roughness coefficient represents the energy loss due to the water friction against bed

surface roughness and this roughness in bed surface increases the depth of flow in the channel.

5.3.2 Impact of Manning's n on river stage-discharge rating curve

Stage-discharge rating curve were drawn for different Manning's n at Bantwal gauging station for the year 2007, 2008 and 2009.

Stage-discharge rating curve for different Manning's n for the year 2007 presented in Figure 5.16.

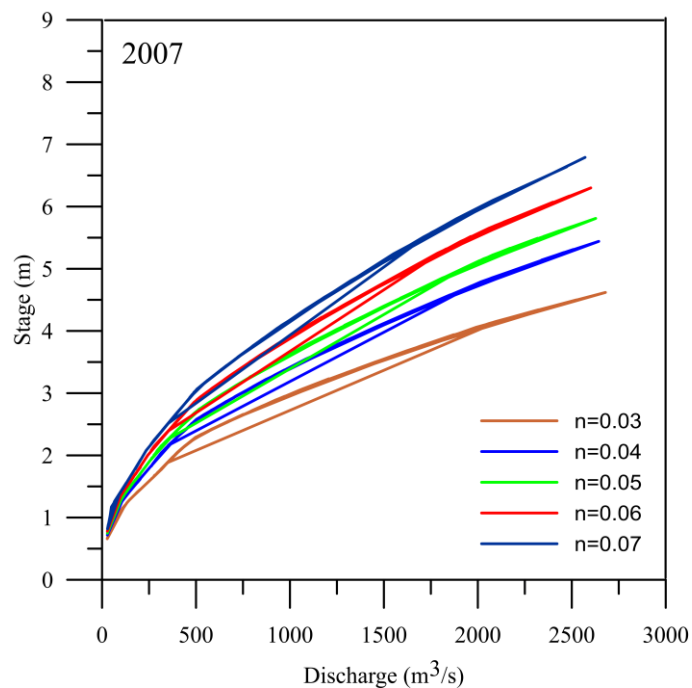


Figure 5.16 Stage-discharge rating curve for different Manning's n in the year 2007

From the Figure 5.16 it is observed that, the stage values (in m) were found to be 2.984, 3.417, 3.633, 3.912 and 4.18 for $n=0.030$, 0.04, 0.05, 0.06 and 0.07 respectively for the considered discharge of $1000 \text{ m}^3/\text{sec}$. Additionally for the discharge values of $2500 \text{ m}^3/\text{sec}$ the stage values were estimated to be 4.48, 5.302, 5.680, 6.185 and 6.680 for $n=0.030$, 0.04, 0.05, 0.06 and 0.07 respectively for the year 2007. The stage discharge rating curve illustrates the irregularity in the prediction due to unrealistic data that might have emerged during field data measurement. The loop in the rating curve represents the temporary shift in in the prediction that can be neglected due to the consideration of unsteady flow condition in the hydraulic model.

Stage-discharge rating curve for different Manning's n for the year 2008 is presented in Figure 5.17.

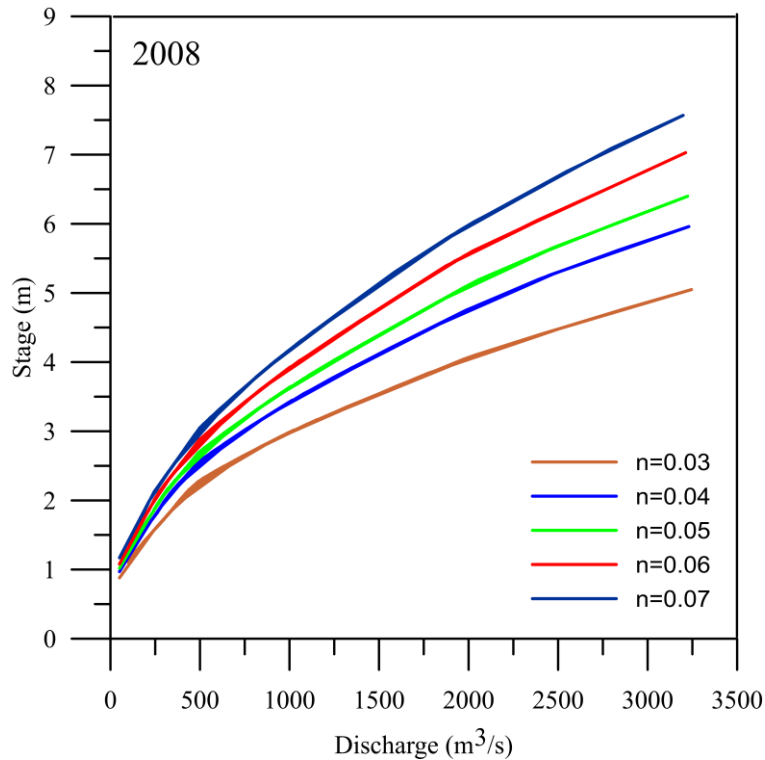


Figure 5.17 Stage-discharge rating curve for different Manning's n in the year 2008

The stage values (in m) were found to be 2.986, 3.842, 3.420, 3.907 and 4.173 for $n=0.030$, 0.040 , 0.05 , 0.060 and 0.07 respectively for the considered discharge of $1000 \text{ m}^3/\text{sec}$. Additionally for the discharge values of $2500 \text{ m}^3/\text{sec}$ the stage values were estimated to be 4.478, 5.300, 5.674, 6.182 and 6.682 for $n=0.03$, $n=0.04$, 0.05 , 0.06 and 0.07 respectively for the year 2008.

Stage-discharge rating curve for different Manning's n for the year 2009 presented in Figure 5.18.

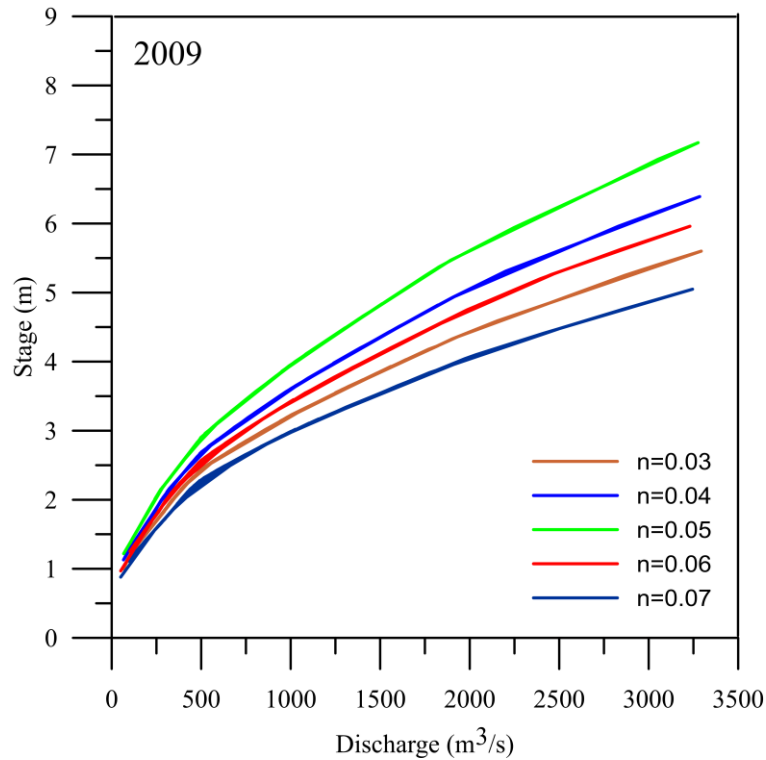


Figure 5.18 Stage-discharge rating curve for different Manning's n in the year 2009

The stage values (in m) were found to be 3.125, 3.606, 3.949, 4.273 and 4.569 for $n=0.030$, 0.040 , 0.05 , 0.06 and 0.07 respectively for the considered discharge of $1000 \text{ m}^3/\text{sec}$. Additionally for the discharge values of $2500 \text{ m}^3/\text{sec}$ the stage values were estimated to be 4.896, 5.608, 6.242, 6.824 and 7.396 for $n=0.03$, 0.04 , 0.05 , 0.060 and 0.07 respectively for the year 2009.

From result, it can be observed that which increase in Manning's coefficient, the stage value is increased relatively and attenuates the associated peak discharge. The variation of Manning's n shows that an increase in 'n' in the channel increases the simulated stage and reduces the associated peak discharge. From the rating curve, it is very clear that as discharge increases, the effect of Manning n on stage relatively increases which shows that roughness is highly sensitive at higher discharges.

5.4 HYDRAULIC FLOOD ROUTING

The HEC-RAS model is developed for the Nethravathi River. 45 km stretch is considered along the river with 80 cross-sections extracted from the DEM. The cross-section width and interval are 2000 m and 500 m respectively as shown in Figure 5.19. Along the river length Manning's coefficient is set as 0.032 for channel and 0.070 for flood plain since the river bed is covered with gavels, few boulders and cobbles (Chow, 1959). By using the Mixed Flow Regime option for Unsteady Flow Analysis, the flow regime is set as mixed. From mixed flow regime, RAS can handle transitions from subcritical to supercritical flow. The daily discharge is set as an upstream boundary condition and normal depth (friction slope=0.001) as a downstream boundary condition. The simulation is done as an unsteady state flow analysis. Figure 5.20 illustrates the water surface profiles, critical water surface, and energy gradient.

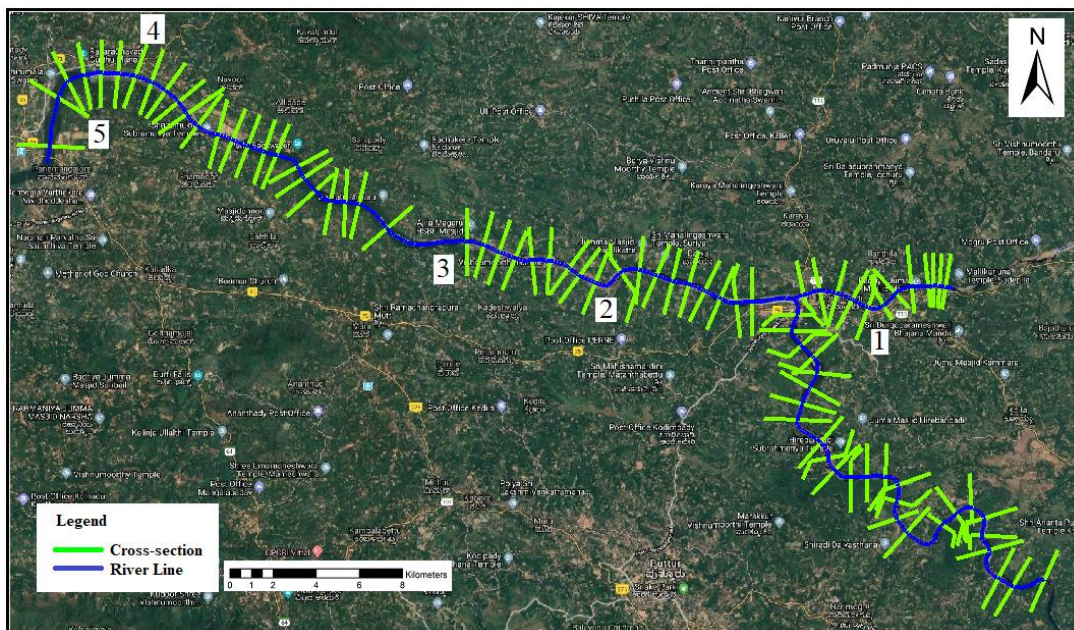


Figure 5.19 Cross-section layout of Nethravathi river system

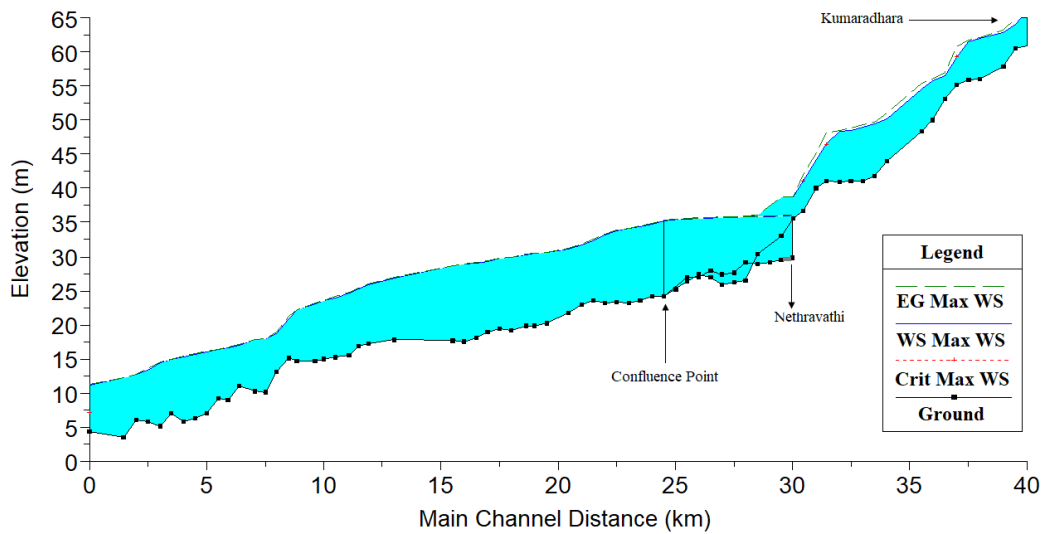


Figure 5.20 Longitudinal section of water surface elevation (maximum)

5.4.1 Model calibration and validation for flood analysis

The flow hydrograph for the monsoon months 1st June to 31st October of the years 2007 to 2010 have been used. The model has calibrated by assigning flow roughness factors, expansion/contraction coefficient and varying the Manning's co-efficient in the river reach. During the calibration adjusted the Manning's n value until the observed and simulated discharge values are in close agreement. The performance of the model during calibration and validation is evaluated using Coefficient of Determination (R^2), Nash-Sutcliffe efficiency (NSE), index of agreement (d), Normalized Root Mean Squared Error (NRMSE) and Mean Absolute Error (MAE).

5.4.1.1 Model Calibration for the year 2007

The observed and estimated discharge and stage hydrographs which are calibrated for the year 2007 at Bantwal gauging station are presented in Figure 5.21

From Figure 5.21, it is observed that the observed and estimated discharge hydrographs are reasonably matching except at the peak flow. Accordingly, the following observations are made. The estimate discharges are lower than those observed in most periods. The simulated discharge is under-estimated when the flow is less than 1800 m³/sec.

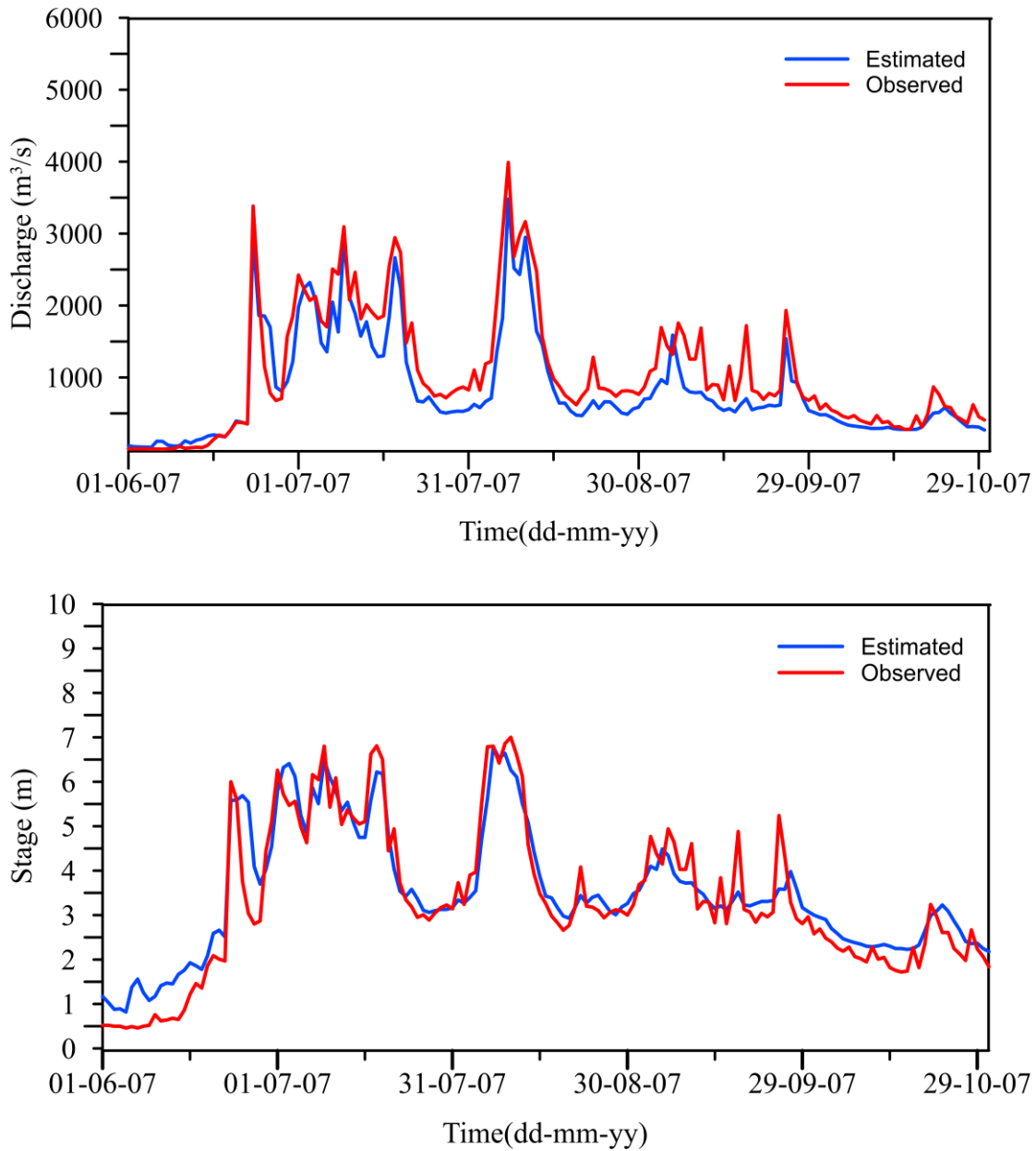


Figure 5.21 Observed and estimated discharge and stage hydrograph for calibration period of 2007 (mixed regime) at Bantwal gauging station

The model result showed good consensus between estimated and observed flow discharge. The computation accuracy of peak discharge is about 87.2% for the year 2007. The Coefficient of Determination (R^2) is 0.896, Nash-Sutcliffe efficiency (NSE) is 0.820, index of agreement (d) is 0.947, Normalized Root Mean Squared Error (NRMSE) is 0.338 and Mean absolute error (MAE) is 0.370 for the calibration period of 2007 at gauging sites, which shows a very close agreement between the observed

and simulated discharge. Figure 5.21 is also shows good agreement between observed and simulated stage values during the medium flow condition. The following analysis is made subsequently. As can be seen in Figure 5.21, the highest peak stage was underestimated by approximately 0.59 m. The Coefficient of Determination (R^2) is 0.918, Nash-Sutcliffe efficiency (NSE) is 0.901, index of agreement (d) is 0.971, Normalized Root Mean Squared Error (NRMSE) is 0.160. and Mean absolute error (MAE) is 0.148 for the calibration period of 2007 at gauging sites. It is worth noting that the number of data containing high flows was significantly lower than medium to low flow. Additionally, the measurement of gauging stations might not measure the water level accurately over the flooding events. Therefore, such a difference between observed and simulated peak might be also the result of poor and un-calibrated measurements. The variation in peak stage value for the Nethravathi river show a good agreement between the observed and computed peak stage.

The scatter plot with 1:1 line of the observed and estimated discharge and stage values after calibration for the year 2007 at Bantwal gauging station is shown in Figure 5.22. The performance of the model during calibration is evaluated using five error functions presented in table 5.3.

The simulation results for the calibration are compared with the observed discharge and stage are presented in Figure 5.22 which shows the correlation of observed and estimated discharge and stage. The simulated results give R^2 statistics of 0.896 and 0.918 which show a higher correlation between observed and simulated discharge and stage respectively.

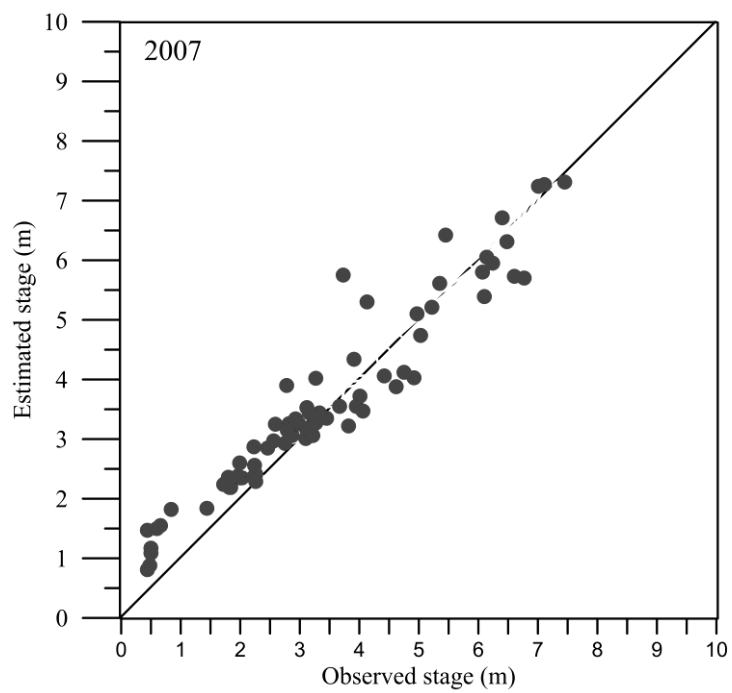
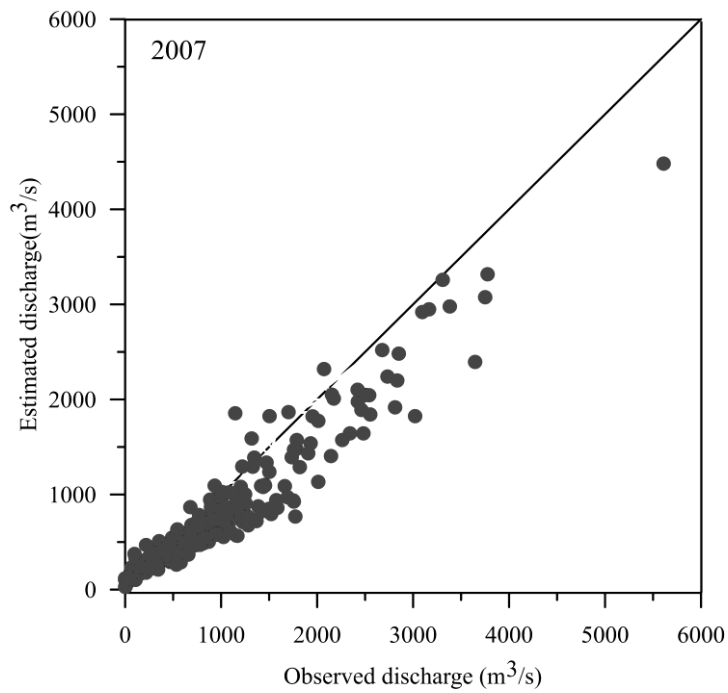


Figure 5.22 Scatter plot of the observed and simulated discharge and stage values during calibration period of 2007(mixed regime) at Bantwal gauging station

5.4.1.2 Model Calibration for the year 2008

The observed and estimated discharge and stage hydrographs which are calibrated for the year 2008 at Bantwal gauging station are shown in Figure 5.23

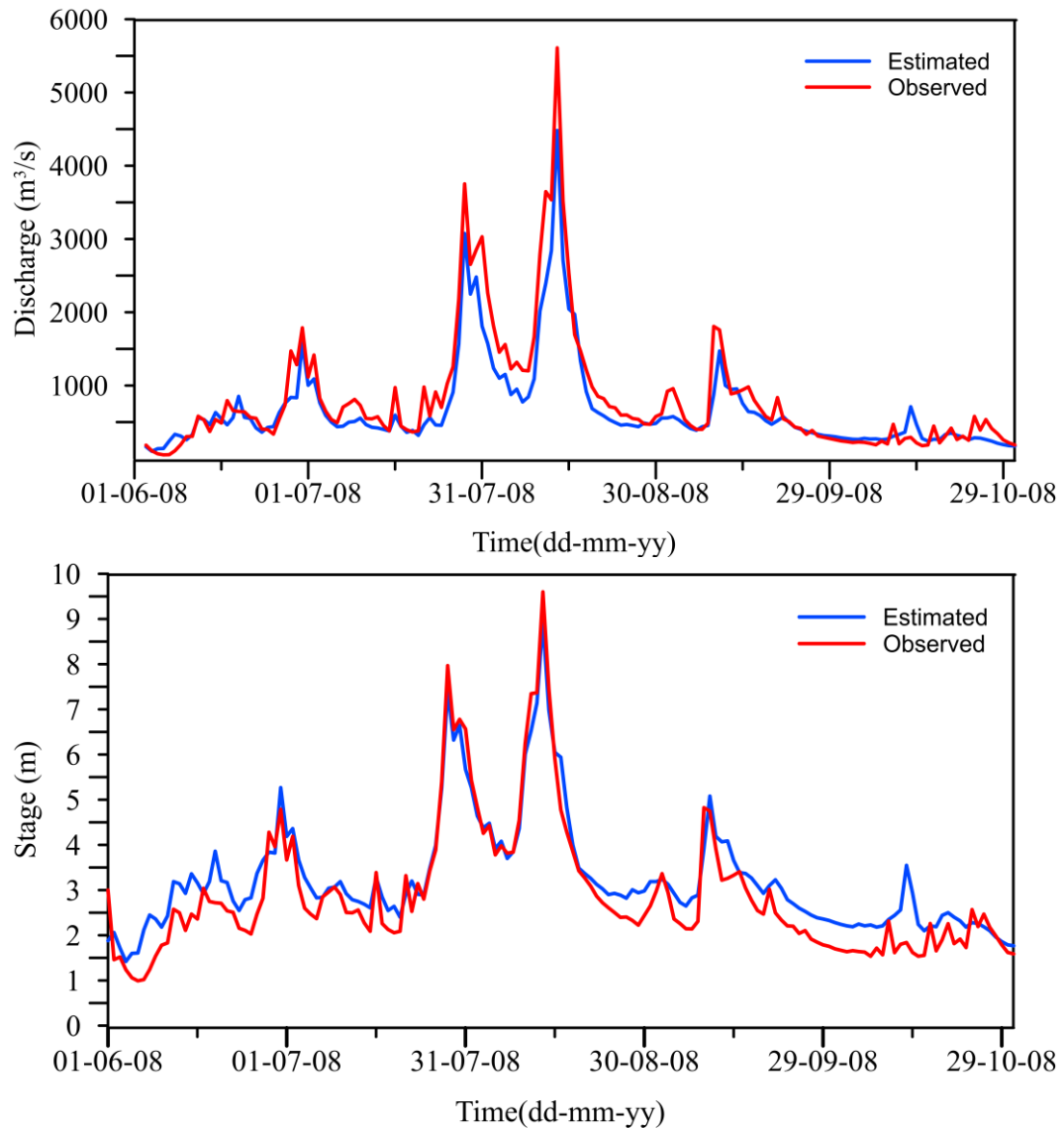


Figure 5.23 Observed and estimated discharge and stage hydrograph for calibration period of 2008 (mixed regime) at Bantwal gauging station

From Figure 5.23, it is observed that the observed and estimated discharge hydrographs are reasonably matching except at the peak flow. Accordingly, the following observations are made. The estimated discharges are lower than those observed in most periods. The simulated discharge is over-estimated when the flow is less than 800 m³/sec. The model result showed good consensus between estimated and observed flow

discharge. The computation accuracy of peak discharge is about 79.80% for the year 2008. The Coefficient of Determination (R^2) is 0.945, Nash-Sutcliffe efficiency (NSE) is 0.864, index of agreement (d) is 0.955, Normalized Root Mean Squared Error (NRMSE) is 0.376 and Mean absolute error (MAE) is 0.295 for the calibration period of 2008 at gauging sites, which shows a very close agreement between the observed and simulated discharge. Figure 5.23 also shows good agreement between observed and simulated stage values during the medium flow condition. The following analysis is made subsequently. As can be seen in Figure 5.23, the highest peak stage was underestimated by approximately 0.59 m. The Coefficient of Determination (R^2) is 0.927, Nash-Sutcliffe efficiency (NSE) is 0.862, index of agreement (d) is 0.959, Normalized Root Mean Squared Error (NRMSE) is 0.175 and Mean absolute error (MAE) is 0.157 for the calibration period of 2008 at gauging station. The variation in peak stage value for the Nethravathi river shows a good agreement between the observed and estimated peak stage.

The scatter plot with 1:1 line of the observed and estimated discharge and stage values after calibration for the year 2008 at Bantwal gauging station is shown in Figure 5.24.

The simulated results for the calibration are compared with the observed discharge and stage and are presented in Figure 5.24 which shows the correlation of observed and simulated discharge and stage. The simulated results give R^2 statistics of 0.945 and 0.927 which show a higher correlation between observed and simulated discharge and stage respectively.

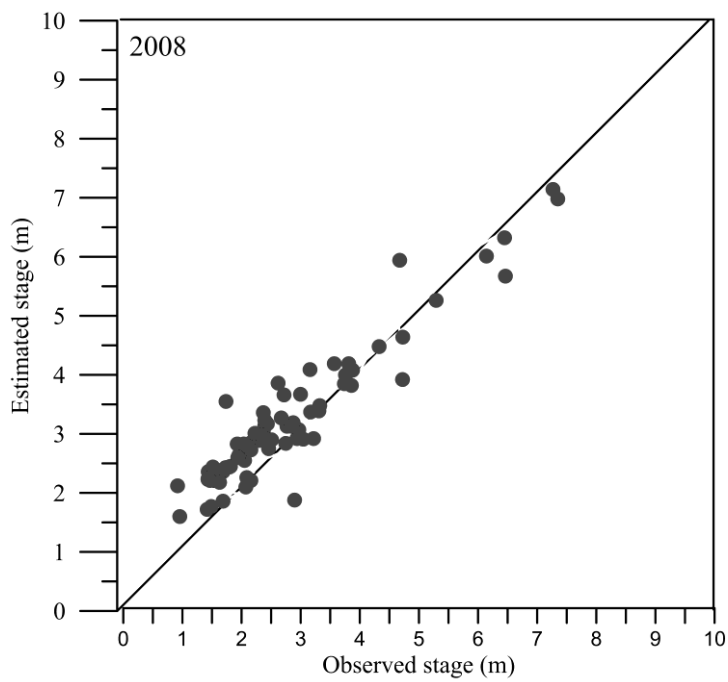
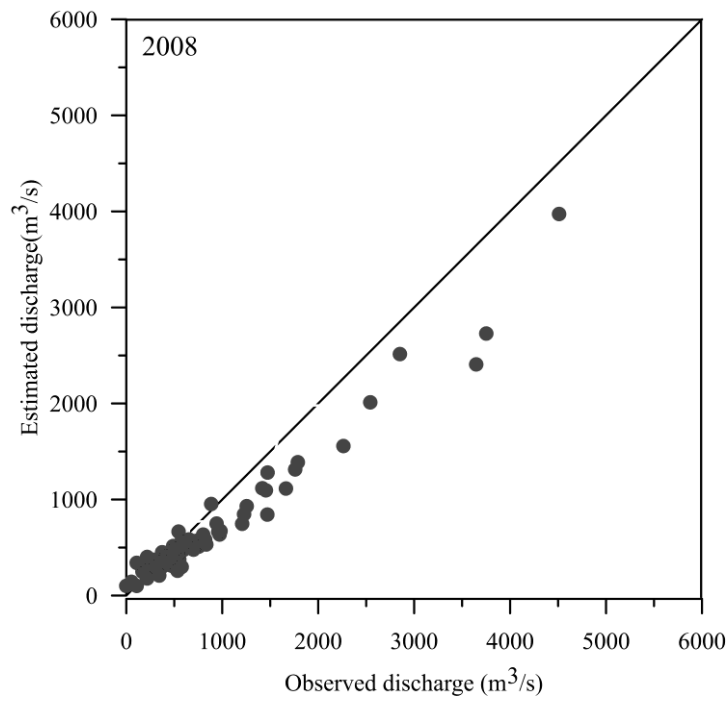


Figure 5.24 Scatter plot of the observed and simulated discharge and stage values during the calibration period of 2008 (mixed regime) at Bantwal gauging station

5.4.1.3 Model Calibration for the year 2009

The observed and estimated discharge and stage hydrographs which are calibrated for the year 2009 at Bantwal gauging station are shown in Figure 5.25

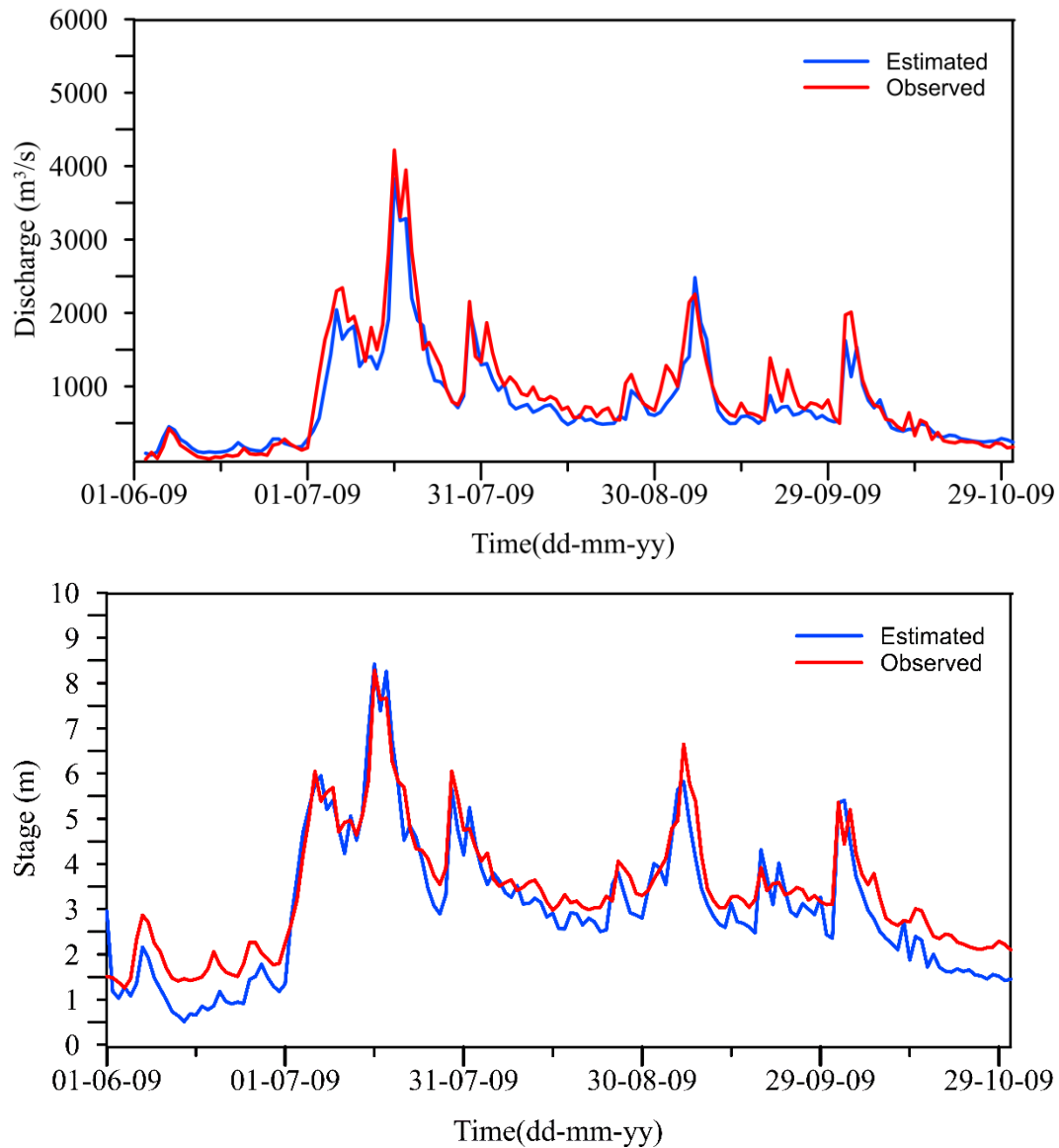


Figure 5.25 Observed and estimated discharge and stage hydrograph for calibration period of 2009 (mixed regime) at Bantwal gauging station

From Figure 5.25, it is observed that the observed and estimated discharge hydrographs are reasonably matching except at the peak flow. Accordingly, the following observations are made. The estimated discharges are lower than those observed in most periods. The simulated discharge is over-estimated when the flow is less than 500

m³/sec. The model result showed good consensus between estimated and observed flow discharge. The computation accuracy of peak discharge is about 83.02% for the year 2009. The Coefficient of Determination (R^2) is 0.927, Nash-Sutcliffe efficiency (NSE) is 0.891, index of agreement (d) is 0.967, Normalized Root Mean Squared Error (NRMSE) is 0.288 and Mean absolute error (MAE) is 0.283 for the calibration period of 2009 at gauging sites, which shows a very close agreement between the observed and simulated discharge. Figure 5.24 also shows good agreement between observed and simulated stage values during the medium flow condition. The following analysis is made subsequently. As can be seen in Figure 5.25, the highest peak stage was underestimated by approximately 0.24 m. The Coefficient of Determination (R^2) is 0.928, Nash-Sutcliffe efficiency (NSE) is 0.863, index of agreement (d) is 0.961, Normalized Root Mean Squared Error (NRMSE) is 0.192 and Mean absolute error (MAE) is 0.187 for the calibration period of 2009 at gauging station. The variation in peak stage value for the Nethravathi river shows a good agreement between the observed and estimated peak stage.

The scatter plot with 1:1 line of the observed and estimated discharge and stage values after calibration for the year 2009 at Bantwal gauging station is shown in Figure 5.26.

The simulated results for the calibration are compared with the observed discharge and stage and are presented in Figure 5.26 which shows the correlation of observed and simulated discharge and stage. The simulated results give R^2 statistics of 0.927 and 0.928 which show a higher correlation between observed and simulated discharge and stage respectively. This shows that the calibration of the hydraulic model is reasonably well applicable for analyzing streamflow and water level.

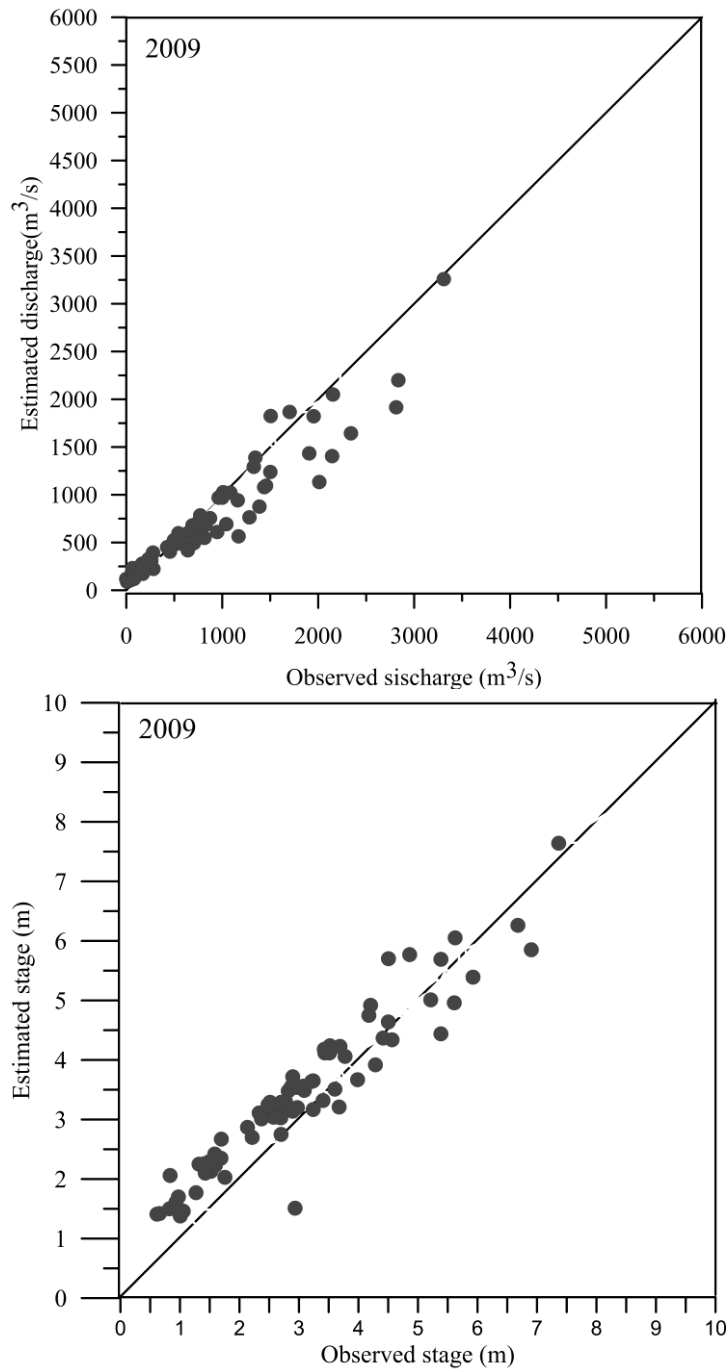


Figure 5.26 Scatter plot of the observed and simulated discharge and stage values during the calibration period of 2009 (mixed regime) at Bantwal gauging station

5.4.1.4 Model validation for the year 2010

The calibrated HEC-RAS model is validated for the monsoon and post-monsoon period from 1st June to 31st October of the year 2010. The validation of the model is carried out for the Bantwal gauging station used during calibration. The observed and estimated discharge and stage hydrograph at Bantwal gauging station are shown in figure 5.27.

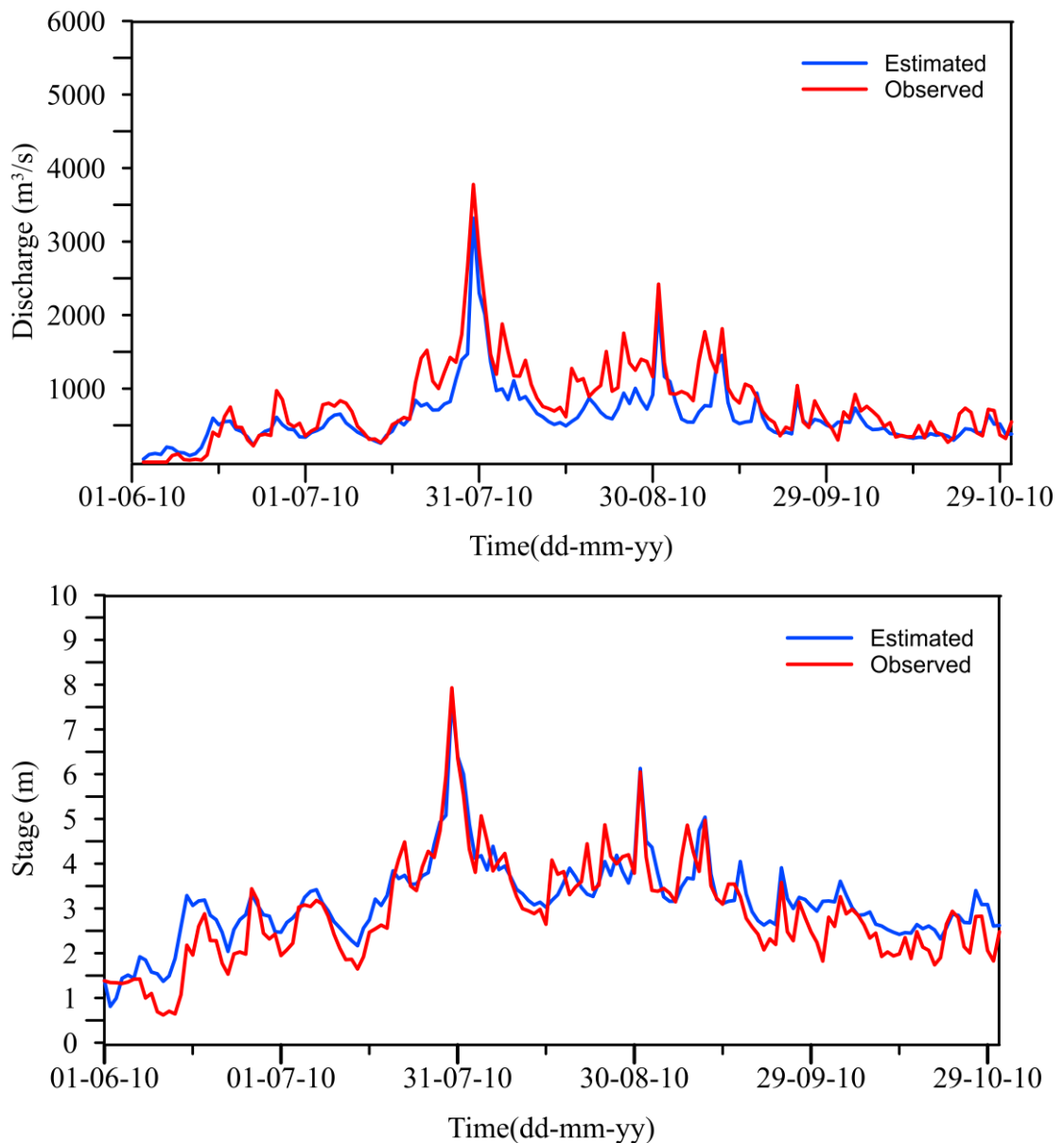


Figure 5.27 Observed and estimated discharge and stage hydrograph for validation period of 2010 (mixed regime) at Bantwal gauging station

The performance of the model during validation are presented in table 5.3. For simulated discharge, the Coefficient of Determination (R^2) is 0.840, Nash-Sutcliffe efficiency (NSE) is 0.704, index of agreement (d) is 0.900, Normalized Root Mean Squared Error (NRMSE) is 0.510 and Mean absolute error (MAE) is 0.340 for the validation period. For simulated stage value, the Coefficient of Determination (R^2) is 0.843, Nash-Sutcliffe efficiency (NSE) is 0.789, index of agreement (d) is 0.934, Normalized Root Mean Squared Error (NRMSE) is 0.183 and Mean absolute error (MAE) is 0.156 for the validation period of 2010. The peak discharge and stage value show good agreement between the observed and estimated discharge and stage.

The scatter plot with 1:1 line of the observed and estimated discharge and stage values for the validation period for the year 2010 at Bantwal gauging station is shown in Figure 5.28. The simulated results for the calibration are compared with the observed discharge and stage are presented in Figure 5.28 which shows the correlation of observed and simulated discharge and stage. The simulated results give R^2 statistics of 0.840 and 0.843 which show the best correlation between observed and simulated discharge and stage respectively.

The error function values during validation are found to be marginally lower in comparison to calibration results. There is a very close agreement of the simulated and observed stage, both during calibration as well as validation. Thus, considering the overall values of the error functions for the gauging station, it is found that the model performs reasonably well during validation. Therefore, the calibrated and validated HEC-RAS model is used for unsteady flow analysis.

Table 5.3. Model Performance

| Perform Indices | Calibration period | | | | | | Validation period | |
|--|--------------------|-----------|-------|-----------|-------|-----------|-------------------|-----------|
| | 2007 | | 2008 | | 2009 | | 2010 | |
| | Stage | Discharge | Stage | Discharge | Stage | Discharge | Stage | Discharge |
| Coefficient of Determination (R^2) | 0.918 | 0.896 | 0.927 | 0.945 | 0.928 | 0.927 | 0.843 | 0.840 |
| Nash-Sutcliffe efficiency (NSE) | 0.901 | 0.820 | 0.862 | 0.864 | 0.863 | 0.891 | 0.789 | 0.704 |
| index of agreement (d) | 0.971 | 0.947 | 0.959 | 0.955 | 0.961 | 0.967 | 0.934 | 0.900 |
| Normalized Root Mean Squared Error (NRMSE) | 0.160 | 0.338 | 0.175 | 0.376 | 0.192 | 0.288 | 0.183 | 0.51 |
| Mean Absolute Error(MAE) | 0.148 | 0.370 | 0.157 | 0.295 | 0.187 | 0.283 | 0.156 | 0.340 |

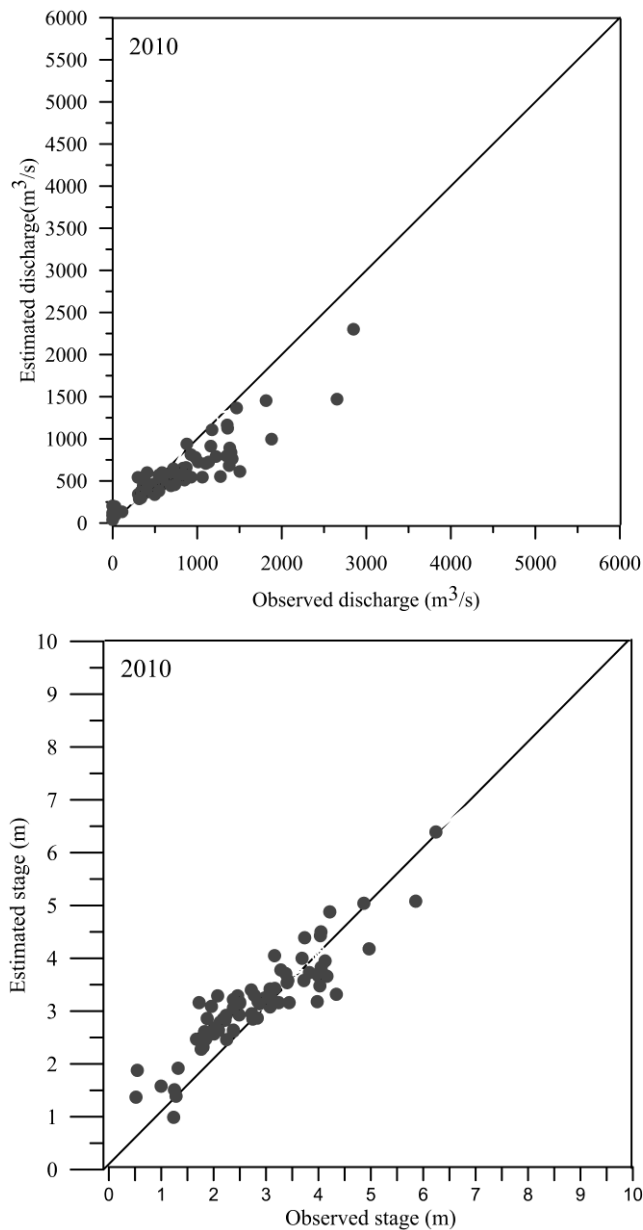


Figure. 5.28 Scatter plot of the observed and estimated discharge and stage for validation period 2010 (mixed regime) at Bantwal gauging station

5.4.2 Unsteady flow analysis in Nethravathi river

The calibrated hydraulic model was used for flood simulation. The various hydraulic parameters of the downstream gauging station of Nethravathi river basin, including the energy grade slope, flow velocity, flow width, flow area, hydraulic radius, conveyance and Froude number are presented in Table 5.4. The Hydraulic parameters generated through a hydrodynamic model simulation along the river reach is and these are

supportive in designing flood protection measures and development of flood inundation map of the lower Nethravathi river basin.

Table 5.4 Model output result at downstream gauging station.

| Parameters | Bantwal Gauging station | | | | |
|-------------------------------------|-------------------------|----------|-----------|----------|------|
| | 2007 | 2008 | 2009 | 2010 | |
| Peak discharge (m ³ /s) | 3704.99 | 4423.72 | 3875.00 | 3540.65 | |
| Maximum velocity (m/s) | 2.30 | 2.45 | 2.34 | 2.26 | |
| Maximum water depth (m) | Estimated | 7.89 | 8.96 | 8.28 | 7.71 |
| | Observed | 8.22 | 9.6 | 8.42 | 7.93 |
| Maximum flow area (m ²) | 1613.31 | 1805.27 | 1658.24 | 1569.15 | |
| Maximum flow width (m) | 345.11 | 350.42 | 345.39 | 344.84 | |
| Hydraulic mean radius (m) | 4.67 | 5.15 | 4.80 | 4.55 | |
| Froude Number | 0.34 | 0.34 | 0.34 | 0.34 | |
| Energy Grade Slope | 0.001 | 0.001 | 0.001 | 0.001 | |
| Flow Conveyance (m ³ /s) | 117160.5 | 139886.0 | 122545.6 | 111958.6 | |
| Inundated area (m ²) | 13604680 | 14468816 | 136150692 | 9456174 | |

5.4.2.1 Flood Simulation for the year 2007

Flood simulation was carried out for the year 2007 and consist of water depth, flow velocity and water surface elevation are as follows.

a) Computed depth of water in the year 2007

The maximum water depth along the river reach is 14.12 m which is in the stream channel. The water depth ranges from 0.01 m to 14.12 m. as shown in figure 5.29. The maximum depth of water observed at Bantwal is 7.89 m.

b) Flow velocity in the year 2007

The complex flow regimes in the main channel and side bank is shown in figure 5.30 In the main channel and flood plain, flow velocity values range from 0.01 to 4.96 m/s. For the overland flow on the floodplain, the maximum water velocity is 0.3 m/s. However, at some location close to channel the values are found to be high (≈ 1.8 m/s). The maximum velocity was found to be 4.96 m/s close to downstream of Nethravathi River and at Bantwal gauging station velocity was observed as 2.3 m/s

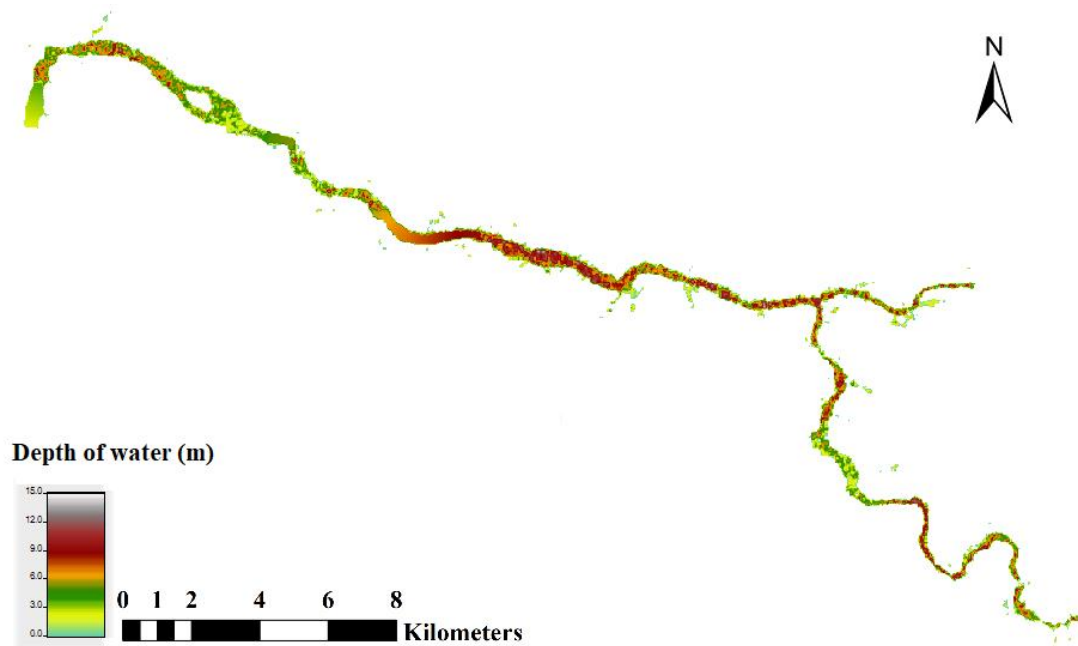


Figure 5.29 Water depth in river channel and floodplain in the year 2007

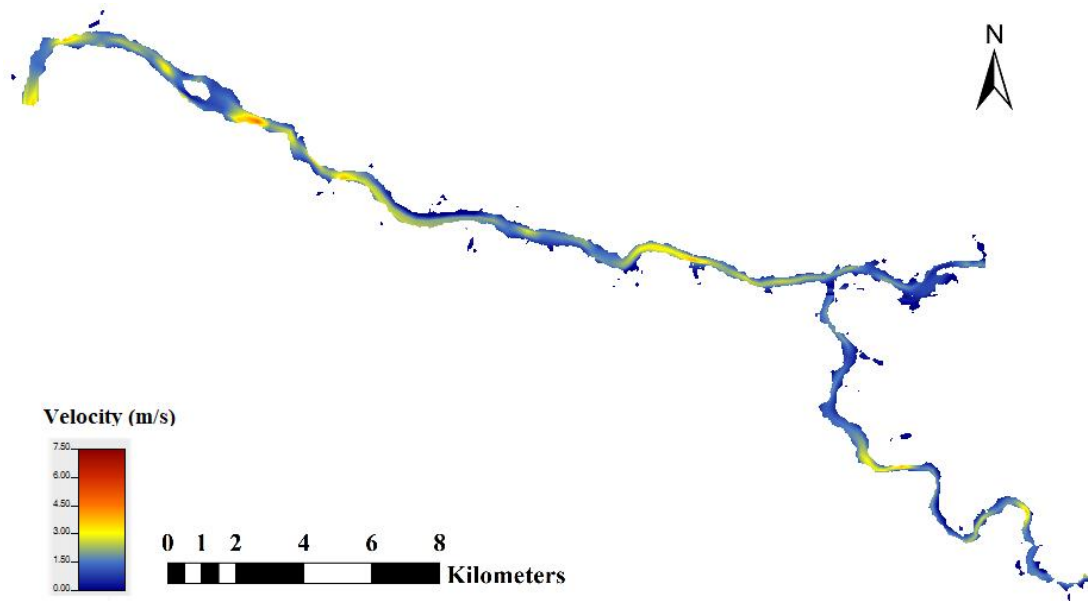


Figure 5.30 Flow velocity in river channel and floodplain in the year 2007

c) Water surface elevation in the year 2007

The water surface elevation of the Nethravathi river is shown in Figure 5.31. the water surface elevation ranges from 68.63m to 10.09 m from mean sea level.

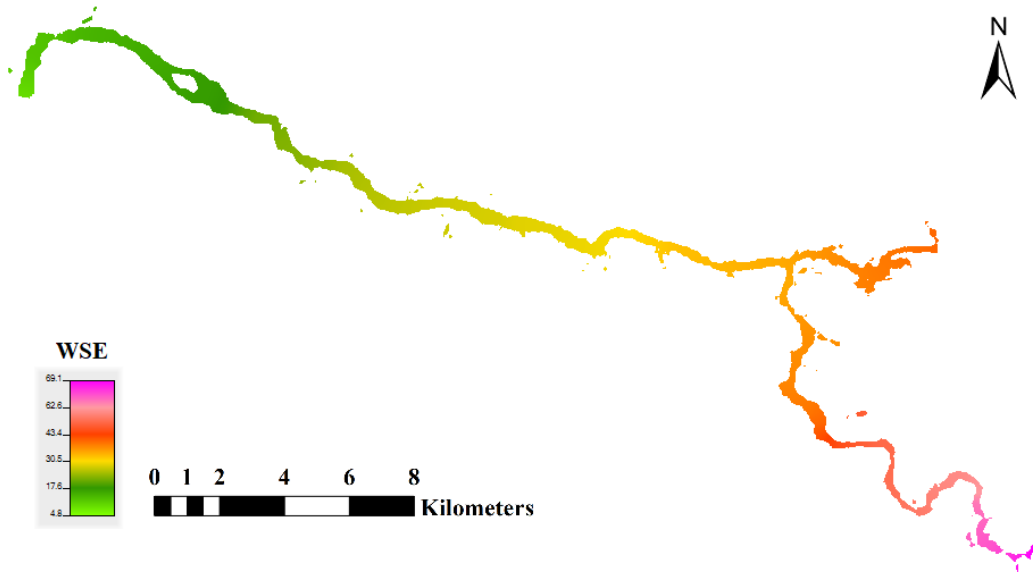


Figure 5.31 Water surface elevation along the river reach in the year 2007

5.4.2.2 Flood Simulation for the year 2008

Flood simulation was carried out for the year 2008 and consist of water depth, flow velocity and water surface elevation are as follows

a) Computed depth of water in the year 2008

The maximum water depth along the river reach is 14.98 m which is in the stream channel. The water depth ranges from 0.01 m to 14.98 m. as shown in figure 5.32. The maximum depth of water observed at Bantwal is 8.96 m.

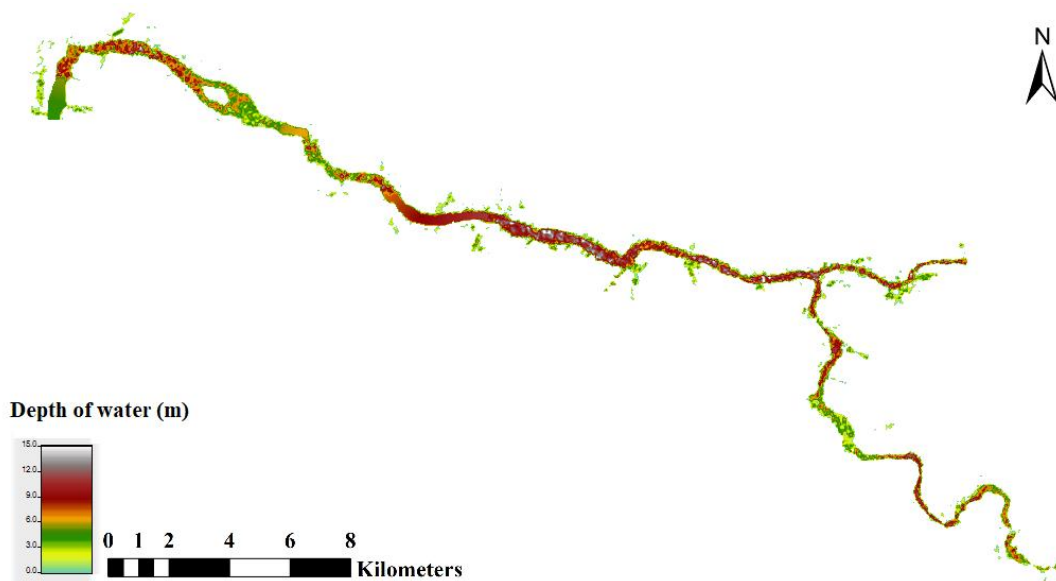


Figure 5.32 Water depth in river channel and floodplain in the year 2008

b) Flow velocity in the year 2008

The complex flow regimes in the main channel and side bank is shown in figure 5.33. In the main channel and flood plain flow velocity values range from 0.01 to 5.54 m/s. For the overland flow on the floodplain, the maximum water velocity is 0.4 m/s. However, at some location close to channel the values are found to be high (≈ 2.20 m/s). The maximum velocity was found to be 5.54 m/s close to upstream of Kumaradhara River reach and at Bantwal gauging station velocity was observed as 2.45 m/s.

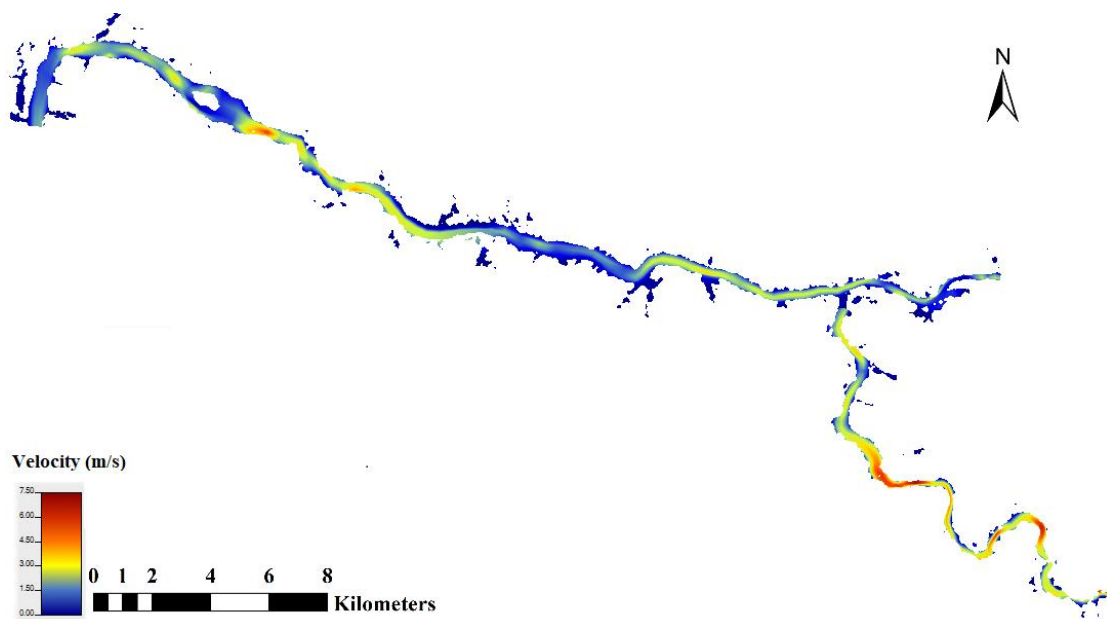


Figure 5.33 Flow velocity in river channel and floodplain in the year 2008

c) Water surface elevation in the year 2008

The water surface elevation of Nethravathi river is shown in Figure 5.34. The water surface elevation ranges from 69.1m to 10.65 m from mean sea level.



Figure 5.34 Water surface elevation along the river reach in the year 2008

5.4.2.3 Flood Simulation for the year 2009

Flood simulation was carried out for the year 2009 and consist of water depth, flow velocity and water surface elevation are as follows

a) Computed depth of water in the year 2009

The maximum water depth along the river reach is 14.25 m which is in the stream channel. The water depth ranges from 0.01 m to 14.25 m. as shown in figure 5.35. The maximum depth of water observed at Bantwal is 8.28 m.

b) Flow velocity in the year 2009

The complex flow regimes in the main channel and side bank is shown in figure 5.36. In the main channel and flood plain flow velocity values range from 0.01 to 5.12 m/s. For the overland flow on the floodplain, maximum water velocity is 0.32 m/s. However, at some location close to channel the values are found be high (≈ 2 m/s). The maximum velocity was found to be 5.12 m/s close to downstream of Nethravathi River and at Bantwal gauging station velocity was observed as 2.34 m/s

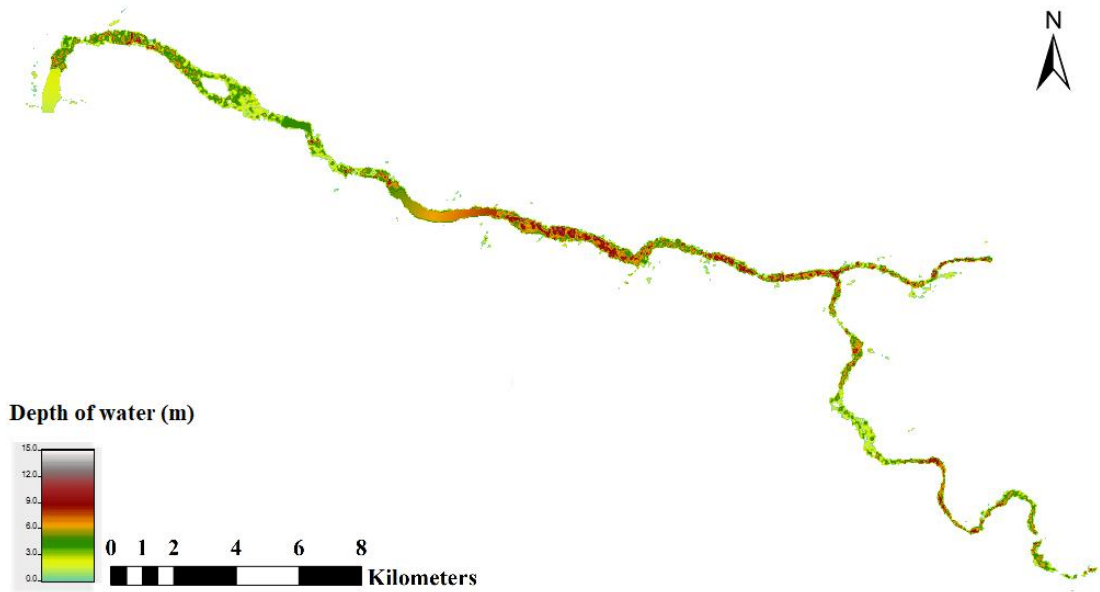


Figure 5.35 Water depth in river channel and floodplain in the year 2009

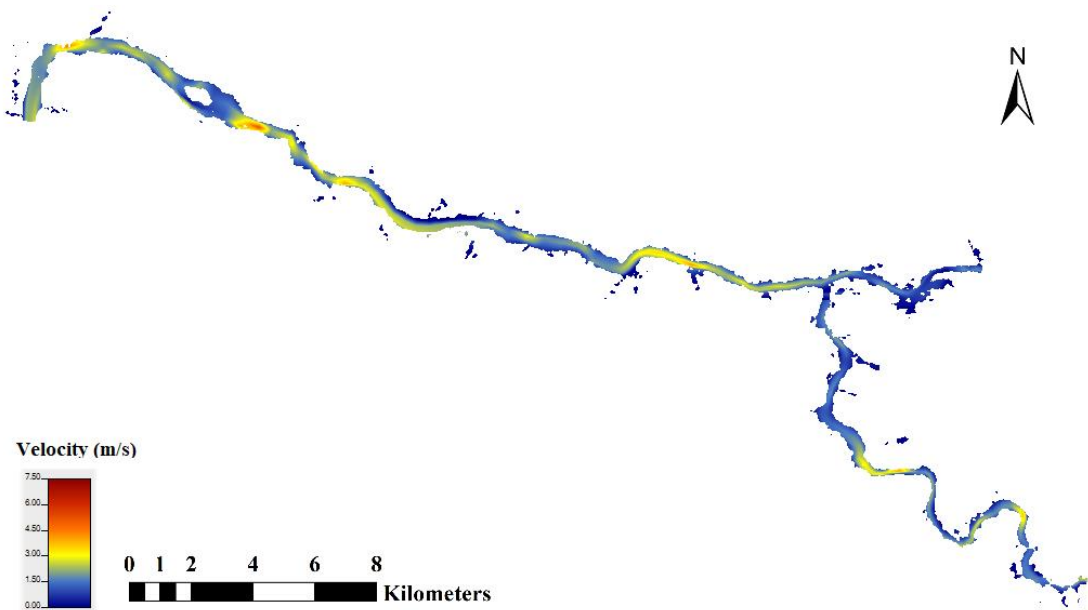


Figure 5.36 Flow velocity in river channel and floodplain in the year 2009

c) Water surface elevation in the year 2009

The water surface elevation of the Nethravathi river is shown in figure 5.37. The water surface elevation ranges from 68.65m to 10.10 m from mean sea level.

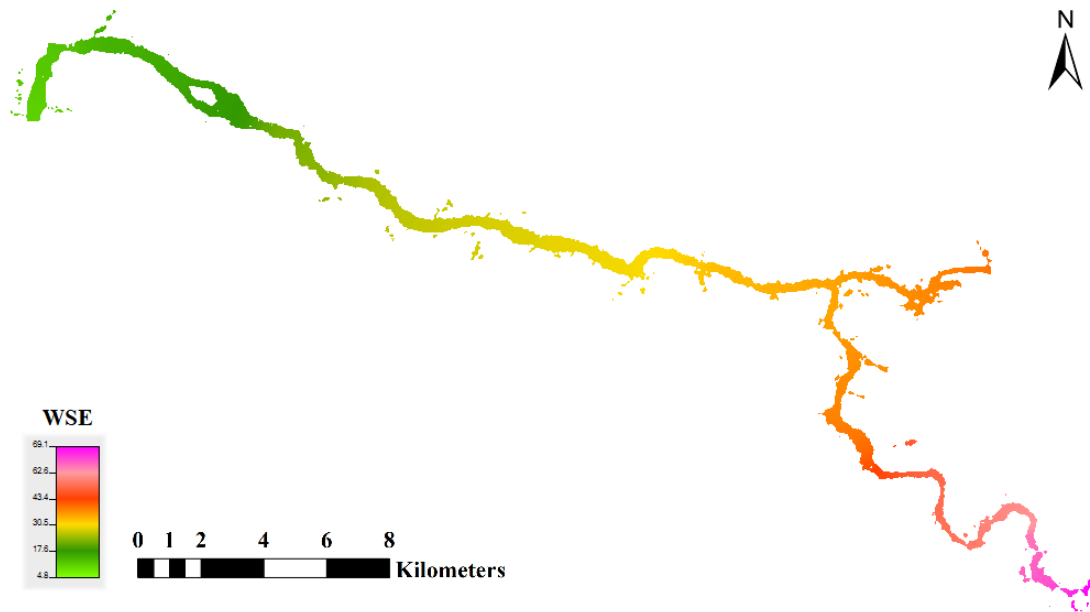


Figure 5.37 Water surface elevation along the river reach in the year 2009

5.4.2.4 Flood Simulation for the year 2010

Flood simulation was carried out for the year 2010 and consist of water depth, flow velocity and water surface elevation are as follows

a) Computed depth of water in the year 2010

The maximum water depth along the river reach is 13.89 m which is in the stream channel. The water depth ranges from 0.01 m to 13.89 m. as shown in figure 5.38. The maximum depth of water observed at Bantwal is 7.71 m.

b) Flow velocity in the year 2010

The complex flow regimes in the main channel and side bank is shown in figure 5.39. In the main channel and flood plain flow velocity values range from 0.01 to 4.71 m/s. For the overland flow on the floodplain, the maximum water velocity is 0.25 m/s. However, at some location close to channel the values are found be high (≈ 2 m/s). The maximum velocity was found to be 4.71 m/s close to downstream of Nethravathi River and at Bantwal gauging station velocity was observed as 2.26 m/s.



Figure 5.38 Water depth in river channel and floodplain in the year 2010

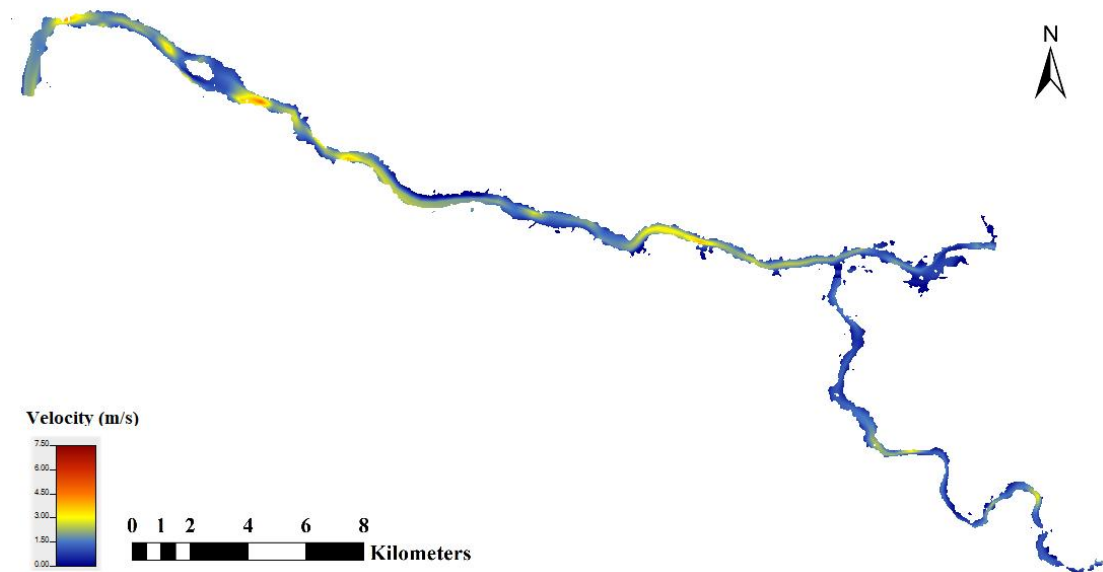


Figure 5.39 Flow velocity in river channel and floodplain in the year 2010

c) Water surface elevation in the year 2010

The water surface elevation of Nethravathi river is shown in figure 5.40. The water surface elevation ranges from 68.15 m to 9.10 m from mean sea level.



Figure 5.40 Water surface elevation along the river reach in the year 2010

5.4.3 Flood inundation mapping for flood event of 2008

RAS Mapper makes automated inundation mapping from HEC-RAS results, provided a terrain model and geo-referenced RAS results. It maps using water surface elevations. Water surface elevation data is imported in RAS mapper to create a continuous water surface. The water surface is then compared with the terrain model to identify the floodplain. Where the land surface is lower than the horizontal water surfaces, storage, area is assigned in addition to the inundation depth grid and floodplain boundary. Adding the Imaginary layer in the RAS mapper helps to identify the extent of flooding, flood depth, and flood velocity. Flood inundation map shows the spatial variation of the flood in the floodplains of the Nethravathi basin. Using the flow hydrograph of the flood event of 2008 as input to the HEC-RAS model, model simulation is carried out. Subsequently, RAS mapper simulation is carried out for obtaining the flood inundation as shown in Figure 5.41. Depth of flood is found to be in the range between 0.1 m to 14.98 m. The velocity of flow in the floodplain is found to vary between 0.01 to 5.54 m/s. The maximum depth of flow in channel and floodplain is 7.75 m and 3.37 m respectively. The maximum velocity in the channel is 5.54 m/s and 0.40 m/s in a floodplain. Enlarged flood inundated area A of downstream and B of river confluence

in the DEM map are shown in Figure 5.41. The computed flood inundation is noticed at peak discharge occurred on 14th August 2008.

It is observed from the computed results that the flooding in the Nethravathi River flood plain first starts near the confluence of Nethravathi and Kumaradhara (Point 1 in figure 5.1). Near Uppinangadi, upstream of the gauging station, floodwater flows over the riverbank. Later about 6 kilometre downstream from the confluence, flooding is noticed at the meandering section (Point 2). In the next section about 10 Kilometers away from the confluence, the downstream channel width is smaller than the upstream (Point 3) due to which upstream section was flooded. Flooding in the downstream near Bantwal (Point 4 and 5) is due to the flooding in section 1, 2, 3 and continuous flow of floodwater in the upstream floodplain through channels.

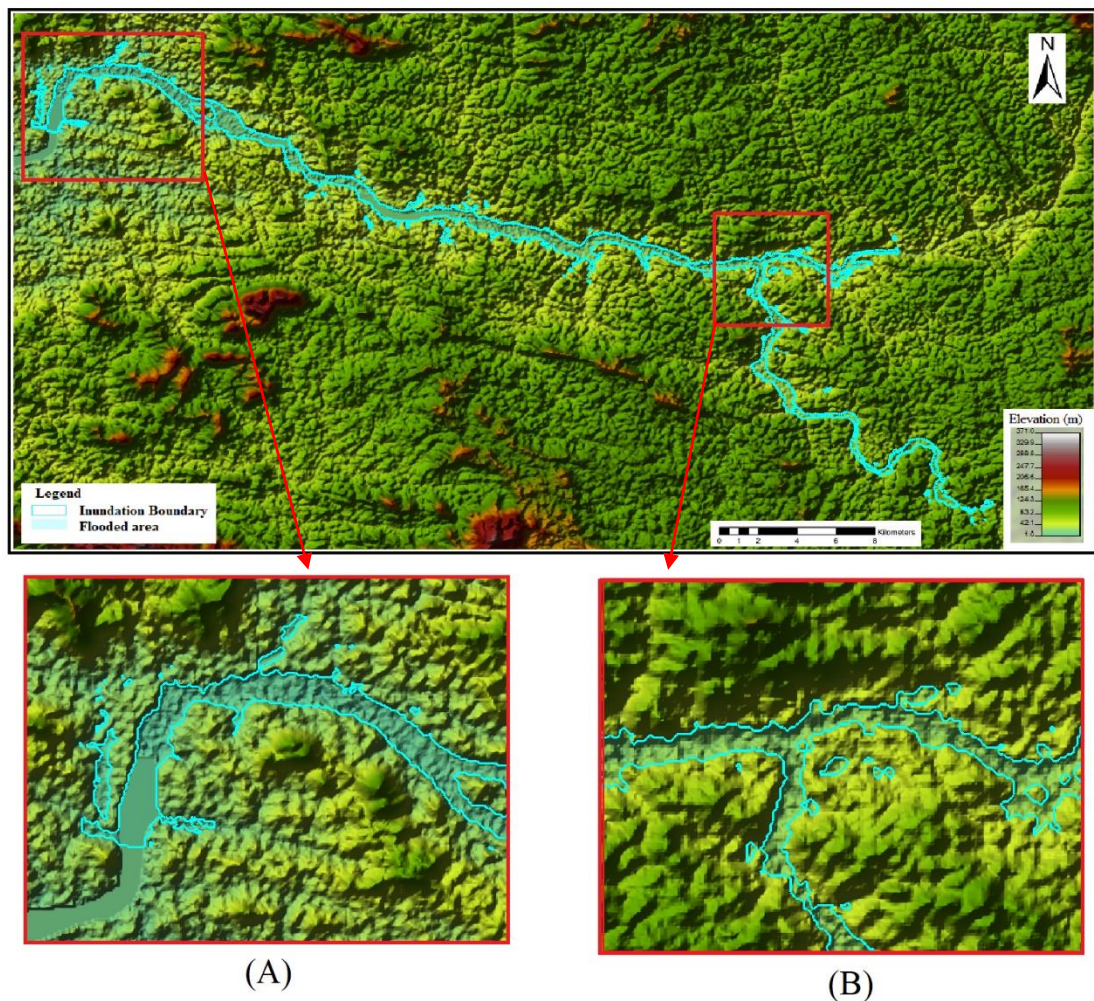


Figure 5.41 Flood inundation map of the Nethravathi river basin

5.5 SENSITIVITY ANALYSIS

The HEC-RAS model uses, channel geometry, upstream and downstream boundary conditions and roughness coefficients to compute a water-surface profile. In this study, a sensitivity analysis was carried out for the 1D HEC-RAS model to determine the impact of some geometric and computational parameters on model results and stability. The parameters that were investigated in the sensitivity analysis are Manning's roughness coefficient, downstream boundary condition (normal depth), computational time step, θ -weighting parameter. The sensitivity analysis was performed for Manning's roughness and bed slope varying $\pm 10\%$, $\pm 20\%$ and $\pm 30\%$ for θ -weighting parameter varying 0.6 to 1 and the computational time step 10 sec, 30 sec, 2 min, 6 min, 15 min and 30 min.

5.5.1 Sensitivity analysis for time step

In the development of an unsteady flow model, stability and numerical accuracy can be improved by selecting a time step that satisfies the Courant condition. This is very important for an unsteady flow model. If the computation time step is too large the change in hydraulic properties between two consecutive time steps might be too large, causing instability. A too small-time step can also cause instability issues. The time step sensitivity analysis was carried out to investigate how the choice of time step influences stability and simulation results. The sensitivity of time step on output result shown in Figure 5. 42.

The result shows when time step increases the peak stage is reduced but the more change is not noticeable until the time step exceeds 30 sec. The reduction of peak stage reflects a general flattening of the hydrograph, which could be a result of numerical diffusion due to the time step being too large (Brunner, 2016a). When the time step is increased the timing of the peak is delayed. This is due to the variations on a smaller time scale than the model time step cannot be captured, a model with a 1-hour time step cannot capture a peak occurring at a given half-hour.

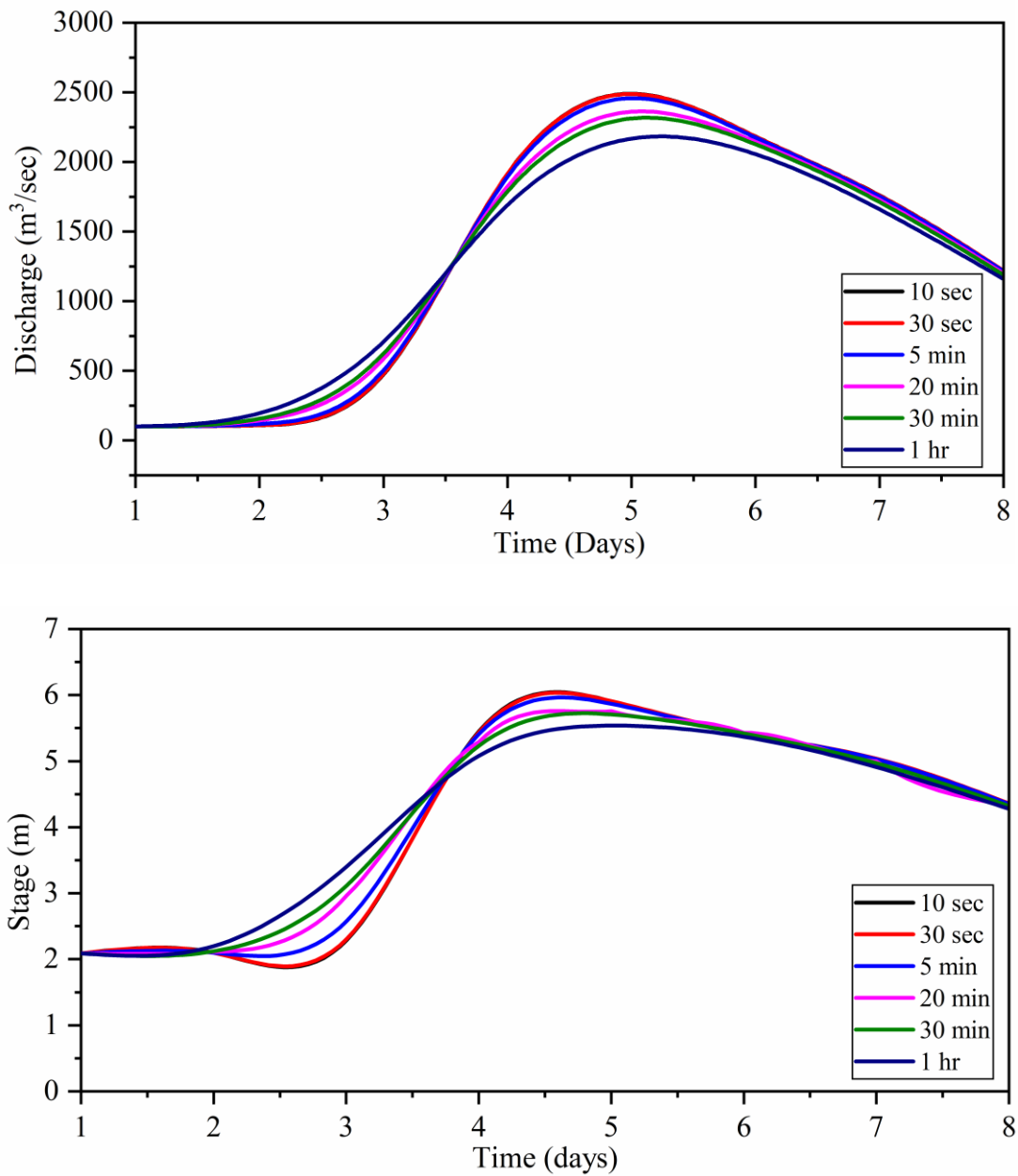


Figure 5.42 Sensitivity of time step on stage and discharge at downstream gauging station.

5.5.2 Sensitivity analysis for weighting factor (Theta)

When the hydraulic computations are performed, the governing differential, equations are solved using numerical approximations of the derivatives. The spatial derivatives are evaluated at an interior point $(n + \theta) \Delta t$, with $0.6 < \theta < 1$. Generally, a lower θ -value will produce a higher accuracy but may reduce model stability. (Brunner, 2016b). In

order to investigate how the choice of θ -value impacts the model results, a sensitivity analysis was carried out. When θ is reduced to values smaller than 0.6 the model unstable. However, comparing the output results from Theta 0.7, 0.8, and 0.9 with the $\theta = 1$, no difference in output stage but in a very small increase in discharge $0.1 \text{ m}^3/\text{sec}$ which is negligible. From the result, it shows that the accuracy associated with θ -parameter was insignificant in the Nethravathi river model.

5.5.3 Sensitivity analysis for normal depth

Downstream boundary conditions are important for all hydraulic models, especially unsteady flow models. Downstream boundary conditions can often be a source of model error, as well as model instability. More often than not, the true stage for a given flow at the downstream end of our models is not known. The normal depth boundary condition requires the user to enter a single energy slope, which is then in turn used in Manning's equation to compute the downstream stage for any flow occurring. To investigate how the downstream boundary conditions, impact the model results, a sensitivity analysis was carried out.

The results of the sensitivity analyses for normal depth shows in Figure 5.43. Varying the normal depth value by $\pm 10\%$ changed the estimated peak depth of flow by 0.12 m from the base value and the estimated discharge is not changed. Varying the normal depth for the study reaches by $\pm 20\%$ the estimated peak depth of flow changed by an average of 0.22 m to 0.27 m and the estimated discharge is charged by $0.14 \text{ m}^3/\text{sec}$, where even a change of $\pm 30\%$ in normal depth corresponded to 0.32 m to 0.44 m change in estimated peak stage and $0.18 \text{ m}^3/\text{sec}$ in the estimated discharge. The result shows that the normal depth is more sensitive to model accuracy of stage output result rather than discharge.

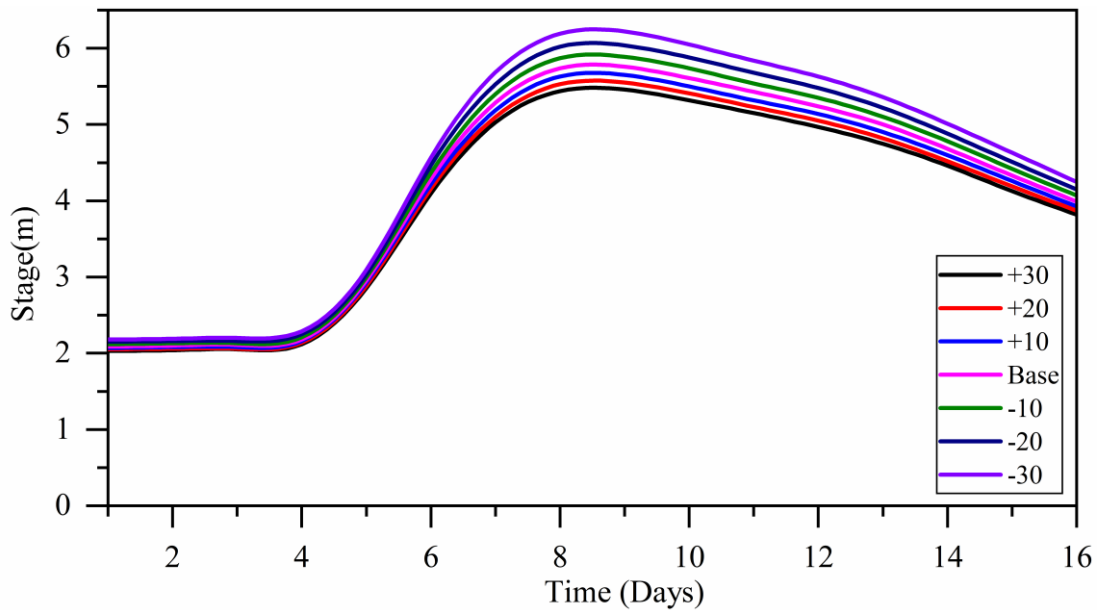


Figure 5.43 Sensitivity of Normal depth on stage at downstream gauging station.

5.5.4 Sensitivity analysis for cross-section spacing (Δx)

For sensitivity analysis, the simulation period July 1 to July 16 period is considered. In each case, input discharge is defined by considering the average value of the day and a constant bed slope of 0.001 is considered. The different cross-section spacing (Δx) ranging from around 100 m to 2000 m and the study is selected for one typical case of Δt 5 min, $n=0.032$ in channel an $n=0.070$ in floodplain, normal depth of 0.001, and average peak discharge of 2610 m^3/s . The results of sensitivity analysis for cross-section spacing is presented in Table 5.5.

Table. 5.5 sensitivity results obtained at the downstream gauging station

| Cross-section spacing (Δx) | Discharge (m^3/s) | Stage (m) |
|--------------------------------------|-----------------------|-----------|
| 2000 | 2679.23 | 6.01 |
| 1000 | 2643.63 | 5.91 |
| 500 | 2610 | 5.87 |
| 200 | 2589.10 | 5.84 |
| 100 | 2581.90 | 5.831 |

The sensitivity analysis for different cross-section spacing ranging between 100 m to 2000 m did not show significant differences. Although model performance for flow depth at downstream gauging station is not significantly affected by model spacing.

5.5.5 Sensitivity analysis for Manning's roughness

Manning's n is a friction parameter reflecting the resistance against the flow from the bottom surface. A high Manning's n value reflects a high frictional resistance, and will thus produce a slower flow and higher water levels, whereas a lower Manning's n will allow more rapid flow and lower stage. The impact on stage and flow hydrographs and inundation extent of changing Manning's n was investigated. Manning's n is often used as a calibration parameter, and it is valuable to have an approximate idea of the magnitude of the response to a change in Manning's n .

Varying the n -value by $\pm 10\%$ changed the estimated peak depth of flow by 0.22 to 0.25 m from the base value and the estimated discharge is changed by 33 m^3/sec to 36 m^3/sec . Varying the n -value for the study reaches by $\pm 20\%$ the estimated peak depth of flow changed by an average of 0.32 m to 0.44 m and the estimated discharge is charged by 71 m^3/sec to 110 m^3/sec , where even a change of $\pm 30\%$ in normal depth corresponded to 0.49 m to 0.66 m change in estimated peak stage and 130 m^3/sec to 178 m^3/sec in the estimated discharge. The results from the sensitivity analysis show that the model is very sensitive to the choice of Manning's n . Reducing Manning's n will decrease the magnitude of peak and stage, and reduce the total inundation extent. Figure 5.44 shows the response of changes n -value in a cross-section in the Nethravathi River. It can also be noted that the change in output as a result of changing Manning's n was significantly larger than the changes due to change in time step, θ -parameter and normal depth. This indicates that the choice of friction coefficient can to some extent overshadow the uncertainties related to insufficient geometry data and the numerical solution.

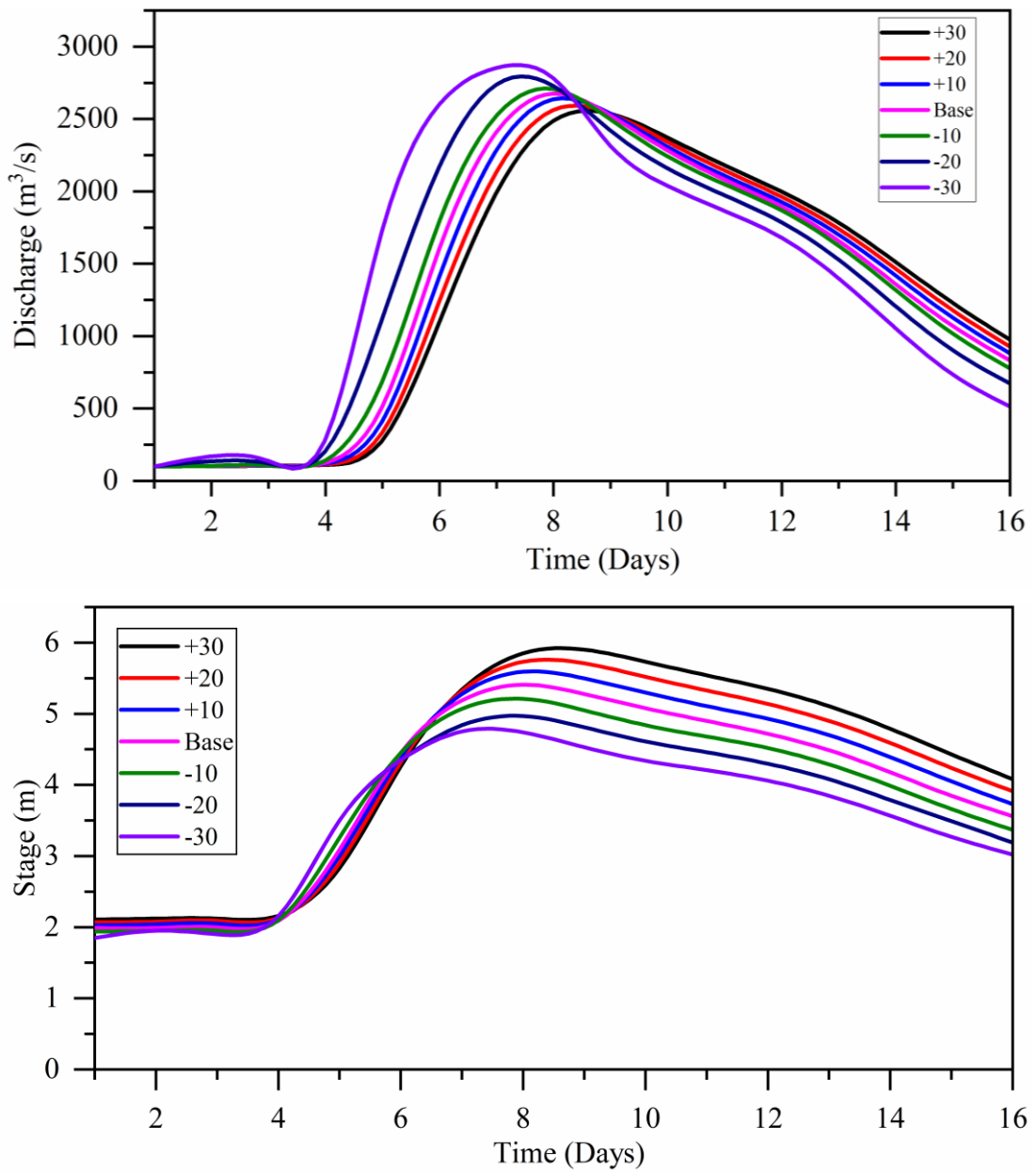


Figure 5.44 Sensitivity of Manning's n on stage and discharge at downstream gauging station.

SUMMARY AND CONCLUSIONS

6.1 SUMMARY

In natural channels such as rivers, the flow behaviour is a highly complicated phenomenon due to unsteady and non-uniform flow. Hydraulic modeling is essential for the study of characteristics of unsteady flow in rivers. Changes in riverbed morphology influence the increase in depth of flow in rivers. In the present study, the roughness coefficient is varied to match the natural condition. The study is carried out using the Hydrologic Engineering Centres—River Analysis System (HEC-RAS). A river length of 45 km of the Nethravathi river regime, Karnataka from Uppinangadi and Kumaradhara to Bantwal is considered for the study. Daily river stage and discharge data are collected from the Central Water Commission (CWC) gauged at Bantwal station. GIS interface of HEC-GeoRAS is also used to extract the cross-section, bed slope, and length of the river channel from 30 m resolution DEM data. The cross-sections are represented for each 500 m length of the river. Since accurate data is unavailable in the study area, cross-sections are simplified. HEC-RAS model was used for the simulation of surface water levels and discharge values.

Manning's roughness coefficient and river cross-sections were defined for the calibration of observed river stage and discharge data. The model is built to examine the hydraulic response in the Nethravathi River basin for a calibration period of 2007 - 2009 and the validation period of 2010. The impact of roughness coefficient is determined using observed stage and discharge hydrograph. Consequently, the river stage and discharge along the cross-section of flow are disturbed resulting in the flooding of river banks and inundation of low lying areas. In the present study, a sensitivity analysis of flood routing parameters was carried out using a calibrated and validated parameter values of the Nethravathi river regime. The channel parameters such as Manning's roughness coefficient, normal depth, time step and θ -weighting parameter were considered to test the model sensitivity.

6.2 CONCLUSIONS

From the present study, the following conclusions are made:

1. Manning's roughness plays an important role in flow analysis of natural river. In the present study, it is observed that Manning's co-efficient of 0.032 for channel and 0.05 to 0.07 for floodplain was found be apt. This shows that for flood plain relatively a high value of n is acceptable.
2. It is observed that the maximum depth of flood for the study area in the upstream region was found to be 14.98 m and at downstream region was found to be 9.6 m.
3. The accurate representation of longitudinal section of bed elevation in the 1-D model using DEM was found to be critical in calculating the maximum depth of water level.
4. The peak discharge for the upstream region of the natural channel was found to be 2328 m³/s with a maximum velocity of 6.7 m/s due to narrow width of river along the valley portions with boulder and vegetation across along the river bed leading to non-uniform flow in the river section.
5. The peak discharge for the downstream stream region of the natural channel was found to be 5610 m³/s with a maximum velocity of 5.54 m/s due to increase in the width of river along the valley portions with boulder and vegetation across along the river bed covered with find sand resulting in uniform flow in the river section.
6. The model accuracy was found to be 93.33% and 97.23% for calibration and validation period respectively in case of depth of flow while The corresponding value are 80% and 88% for discharge.
7. From flood inundation map it is observed that, floodwater flows over the riverbank in the upstream of the Uppinangadi gauging station, near the Nethravathi-Kumaradhara river confluence and at the meandering section in upstream of the Bantwal gauging station.
8. The model is very sensitive to the choice of Manning's n . The change in model output as a result of changing Manning's n was significantly larger than the changes due to change in time step, θ -parameter and normal depth.

6.3 CONTRIBUTIONS

- The present study has determined Manning's roughness coefficient 'n' for the selected stretch of the Nethravathi river using the available information related to discharge and stage hydrograph. Such numerical study has not been attempted earlier, therefore it helps in determining the flood depth and stage hydrograph at any cross-section of the selected river reach.
- The present study is the application of variability in hydraulic model parameters such as Manning's roughness coefficient to assess the model response, which helps to understand the behaviour of the river under varying hydrological and hydrogeological conditions.
- The severity and spatial variation of flood conditions in the river are derived from flood inundation maps.
- The parameter perturbation technique was utilized to carry out a sensitivity analysis in the 1D HEC-RAS model to identify the parameters that accurately represent the hydraulic characteristics in the catchment. This shows that the parameter perturbation technique is effectively used to assess the relative sensitivity of parameters.
- The sensitivity analysis recognized that the calibrated unsteady flow hydraulic model is very sensitive to the value of Manning's roughness coefficient 'n' chosen for the study area. The sensitivity of model accuracy towards the flow depth output rather than discharge.
- The study helps in preparing water management strategy and planning for flow analysis in a natural river. The result of flood inundation mapping during the various flood for different roughness in the upper, middle, and lower reach of a river. This will help in preparing a statistic plan for administration to guide the concerning flood protections, evacuations, LU/LC and suggestions for stakeholders near the bank in upstream and downstream regions.

6.4 LIMITATIONS OF THE STUDY

- HEC-RAS yields one-dimensional results and hence the results are limited to analyse the flood routing in a narrow channel.

- The present study has not considered the lateral flow, groundwater contribution and bank storage due to non-availability of information. Hence, the vertical heterogeneity of hydro-geological parameters contribution has not been analysed due to lack of sufficient bore-log data for the selected study area.
- The implication of change in land use/land cover on the fluvial cross-section of the river has not been considered while predicting the inundation in the study area.

6.5 SCOPE FOR FUTURE RESEARCH

- The precision of the simulations can be improved by utilizing/predicting higher resolution DEM, groundwater level information and discharge information of lower-order streams joining the river reach.
- The present study can be improvised for the 2-Dimensional or 3-Dimensional model which requires varied hydrological input data.

REFERENCES

- Abdelbasset, M., Abderrahim, L., Ali, C. A., Abdellah, B., Lahcen, B. and Laila, B. (2015). "Integration of GIS and HEC-RAS in floods modeling of the Ouergha river, Northern Morocco." *Eur. Sci. J.*, 11(2).
- Abu-Aly, T. R., Pasternack, G. B., Wyrick, J. R., Barker, R., Massa, D. and Johnson, T. (2014). "Effects of LiDAR-derived, spatially distributed vegetation roughness on two-dimensional hydraulics in a gravel-cobble river at flows of 0.2 to 20 times bankfull." *Geomorphology.*, 206, 468-482.
- Akbari, G. H., and Barati, R. (2012). Comprehensive analysis of flooding in unmanaged catchments. *In Proc., Int. Civil Engineers-Water Management* (Vol. 165, No. 4, pp. 229-238). Thomas Telford Ltd.
- Akbari, G. H., Nezhad, A. H. and Barati, R. (2012). "Developing a model for analysis of uncertainties in prediction of floods." *J. Adv. Res.*, 3(1), 73-79.
- Al Faruque, M. A. and Balachandar, R. (2015). "Variation of Streamwise and Vertical Turbulence Intensity in a Smooth and Rough Bed Open Channel Flow." *Int. j. aerosp.*, 9(12), 2047-2050.
- Al Faruque, M. A., Wolcott, S., Goldowitz, J. and Wolcott, T. (2014). "Open channel flow velocity profiles for different Reynolds numbers and roughness conditions." *Int. j. aerosp.*, 3(01), 400-405.
- Alegre., Porto., Danieli Mara Ferreira. and Julio Gomes. (2017). "Verification of Saint-Venant Equations Solution Based on the Lax Diffusive Method for Flow Routing in Natural Channels." *RBRH*, 22
- Alekseevskii, N. I., Krylenko, I. N., Belikov, V. V., Kochetkov, V. V. and Norin, S. V. (2014). "Numerical Hydrodynamic Modeling of Inundation." in Krymsk on 6–7 July 2012. *Power Tech. and Eng.*, 48(3), 179-186.
- Ardıçlıoğlu, M. and Kuriqi, A. (2019). "Calibration of channel roughness in intermittent

rivers using HEC-RAS model: Case of Sarimsakli creek, Turkey.” *SN Applied Sciences*, 1(9), 1080.

Arora, V. K., & Boer, G. J. (1999). “A variable velocity flow routing algorithm for GCMs.” *J. Geophys. Res.: Atmos.*, 104(D24), 30965-30979.

Arora, Vivek., Frank Seglenieks., Nick Kouwen. and Eric Soulis. (2001). “Scaling Aspects of River Flow Routing.” *Hydrological processes*, 15(3), 461–77.

Atallah, M. H., Hazzab, A., Seddini, A., Ghenaim, A. and Korichi, K. (2016). “Hydraulic flood routing in an ephemeral channel: Wadi Mekerra, Algeria.” *Modeling Earth Systems and Environment*, 2(4), 1-12.

Awad, A. M. (2016). “Hydraulic Model Development using HEC-RAS and Determination of Manning Roughness Value for Shatt Al-Rumaith.” *Muthanna J. Engg. Tech.*, 4(1), 9-13.

Bao, H. J. and Zhao, L. N. (2011). “Hydraulic model with roughness coefficient updating method based on Kalman filter for channel flood forecast.” *Water Sci. Eng.*, 4(1), 13-23.

Barati, R. (2011). “Parameter estimation of nonlinear Muskingum models using Nelder-Mead simplex algorithm.” *J. Hydrol. Eng.*, 16 (11), 946-954.

Barati, Reza., Sajjad Rahimi. and Gholam Hossein Akbari. (2012). “Analysis of Dynamic Wave Model for Flood Routing in Natural Rivers.” *Water Sci. Eng.*, 5(3), 243–58. <http://dx.doi.org/10.3882/j.issn.1674-2370.03.001>.

Barnes, H. H. (1967). *Roughness characteristics of natural channels* (No. 1849). US Government Printing Office.

Becker, L. and Yeh, W. W. G. (1972). “Identification of parameters in unsteady open channel flows.” *Water Resour. Res.*, 8(4), 956-965.

Belicci, R. (2014). “Advance Hydraulic modeling using HEC-RAS, Baraolt river, Romania.” *J. Agric. Sci*,

- Bong, C. H. J. and Mah, D. Y. S. (2008). “Study of Flow in a Non-Symmetrical Compound Channel with Rough Floodplain.” *Journal - IEM.*, 69(2),18–26.
- Boulomytis, V. T. G., Zuffo, A. C., Dalfré Filho, J. G. and Imteaz, M. A. (2017). “Estimation and calibration of Manning’s roughness coefficients for ungauged watersheds on coastal floodplains.” *Int. J. River Basin Manag.*, 15(2), 199-206.
- Brunner, G. W. (2016). *HEC-RAS River Analysis System. Hydraulic Reference Manual. Version 5.0.* Hydrologic Engineering Center Davis CA.
- Casas, A., Benito, G., Thorndycraft, V. R., and Rico, M. (2006). “The topographic data source of digital terrain models as a key element in the accuracy of hydraulic flood modelling.” *Earth Surf Proc Land.*, 31, 444–456. doi:10.1002/esp.1278.
- Castellarin, A., Di Baldassarre, G., Bates, P. D. and Brath, A. (2009). “Optimal cross-section spacing in Preissmann scheme 1-D hydrodynamic models.” *J. Hydraul. Eng.*”, 135(2), 96–105. doi: 10.1061/(ASCE)0733- 9429(2009)135:2(96).
- CGWB. (2012). “Ground water information booklet, Dakshina Kannada district, Karnataka.” Central Ground Water Board, Ministry of Water Resources, Government of India, South Western Region, Bangalore., 10-11.
- Chagas, Patricia (2005). “Solution of Saint Venant’s Equation to Study Flood in Rivers, through Numerical Methods. Chagas, Patricia 1.” *J. Hydrol.*, (55), 205–10.
- Chaturvedi, A. (2000). “Accuracy assessment of DTM data: a cost-effective approach for a large-scale digital mapping project.” *Int. arch. photogramm. remote sens.*, 33(B2; PART 2), 105-111.
- Chaudhry, M. H. (1993). *Open-Channel Flow*, Prentice Hall, Englewood Cliffs, New Jersey
- Chow, V. T. (1959). *Open-channel hydraulics. McGraw-Hill civil engineering series.*
- Cook, A. and Merwade, V. (2009) “Effect of topographic data, geometric configuration and modelling approach on flood inundation mapping.” *J. Hydrol.*, 377 (1-2), 131-142.

Cook, A. C. (2008). "Comparison of one-dimensional HEC-RAS with two-dimensional FESWMS model in flood inundation mapping." Mtech thesis, Graduate School, Purdue Univ., West Lafayette.

Cunge, J.A., 1969. "On the subject of a flood propagation computation method (Muskingum method)." *J. Hydraul. Res.* 7, 205e230.

Cunge, J.A., Holly, F.M., Verwey, A. (1980). "*Practical aspects of computational river hydraulics*" Pitman Publishing Ltd. London.

Cunge., Jean A. and Marc Erlich. (1999). "Hydroinformatics in 1999: What Is to Be Done ?" *Journal of Hydroinformatics*, 1(1), 21–31.

Di Baldassarre, G., Castellarin, A., Montanari, A. and Brath, A. (2009), "Probability weighted hazard maps for comparing different flood risk management strategies: a case study." *Nat Hazards.*, 50, 479-496.

Ding, Y., Jia, Y. and Wang, S. S. (2004). "Identification of Manning's roughness coefficients in shallow water flows." *J. Hydraul. Eng.*, 130(6), 501-510.

Ding, Y., Liu, Y., Liu, X., Chen, R. and Shao, S. (2017). "Applications of coupled explicit–implicit solution of SWEs for unsteady flow in Yangtze River." *Water Res.*, 9(3), 91.

Duvvuri, S. and Narasimhan, B. (2013). "Flood inundation mapping of thamiraparani river basin using hec-geo ras and swat." *Int. J. Eng. Res. Technol.*, 2(7).

Ebissa, G. K. (2017). "Estimation of Open Channel Roughness by using Gradual Varied Flow Profiles." *Int. J. Sci. Res.*, 6(5), 1295-1304.

Elhanafy H. and Copeland G.J.M., "*Modified method of characteristics for the shallow water equation*" civil engg. Dept., Strathclyde University, UK.

Elhanafy, H., and Copeland, G. M. (2007). "Modified method of characteristics for the shallow water equations." In 2nd IMA International Conference on flood Risk Assessment

- Ezz, H. (2018). "Integrating GIS and HEC-RAS to model Assiut plateau runoff." *Egypt. J. Remote. Sens. Space Sci.*, 21(3), 219-227.
- Faruque, M. D. and Balachandar, R. (2016). "Study the Effect of Roughness on the Higher Order Moment to Extract Information About the Turbulent Flow Structure in an Open Channel Flow." *Int. J. Mech. Aerospace. Indst. Mechatro. Manufact. Engg.*, 10(5), 806-811.
- Faruque., Abdullah Al., Scott Wolcott., Joshua Goldowit., and Teresa Wolcott. (2014). "Open Channel Flow Velocity Profiles for Different Reynolds Numbers and Roughness Conditions." *Int. J. Eng. Technol.*, 03(2003), 400–405.
- Ferreira, D. M., Fernandes, C. V. S. and Gomes, J. (2017). "Verification of Saint-Venant equations solution based on the lax diffusive method for flow routing in natural channels." *Revista Brasileira de Recursos Hídricos Brazilian J. Water Res.*, 22, e25.
- Gadissa, E. and Teshome, A. (2018). "Estimation of Open Channel Flow Parameters by Using Genetic Algorithm." *J Optimiz Theory App.*, 7(03), 51.
- Gori, A., Blessing, R., Juan, A., Brody, S. and Bedient, P. (2019). "Characterizing urbanization impacts on floodplain through integrated land use, hydrologic, and hydraulic modeling." *J. Hydrol.*, 568, 82-95.
- Graff, W., and Altinakar, M.S., (1996). "Ecoulement nonpermanent et phenomenes de transport." *Presse Polytechnique et Universitaires Romandes, Lausanne.*
- Hameed, L. K. and Ali, S. T. (2013). "Estimating of Manning's roughness coefficient for Hilla River through calibration using HEC-RAS model." *Jordan J. Civ. Eng.*, 159(701), 1-10.
- Hempel, C.G. (1963). "Explanations and Predictions by Covering Laws." In *Philosophy of Science*, John Wiley, 107–33.
- Hasani, H. (2013). "Determination of Flood Plain Zoning in Zarigol River Using the Hydraulic Model of HECRAS." *Int. j. sci.: basic appl.*, 5(3), 399-403.
- Horritt, M. S. and Bates, P. D. (2002). "Evaluation of 1D and 2D numerical models for

predicting river flood inundation.” *J. Hydrol.*, 268(1-4), 87-99.

Hughes, J. D., Langevin, C. D., and White, J. T. (2015). “MODFLOW-based coupled surface water routing and groundwater-flow simulation.” *Groundwater.*, 53(3), 452-463.

Ingale, H. and Shetkar, R. V. (2017). “Flood analysis of Wainganga River by using HEC-RAS model.” *Int. j. sci.*, 6(7), 211-215.

Jacob, X. K., Bisht, D. S., Chatterjee, C. and Raghuwanshi, N. S. (2019). “Hydrodynamic Modeling for Flood Hazard Assessment in a Data Scarce Region: A Case Study of Bharathapuzha River Basin.” *Environ. Model. Assess.*, 1-18.

Jahandideh-Tehrani, M., Helfer, F., Zhang, H., Jenkins, G. and Yu, Y. (2020). “Hydrodynamic modelling of a flood-prone tidal river using the 1D model MIKE HYDRO River: calibration and sensitivity analysis.” *Environ. Model. Assess.*, 192(2), 97.

Jena, P. P., Panigrahi, B. and Chatterjee, C. (2016). “Assessment of Cartosat-1 DEM for modeling floods in data scarce regions.” *water resous. manag.*, 30, 1293–1309.

Jia, Y. and Wang, S. S. Y. (1999) “Numerical model for channel flow and morphological change studies.” *J. Hydraul. Eng.*, 125~9!, 924– 933.

Johnson, P. A. (1996). “Uncertainty of hydraulic parameters.” *J. Hydraul. Eng.*, 122(2), 112-114.

Kadam, P., and Sen, D. (2012). “Flood inundation simulation in Ajoy River using MIKE-FLOOD.” *J. Hydraul. Eng.*, 18(2), 129-141.

Kalita, H. M. and Sarma, A. K. (2012). “Efficiency and performances of finite difference schemes in the solution of saint Venant's equation.” *Int. j. civ.*, 2(3), 950-958.

Kardavani, P. and Qalehe, M. H. (2013). “Efficiency of Hydraulic Models for Flood Zoning Using GIS (Case Study: Ay-Doghmarsh River Basin).” *Life Sci.*, 10(2).

Keupers, I., Nguyen Thanh, T. and Willems, P. (2015). “Modelling the time variance of

the river bed roughness coefficient for improved simulation of water levels.” *Int. J. River Basin Manag.*, 13(2), 167-178.

Khalfallah, C. B. and Saidi, S. (2018). “Spatiotemporal floodplain mapping and prediction using HEC-RAS-GIS tools: Case of the Mejerda river, Tunisia.” *J. Afr. Earth Sci.*, 142, 44-51.

Khatua, K. K., Patra, K. C. and P K Mohanty. (2012). “Stage-Discharge Prediction for Straight and Smooth Compound Channels with Wide Floodplains.” *J. Hydraul. Eng.*, 138(January): 93–99.

Kim, J. S., Lee, C. J., Kim, W., and Kim, Y. J. (2010). “Roughness coefficient and its uncertainty in gravel-bed river.” *Water Sci. Eng.*, 3(2), 217-232.

Knebl, M. R., Yang, Z. L., Hutchison, K. and Maidment, D. R. (2005). “Regional scale flood modeling using NEXRAD rainfall, GIS, and HEC-HMS/RAS: a case study for the San Antonio River Basin Summer 2002 storm event.” *J Environ Manage.*, 75(4), 325-336.

Knight, D. W., Omran, M. and Tang, X. (2007). “Modeling depth-averaged velocity and boundary shear in trapezoidal channels with secondary flows.” *J. Hydraul. Eng.*, 133(1), 39-47.

Knight, Donald W., Mazen Omran, and Xiaonan Tang. (2013). “Modeling Depth-Averaged Velocity and Boundary Shear in Trapezoidal Channels with Secondary Flows.” *J. Hydraul. Eng.*, 133(1): 39–47.

Kumar, A., Jayappa, K. S. and Deepika, B. (2010). “Application of remote sensing and geographic information system in change detection of the Netravati and Gurpur river channels, Karnataka, India.” *Geocarto Int.*, 25(5), 397-425.

Kumar, S. H. and Nagaraj, M. K. (2018). “Assessment of Interactions between River and Aquifer in the Gowri-hole Sub-catchment.” *J. Geol. Soc.*, 92(4), 435-440.

Kuta, R. W., Annable, W. K. and Tolson, B. A. (2010). “Sensitivity of field data estimates in one-dimensional hydraulic modeling of channels.” *J. Hydraul. Eng.*,

136(6), 379-384.

Kute, S., Kakad, S., Bhoje, V. and Walunj, A. (2014). "Flood modeling of river Godavari using HEC-RAS." *Int J Res Eng Technol.*, 3(09), 81-87.

Lamichhane, N. and Sharma, S. (2018). "Effect of input data in hydraulic modeling for flood warning systems." *Hydrolog Sci J.*, 63(6), 938-956.

Leopold, L.B., Wolman, M.G., and Miller, J.P., (1964). "Fluvial Processes in Geomorphology." W.H. Freeman, San Francisco, California, USA.

Li, Z., Zhu, C. and Gold, C. (2004). *Digital terrain modeling: principles and methodology*. CRC press , Boca Raton London New York Washington, D.C.

Liu, Z., Merwade, V. and Jafarzadegan, K. (2019). "Investigating the role of model structure and surface roughness in generating flood inundation extents using one-and two-dimensional hydraulic models." *J. Flood Risk Manag.*, 12(1), e12347.

Logah, F. Y., Amisigo, A. B., Obuobie, E. and Kankam-Yeboah, K. (2017). "Floodplain hydrodynamic modelling of the Lower Volta River in Ghana." *J. Hydrol.*, 14, 1-9.

Logah, F. Y., Amisigo, A. B., Obuobie, E., & Kankam-Yeboah, K. (2017). Floodplain hydrodynamic modelling of the Lower Volta River in Ghana. *Journal of Hydrology: Regional Studies*, 14, 1-9.

Maidment, D. R. (1993). *Handbook of Hydrology*. McGraw-Hill, Inc. P10.1

Manandhar, B. (2010). "Flood plain analysis and risk assessment of Lothar Khola. Master of Science Thesis in Watershed Management." Tribhuvan Univ., Institute of Forestry Pokhara, Nepal.

Marko, K., Elfeki, A., Alamri, N. and Chaabani, A. (2019). "Two-Dimensional Flood Inundation Modelling in Urban Areas Using WMS, HEC-RAS and GIS (Case Study in Jeddah City, Saudi Arabia)." *Int Conference of the Arabian J. Geoscie.*, Springer, Cham., 265-267

Matori, A. N., Dedi Atunggal, S. P. and Cahyono, B. K. (2008). "Quality assessment of

DTM generated from RTK GPS data on area with various sky views” In *Proceedings of the 21st International Technical Meeting of the Satellite Division of The Institute of Navigation*, 1462-1469.

McCarthy, G. T. (1938). “The unit hydrograph and flood routing.” *Proc. Int. Conf. of North Atlantic Division*. US Army Corps of Engineers, 608-609.

Mitra, Lakshmi, and Mimi Das Saikia. (2016). “Analysis of Flow Resistance for Different Bed Materials with Varying Discharge.” *Int J Innov Res Sci Eng Technol.*, 5(2): 1817–23

Mockus, V. (1964). *National engineering handbook*. US Soil Conservation Service: Washington, DC, USA, 4.

Mohammed Siwan shamkhi and Zainab Shakir Attab (2018). “Estimation of Manning’s Roughness Coefficient for Tigris River by Using HEC-RAS model.” *Wasit J. Engg. Scien.*, 6(3), 90-97.

Moharana, S. and Khatua, K. K. (2014). “Prediction of roughness coefficient of a meandering open channel flow using Neuro-Fuzzy Inference System.” *Measurement.*, 51, 112-123.

Mokhtar, E. S., Pradhan, B., Ghazali, A. H. and Shafri, H. Z. M. (2018). “Assessing flood inundation mapping through estimated discharge using GIS and HEC-RAS model.” *Arab. J. Geosci.*, 11(21), 682.

Moya Quiroga, V., Popescu, I., Solomatine, D.P. and Bociort, L. (2013). “Cloud and cluster computing in uncertainty analysis of integrated flood models. *J. Hydroinformatics.*, 15(1), 55-69, doi:10.2166/hydro.2012.017.

Nareth, N. and Plermkamon, V. (2013). “Estimation of Flood Damages on Nam Phong River by HEC-RAS.” *Proc.14th TSAE nat. Confr.and 6th TSAE Int. Conf.*, Prachuap Khiri Khan, 179– 186.

Nash, J. E. (1957). “The form of the instantaneous unit hydrograph.” *Int. Assoc.of Scienti. Hydrol.*, 3, 114-121.

- Nassar, M. A. (2011). "Multi-parametric sensitivity analysis of CCHE2D for channel flow simulations in Nile River." *J Hydro-Environ Res.*, 5(3), 187-195.
- Nguyen, H., Degener, J. and Kappas, M. (2015). "Flash flood prediction by coupling KINEROS2 and HEC-RAS models for tropical regions of Northern Vietnam." *J. Hydrol.*, 2(4), 242-265.
- Nut, N., and Plermkamon, V. (2013). "Estimation of flood damages on namphong river by hec-ras." *Proc. Int. Conf. of 6th TSAE*, Thailand, 179-186.
- Oubennaceur, K., Chokmani, K., Nastev, M., Tanguy, M and Raymond, S. (2018). "Uncertainty analysis of a two-dimensional hydraulic model." *Water.*, 10(3), 272.
- Pal, Debasish, and Koeli Ghoshal. 2014. "Effect of Bed Roughness on Grain-Size Distribution in an Open Channel Flow." *J Hydro-Environ Res.*, 8(4): 441–51.
- Papaoiannou, G., Loukas, A., Vasiliades, L. and Aronica, G. T. (2016). "Flood inundation mapping sensitivity to riverine spatial resolution and modelling approach." *Nat Hazards.*, 83(1), 117-132.
- Papaoiannou, G., Vasiliades, L., Loukas, A. and Aronica, G. T. (2017). "Probabilistic flood inundation mapping at ungauged streams due to roughness coefficient uncertainty in hydraulic modelling." *Adv. Geosci.*, 44, 23.
- Pappenberger, F., Beven, K., Horritt, M. and Blazkova, S. (2005). "Uncertainty in the calibration of effective roughness parameters in HEC-RAS using inundation and downstream level observations." *J. Hydrol.*, 302(1-4), 46-69.
- Parhi, P. K. (2013). "HEC-RAS Model for Mannig's Roughness: A Case Study." *Open J. Mod Hydrol.*, 3(03), 97.
- Parhi, P. K. (2018). "Flood management in Mahanadi Basin using HEC-RAS and Gumbel's extreme value distribution." *J. Inst. Eng. India: Series A.*, 99(4), 751-755.
- Patel, A. (2020). "Rainfall-Runoff Modelling and Simulation Using Remote Sensing and Hydrological Model for Banas River, Gujarat, India." *In Adv. in Water Resou. Engg. and Manag.*, Singapore Springer.,153-162.

- Patro, S., Chatterjee, C., Mohanty, S., Singh, R. and Raghuwanshi, N. S. (2009a). "Flood inundation modeling using MIKE FLOOD and remote sensing data." *J. Indian Soc. Remote. Sens.*, 37, 107–118.
- Patro, S., Chatterjee, C., Singh, R. and Raghuwanshi, N. S. (2009b). "Hydrodynamic modelling of a large flood-prone river system in India with limited data." *Hydrol. Process.*, 23, 2774–2791.
- Pinos, J. and Timbe, L. (2019). "Performance assessment of two-dimensional hydraulic models for generation of flood inundation maps in mountain river basins." *Water Sci. Eng.*, 12(1), 11-18.
- Pinos, J., Timbe, L. and Timbe, E. (2019). "Evaluation of 1D hydraulic models for the simulation of mountain fluvial floods: a case study of the Santa Bárbara River in Ecuador." *Water Pract. Technol.*, 14(2), 341-354.
- Puente, I., González-Jorge, H., Martínez-Sánchez, J. and Arias, P. (2013). "Review of mobile mapping and surveying technologies." *Measurement.*, 46(7), 2127-2145.
- Putty, M. R. Y. and Prasad, R. (2000). "Understanding runoff processes using a watershed model—a case study in the Western Ghats in South India." *J. Hydrol.*, 228(3-4), 215-227.
- Ramesh, R., Datta, B., Bhallamudi, S. M. and Narayana, A. (2000). "Optimal estimation of roughness in open-channel flows." *J. Hydraul. Eng.*, 126(4), 299-303.
- Rashid, R. S. M. M., and Chaudhry, M.H. (1995) "Flood routing in channels with flood routing" *J. Hydrol.*, 171(1–2), 75–91.
- Reddy, P. J. R. (2005). *A text book of Hydrology*. Firewall Media. Laxmi Publications
- Rezaei, Bahram, and DW Knight. (2011). "Overbank Flow in Compound Channels with Nonprismatic Floodplains." *J. Hydraul. Eng.*, 137, 815–824.
- Rivera, S., Hernandez, A. J., Ramsey, R. D. and Suarez, G. (2007). "Predicting flood hazard areas: a SWAT and HEC-RAS simulations conducted in Aguan river basin of Honduras, central America." *In ASPRS 2007 Annual Conference*, Tampa, Florida.

Saint-venant, B.D.(1871). “Theory of unsteady water flow, with application to river floods and propagation of tides in river channels.” *French Academy of science*, 73, 148-154, 37-240.

Saleh, F., Ducharme, A., Flipo, N., Oudin, L. and Ledoux, E. (2013). “Impact of riverbed morphology on discharge and water levels simulated by a 1D Saint–Venant hydraulic model at regional scale.” *J. Hydrol.*, 476, 169-177.

Samantaray, D., Chatterjee, C., Singh, R., Gupta, P. K. and Panigrahy, S. (2015). “Flood risk modeling for optimal rice planning for delta region of Mahanadi river basin in India.” *Nat Hazards.*, 76, 347–372.

Samuels, P. G. (1990). “Cross-section location in 1-D models. *Proc. Int. Conf. on River Flood Hydraul.*, White W.R., John Wiley: Chichester; 339-350.

Sanjay, L. D. and Ravindra, A. O. (2012). “Dynamic Flood Routing and Unsteady Flow Modelling: A Case Study of Upper Krishna River.” *Int. j. adv.*, 3(3), 55-59.

Schulze, K., Hunger, M., Doll, P. (2005). “Simulating river flow velocity on global scale.” *J. Adv. Geosci.*, 5, 133–136

Schumann, G., Matgen, P., Cutler, M. E. J., Black, A., Hoffmann, L. and Pfister, L. (2008). “Comparison of remotely sensed water stages from LiDAR, topographic contours and SRTM.” *J. Photogramm. Remote Sen.*, 63(3), 283-296.

Serrano, S. E. (2016). “Propagation of nonlinear flood waves in rivers.” *J. Hydraul. Eng.*, 21(1), 04015053.

ShahiriParsa, A., Noori, M., Heydari, M. and Rashidi, M. (2016). “Floodplain zoning simulation by using HEC-RAS and CCHE2D models in the Sungai Maka river.” *Air, Soil and Water Resc.*, 9, ASWR-S36089.

Soleymani, Mohsen and Mehdi Delphi. (2012). “Comparison of Flood Routing Models (Case Study : Maroon River , Iran)” *World Applied Sciences Journal*, 16(5), 769-775.

Strelkoff, T., (1970). “Numerical solution of Saint–Venant equations.” *J. hydraul. Divis. ASCE*, 96.

- Subramanya K (2008). *Engineering Hydrology*, New Delhi: Tata McGraw-Hill.
- Traore, V. B., Sambou, S., Sambou, H. and Diaw, A. T. (2015). “Steady flow simulation in Anambe River Basin using HEC-RAS.” *Int J Dev Res.*, 5(07), 4968-4979.
- Ullah, S., Farooq, M., Sarwar, T., Tareen, M. J. and Wahid, M. A. (2016). “Flood modeling and simulations using hydrodynamic model and ASTER DEM—A case study of Kalpani River.” *Geosci.*, 9(6), 439.
- Vijay, R., Sargoankar, A. and Gupta, A. (2007). “Hydrodynamic simulation of river Yamuna for riverbed assessment: a case study of Delhi region.” *Environ. Monit. Assess.*, 130(1-3), 381-387.
- Vojtek, M., Petroselli, A., Vojteková, J. and Asgharinia, S. (2019). “Flood inundation mapping in small and ungauged basins: sensitivity analysis using the EBA4SUB and HEC-RAS modeling approach.” *Hydrol. Res.*, 50(4), 1002-1019.
- Wang, G., Yang, H., Wang, L., Xu, Z. and Xue, B. (2014). “Using the SWAT model to assess impacts of land use changes on runoff generation in headwaters.” *Hydrol. Process.*, 28(3), 1032-1042.
- Wang, J., and Zhang, Z. (2019). “Evaluating Riparian vegetation roughness computation methods integrated within HEC-RAS.” *J. Hydraul. Eng.*, 145(6), 04019020.
- Wohl, E. E. (1998). “Uncertainty in flood estimates associated with roughness coefficient.” *J. Hydraul. Eng.*, 124(2), 219-223.
- Woolhiser, D. A. and Liggett, J. A. (1967). “Unsteady one-dimensional flow over a plane: the rising hydrograph.” *Water Resc. Res.* 3 (3), 753-771.
- Xu, Z., Xiong, L., Li, H., Xu, J., Cai, X., Chen, K., and Wu, J. (2019). “Runoff simulation of two typical urban green land types with the Stormwater Management Model (SWMM): sensitivity analysis and calibration of runoff parameters.” *Environ. Monit. Assess.*, 191(6), 343.
- Yalcin, E. (2019). “Two-dimensional hydrodynamic modelling for urban flood risk

assessment using unmanned aerial vehicle imagery: A case study of Kirsehir, Turkey.” *J. Flood Risk Manag.*, 12, e12499.

Yan, K., Di Baldassarre, G., and Solomatine, D. P. (2013). “Exploring the potential of SRTM topographic data for flood inundation modelling under uncertainty.” *J. Hydroinformatics.*, 15(3),

Yeh, W. W. G. (1986). “Review of parameter identification procedures in groundwater hydrology: The inverse problem.” *Water Resour. Res.*, 22(2), 95-108.

Yu, D. and Lane, S. N. (2006). “Urban fluvial flood modelling using a two- dimensional diffusion-wave treatment, part 1: mesh resolution effects.” *Hydrol. Process.*, 20, 1541-1565.

Zarrati, A. R., Jin, Y. C. and Karimpour, S. (2008). “Semianalytical model for shear stress distribution in simple and compound open channels.” *J. Hydraul. Eng.*, 134(2), 205-215.

Zarrati, A. R., Tamai, N. and Jin, Y. C. (2005). “Mathematical modeling of meandering channels with a generalized depth averaged model.” *J. Hydraul. Eng.*, 131(6), 467-475.

Zeinyvand H (2001). Flood hazard zonation Silakhor river hydraulic model HEC-RAS. Master’s Thesis, Department of Natural Resources, Mazandaran university.

LIST OF PUBLICATIONS

International Journals

1. **Kappadi, Pramodkumar**, M. K. Nagaraj, and Paresh, Chandra, Deka (2021). “Effect of Roughness Coefficient on Discharge and Flow Depth by Using Hydraulic Model for Nethravathi River Basin, India.” *International Journal of Hydrology Science and Technology*. 11(1), 114-124. (<https://doi.org/10.1504/IJHST.2020.10033821>)

National/International Conferences

1. **Kappadi, Pramodkumar**, M. K. Nagaraj and Paresh, Chandra, Deka (2021). “Sensitivity analysis of flood routing parameters in the Nethravathi river basin. *Proceedings of 25th Hydro 2020 International Conference on Hydraulics, Water Resources and Coastal Engineering* at National Institute of Technology Rourkela, during 26 to 28 March 2021 [ISBN: 978-93-90631-56-8](#)
2. **Kappadi, Pramodkumar**, M. K. Nagaraj and Paresh, Chandra, Deka (2019). “Effect of Manning’s n on Flow and Stage by Using HEC-RAS.” *8th International Engineering Symposium (IES2019)* at Kumamoto University, Japan during 13 to 15 March 2019
3. **Kappadi, Pramodkumar** and M. K. Nagaraj (2018). “Hydraulic Modeling of River Discharge Subjected to Change in Riverbed Morphology.” *International Conference on "GEOMATICS IN CIVIL ENGINEERING" [ICGCE-2018]* at Roorkee, India during 05-06 April 2018
4. **Kappadi, Pramodkumar** and M. K. Nagaraj (2018). “Flood Risk Assessment: The Impact of Riverbed Morphology on Surface Water Level Using Hydraulic Modelling A Review.” *CHESD National Conference on Environment Law, Health and Sustainable Development organized by Centre for Health & Environmental Studies*, Dehradun during 07 January 2018

Scopus Indexed Book Chapters

1. **Kappadi, Pramodkumar** and M. K. Nagaraj (2020). “Hydraulic Modeling of River Discharge Subjected to Change in Riverbed Morphology.” *In Applications of Geomatics in Civil Engineering* (pp. 165-174). Springer, Singapore. Part of the Lecture Notes in Civil Engineering book series (LNCE) (https://doi.org/10.1007/978-981-13-7067-0_12).

CURRICULUM VITAE



| | |
|--------------|--------------------|
| Name: | PRAMODKUMAR |
|--------------|--------------------|

| | |
|---------------------------|--|
| Permanent Address: | S/o Neelkanth Kappadi, Plot No. 41, R. T. Nagar, Ring Road, Near Shree Guru College Gulbarga, Karnataka - 585102 |
|---------------------------|--|

| | |
|-------------------|--|
| EDUCATION: | MASTER OF TECHNOLOGY (2014-16) <i>Discipline:</i> Hydraulic Engineering National Institute of Engineering, Mysore Karnataka <i>Affiliated to:</i> Visvesvaraya Technological University, Belgaum. |
| | BACHELOR OF ENGINEERING <i>Discipline:</i> Civil Engineering Basavakalyan Engineering College, Basavakalyan. <i>Affiliated to:</i> Visvesvaraya Technological University, Belgaum. |

| | |
|---------------------|----------------|
| Contact No.: | +91-9008754540 |
|---------------------|----------------|

| | |
|------------------|-------------------------|
| Email ID: | pramodkappadi@gmail.com |
|------------------|-------------------------|

| | |
|---------------|---|
| ORCID: | https://orcid.org/0000-0002-8775-351X |
|---------------|---|
